INVESTIGATION OF PHOTOCATALYSIS AS AN ALTERNATIVE TO OTHER ADVANCED OXIDATION PROCESSES FOR THE TREATMENT OF FILTER BACKWASH WATER

Report to the
Water Research Commission

by

MN Evans Chirwa & Emomotimi E Bamuza-Pemu
University of Pretoria

WRC Report No 1717/1/10
ISBN No 978-1-77005-988-7

March 2010

DISCLAIMER

This report has been reviewed by the Water Research Commission (WRC) and approved for publication. Approval does not signify that the contents necessarily reflect the views and policies of the WRC, nor does mention of trade names or commercial products constitute endorsement or recommendation for use.

EXECUTIVE SUMMARY

Background

Studies conducted in the year 1996 on behalf of the Department of Water Affairs and Forestry (DWAF) projected that by the year 2025, South Africa will be expecting severe water shortage (Basson et al., 1997). This projection was based on the impacts of population growth and urbanisation, and the semi arid climatic conditions of the region. Additionally, increased urbanisation and industrialisation increases the pollution in the natural water bodies thereby reducing the amount of available clean water supply sources.

The quality of drinking water has dramatically declined over the years due to agricultural, municipal and industrial pollution (Jyoti and Pandit, 2001). Poor quality water sources include eutrophied surface water (from dams), previously wasted filter backwash water and industrial wastewater. Supplementing fresh water supply by recycling treated wastewater is a trend that is rapidly gaining acceptability but its practise is limited by the problems of accumulation of toxic organic pollutants in industrial and municipal wastewaters; and the presence of taste and odours caused by microbial metabolites geosmin and 2-methylisoborneol (2-MIB).

Humic substances, also known as natural organic materials, are produced in large amounts in highly eutrophic water bodies. These contribute to volatile organic compounds (VOC) content and they serve as precursors of disinfection by-products (DBPs) during chlorination.

Both components (odour causing compounds and humic substances) contribute refractory organic pollutants that are persistent in the potable water treatment process. It is feared that, if recycled directly, organic pollutants may accumulate in the backwash water. This research was thus aimed at investigating methods for destroying the organics in the backwash water stream using a semiconductor photocatalytic process. The feasibility of the proposed process is compared with other known organic pollutant removal processes such as granular activated carbon (GAC) adsorption, ozonation, and ultrasonic cavitation.

Project Objective

The main objective of this study was to evaluate the potential of photocatalysis as a technology for treating backwash water at water treatment plants utilising highly eutrophic raw water sources. This could facilitate the reclamation and recycling of treated backwash water at a lower risk of accumulating natural and anthropogenic organic compounds which serve as precursors for DBPs during disinfection.

The main tasks conducted to achieve the project objective included:

Aim 1
Identification and quantification of natural and anthropogenic organic pollutants present in raw and filter backwash water at two treatments around Pretoria.

Aim 2
Evaluation of the performance of a laboratory scale treatment unit employing a chemical free photocatalytic system for the complete degradation of environmentally significant concentrations of taste and odour compounds in filter backwash water.

Aim 3
Detailed kinetic analysis of the photocatalytic degradation of two taste and odour causing compounds to obtain parameters for possible use in future scale-up design.

Aim 4
Cost and efficiency comparison with other known chemical oxidation technologies such as ozone and Photo-Fenton systems.

Methodology

The project involved research on the feasibility of the photocatalytic process in treating organic compounds commonly found in natural waters. The following overall methodology was followed to achieve the project objectives:

a) A detailed literature review was conducted to evaluate existing technology for treating organic compounds in water. The literature survey covered types of photocatalytic processes, photochemical-based advanced oxidation processes, and ultrasonic cavitation. A performance efficiency and cost analysis was conducted across the common technologies.

b) Raw water and backwash water from dissolved air flotation filters and sand/GAC filters from local water treatment plants (Rietvlei and Roodeplaat Water Treatment Works) were characterised to determine common organic pollutants in the water. This was done in order to determine the compounds on which to focus during the study.

c) The families of the problematic organic species identified through the literature survey and the scan of compounds (geosmin for taste and odour compounds and phenol for humic compounds) were investigated further in batch reactors using titanium dioxide (TiO_2) as the photocatalyst.

d) Optimum reaction conditions were investigated on both compounds. These included the amount of photocatalyst added to the reactor, concentration of the pollutant and the effect of aeration on pollutant removal rate.

e) A simple kinetic analysis was conducted using simple first-order reaction kinetics to determine optimum reaction rate parameters under various pollutant concentrations.

Results and Discussion

Forty-two VOCs and semi-volatile organic compounds (SVOCs) belonging to ten different classes of compounds were qualitatively identified. Taste and odour compounds, geosmin and 2-MIB were positively identified and quantified with analytic standards. Additionally, two phenol derivatives; 2-(1,1-dimethylethyl)-5-methylphenol and 2,6-bis[1,1-dimethylethyl]-4-methylphenol (butylated hydroxyltoluene), commonly used as preservatives and antioxidants

(Eriksson et al., 2003) were identified in the raw inlet and filter backwash water samples from both sources. Phenols are classified as water pollutants and have a maximum contaminant level of 0.5 µg/ℓ set by the European Community Directive (1980), and a United States Environmental Protection Agency (US EPA) limit of 1 mg/ℓ (US EPA, 2009; Steiner et al., 2008 (Appendix D)) in drinking water.

The effect of catalyst loading on the degradation efficiency of geosmin at 220 ng/ℓ was evaluated over a catalyst concentration range of 40-100 mg/ℓ, irradiated with a medium pressure lamp. These effects are presented graphically in the figure below. A system containing only TiO_2 (100 mg/ℓ) without ultraviolet (UV) irradiation was used as control.

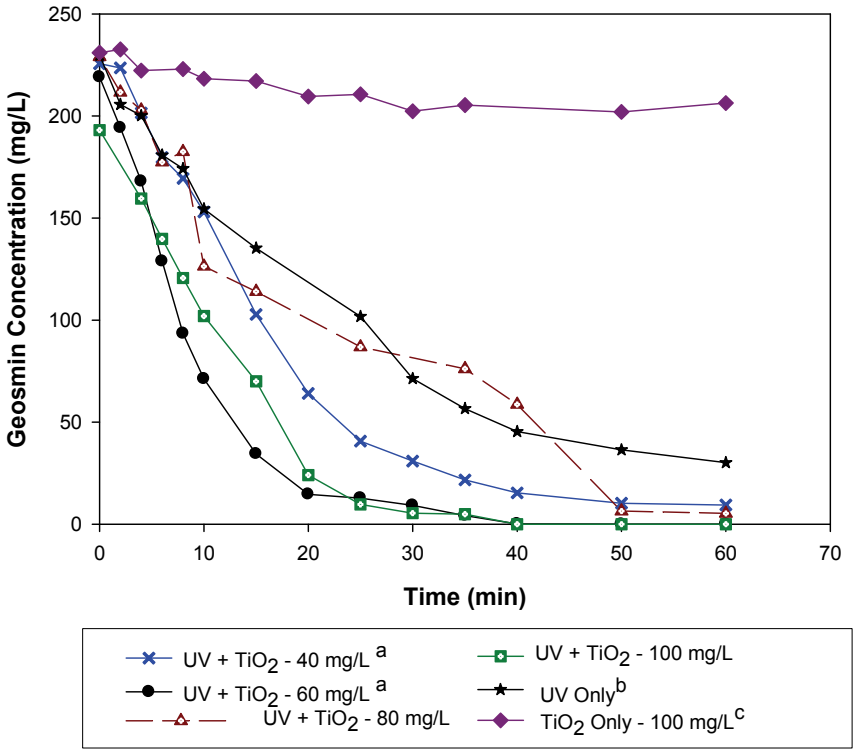

Figure E1: Degradation profile of geosmin (220 ppt). Conditions: (a) Photocatalysis - UV 400 W and TiO_2 (40-100 ng/ℓ) - (b) Photolysis - UV (400 W) only and; (c) TiO_2 only (100 ng/ℓ). All systems were aerated.

Rapid degradation was obtained for all TiO_2 concentrations under photocatalysis. Observed degradation rates increased with increasing TiO_2 concentration to an optimum of 60 mg/ℓ. This is expected for photocatalytic systems as recorded by Herrmann (1999) and Lawton et al. (2003). Complete degradation was achieved at catalyst concentrations of 60 mg/ℓ after 40 min of treatment. This is in line with findings from other studies on photocatalytic degradation of phenolics (Barakat et al., 2005; Hong et al., 2001; Serpone, 1997).

Degradation of phenolic compounds was achieved with catalyst concentrations from 10 mg/ℓ to 100 mg/ℓ within 20 minutes of exposure. Degradation efficiency increased with increasing catalyst concentration to a maximum catalyst concentration of 50 mg/ℓ for phenol solution of 10 mg/ℓ. Further catalyst loading beyond 50 mg/ℓ was detrimental to the system as shown by

the longer reaction times for complete degradation at catalyst concentrations of 100 mg/ℓ (20 minutes) and 150 mg/ℓ (30 minutes).

From the data in the next figure, it becomes obvious that aeration had a significant impact on the rate of pollutant removal. This was shown by the increased degradation rate of phenolics under different TiO_2 concentrations. Aeration led to improved degradation of both the photolytic and the photocatalytic systems at all catalyst concentrations studied.

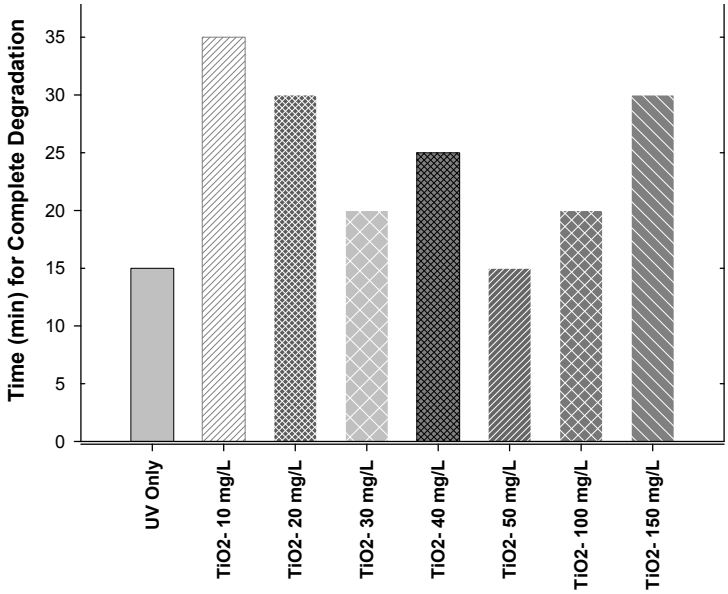

Figure E2: Comparative Photolysis and Photocatalytic Degradation Performance for Phenol (10 mg/ℓ). Conditions: UV 400 W Only, mg/ℓ ([TiO_2] = 10-150 mg/ℓ).

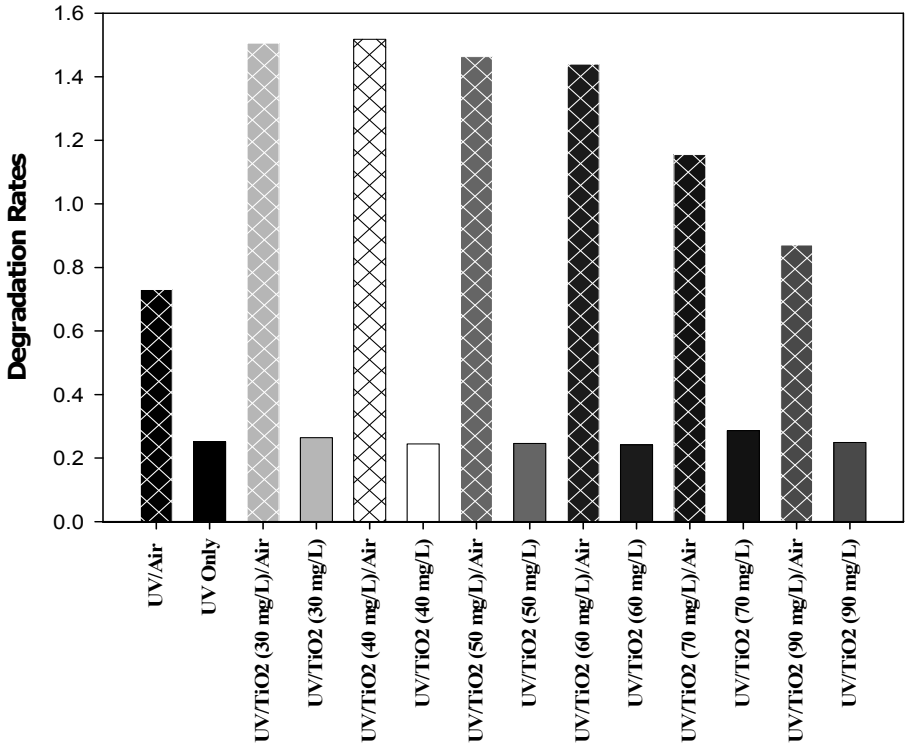

Figure E3: Effect of Aeration on Degradation Rates of Phenol (30 mg/ℓ)

Conclusions

Organic pollutants of concern were detected in the raw water and backwash water of the local water treatment plants (Rietvlei and Roodeplaat Water Treatment Works). The organics of concern detected in the water were the taste and odour causing compounds *trans*-1,10-dimethy-*trans*-9-decalol (geosmin) and 2-methyl-isoborneol (2-MIB), the phenolics – naphthalene, 2-ethenylnaphthalene, 2-(1-methylethyl)naphthalene, 2-(1,1-dimethylethyl)-5-methylphenol and 2,6-bis[1,1-dimethylethyl]-4-methylphenol (butylated hydroxyltoluene), and trace amounts of the herbicide altrazine. The investigation on the biodegradability of these families of compounds was conducted using geosmin to present the semivolatile groups and phenol to represent the non-volatiles. The taste and odour compound, geosmin, completely degraded in the solution after exposure for 40 minutes under an optimum TiO_2 concentration of 50-60 mg/ℓ.

The degradation of the taste and odour compound geosmin at a concentration as high as 230 ng/ℓ is of practical importance since the tested value was an order of magnitude higher than the levels that result in complaints from consumers (1.3 to 6.3 ng/ℓ). The tested range of concentration of phenolics was too high for the purpose of measuring impacts on drinking water treatment.

One of the challenges of the current system is that high temperatures are generated due to the high wattage of the UV lamps used in the study. To circumvent this problem, the lamp sleeve was surrounded by a cooling water jacket. However, this increased the effective circumference of the photoreactor, thereby decreasing light intensity. This could drastically increase the power input to the system to achieve the same efficiency.

Recommendations for Future Research

In future, the cost related to power input using electricity could be lowered by using UV radiation from the sun. Several configurations have been suggested in the full report that could be adopted for use in photocatalysis.

ACKNOWLEDGEMENTS

The authors would like to thank the Reference Group of the WRC Project K5/1717 for the assistance and the constructive discussions during the duration of the project:

Ms ND Basson	Sedibeng Water
Dr JE Burgess	Water Research Commission
Dr AD Ceronio	CSV Water
Ms L Coetzee	City of Tshwane
Ms S Freese	Water Science
Mr J Geldenhuys	Rand Water
Mr R Rajagopaul	Umgeni Water
Prof E Rohwer	University of Pretoria
Mr C van der Walt	CSV Water
Mr M van der Walt	Magalies Water

The authors are grateful to Prof Rohwer and Ms Yvette Naude for assistance with chromatographic analysis and to the staff of Rietvlei and Roodeplaat treatment plants for their support and assistance.

The authors would also like to thank other support personnel of the University of Pretoria, specifically Mrs Alette Devega, for continued assistance with analytical instruments and experimental work.

TABLE OF CONTENTS

LIST OF FIGURES

LIST OF TABLES

ABBREVIATIONS

BTEX	Benzene, toluene, ethylbenzene and xylene
CB	Conductance band
CIS	Cooled inlet system
CPCR	Compound parabolic collecting reactor
CVD	Chemical vapour deposition
DAFF	Dissolved air floatation filters
DCE	Dichloroethane
DCM	Dichloromethane
DCR	Dispersed catalyst reactors
DO	Dissolved oxygen
DOC	Dissolved organic carbon
DSSR	Double skin sheet reactor
DWA(F)	Department of Water Affairs (and Forestry)
E_{bg}	Band gap energy
GAC	Granular activated carbon
GC/MS	Gas chromatography/mass spectrometry
$h^+ e^-$	electron-hole pair
HP	Hewlett Packard
HPLC	High performance liquid chromatography
IPMP	2-Isopropyl-3-methoxypyrazine
MDHP	2-methyl-2,2-dimethyl-1-[2-hydroxylmethyl]propylester
MDMP	2-methyl-1-[1,1-dimethyl]-2-methyl-3-propanediylester
MIB	2-methylisoborneol
MIT	Measuring instruments technology
MLC	Maximum contaminant level
MLCG	Maximum contaminant level goal
MLD	Megalitres per day
NA	Not available
NHE	Normal hydrogen electrode
NIST	National Institute of Standards and Technology
NOM	Natural organic matter
NTU	Nephelometric turbidity unit
PAHs	Polycyclic aromatic hydrocarbons
PDA	Photo diode array
PE TMH	Perkin Elmer turbo matrix headspace
PFTBA	Perfluorotributylamine
PSDVB	Polystyrenedivinylbenzene
PTC	Parabolic trough concentrators
PTR	Parabolic trough reactor
SA	South Africa
SADWQS	South African domestic water quality standards
SC	Semiconductor
SEM	Scanning electron microscopy
SHE	Standard hydrogen electrode
SIR	Single ion recording

SPE	Solid phase extraction
SPME	Solid phase microextraction
SRB	Sulphate reducing bacteria
SVOC	Semi-volatile organic carbon
TBT	Tributyltin chloride
TBTO	Bis(tributyltin) oxide
TCA	2,4,6-Trichloroanisole
TCE	Trichloroethene
TDS	Total dissolved solids
TFFBR	Thin film fixed bed reactor
TIC	Total ion chromatogram
TOC	Total organic carbon
TPA	Terephthalic acid
t_R	Retention times
TSS	Total suspended solids
UV	Ultraviolet
VUV	Vacuum ultraviolet
VB	Valence band
VOC	Volatile organic carbon
XRD	x-ray diffractometry

CHAPTER ONE

1 INTRODUCTION

1.1 Background

Conventional potable water treatment consists of suspended solids removal through sedimentation or floatation followed by filtration. Filters are de-clogged and cleaned by backwashing with clean water. The backwash water stream may be discharged or sent back for further treatment or reclamation. In most water treatment systems, the backwash water is not returned into the system to avoid accumulation of unwanted pollutants (Plummer and Edzwald, 1998). Attempts to clean the backwash for reclamation through sedimentation tanks have been met with limited success (Bourgeois et al*.,* 2004).

Apart from the suspended solids in the backwash water, the presence of organic pollutants emanating from human and industrial activities raises concerns over the treatability of backwash water. Some of the organic pollution is indirect in that anthropogenic activities contribute to the accelerated algal growth in water bodies resulting in the accelerated eutrophication. Metabolites from algae (cyanobacteria) cause offensive odour and taste in potable water supplies. The other component of organic pollution is direct. This includes pollution from industrial and agricultural sources.

Both components of pollution contribute refractory organic pollutants that are persistent in the potable water treatment process. Even the less toxic organics emanating from algae and humic substances are potential precursors of volatile organic compounds (VOCs) which form the disinfection products trihalomethane (THM) and haloacetic acid (HAA) during chlorination.

It is feared that, if recycled directly, organic pollutants may accumulate in the backwash water. This research was thus aimed at investigating methods for destruction of the organics in the backwash water stream using the semiconductor photocatalyitc process. The feasibility of the proposed process is compared with other known organic pollutant removal processes such as GAC adsorption, ozonation, and ultrasonic (UV) cavitation.

1.2 Rationale

Studies conducted in the year 1996 on behalf of the Department of Water Affairs and Forestry (DWAF) projected that, by the year 2025, South Africa will be expecting severe water shortage (Basson et al., 1997). This projection was based on the impacts of population growth and urbanisation, and the semi arid climatic conditions of the region. Additionally, increased urbanisation and industrialisation increases the pollution in the natural water bodies thereby reducing the amount of available clean water supply sources.

1.2.1 Impacts of Pollution

The quality of drinking water has dramatically declined over the years due to agricultural, municipal and industrial pollution (Jyoti & Pandit, 2001). Poor quality water sources include eutrophied surface water (from dams), previously wasted filter backwash water and industrial

wastewater. Supplementing fresh water supply by recycling treated wastewater is a trend that is rapidly gaining acceptability but its practise is limited by the problems of accumulation of toxic organic pollutants in industrial and municipal wastewaters; and the presence of taste and odours caused by microbial metabolites geosmin and 2-methylisoborneol (2-MIB). In a survey conducted by Wnorowski (1992) on South African water bodies it was observed that 30% of the water bodies examined had odour problems and 50% of these problems were attributed to geosmin.

The taste and odour compounds *trans*-1,10-dimethy-*trans*-9-decalol (geosmin) and 2-MIB are volatile tertiary alcohols that are produced by secondary metabolites of actinomycetes and cyanobacteria (Zaitlin and Watson, 2006; Sung et al*.,* 2005,). These compounds are responsible for the musty and earthy odours in drinking water even at trace concentrations in the ng/ℓ range. For example, odour is detectable in samples at concentrations as low as 1.3 ng/ℓ and 6.3 ng/ℓ for geosmin and 2-MIB, respectively (Lloyd et al., 1998; Young et al., 1996).

Although there is no proven toxicity resulting from contamination with geosmin and 2-MIB, consumers judge the quality of the water primarily on the aesthetic characteristics. If the water is not appealing in appearance, taste or odour, it may result in psychosomatic illnesses such as stomach upsets, headaches and stress (Lauderdale et al., 2004). South Africa has no clear sensory quality standards with regards to taste and odour; instead the term “not objectionable” has been previously used (Pieterse, 1989; le Roux, 1988).

Due to their complex tertiary structure, both geosmin and 2-MIB motifs (Figure 1.1) are resistant to oxidation by ozone ($O_{3)}$ and other aquatic oxidants (Ho et al., 2007; 2002). They are resistant to chlorination even at high dosages (Lalezary et al., 1986). For this reason, the conventional physical-chemical processes have not been used successfully for treating these compounds.

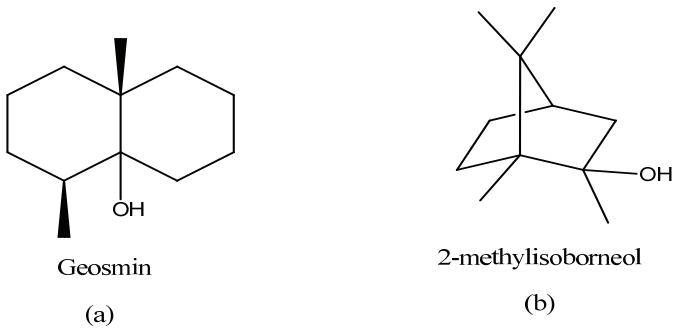

Geosmin (a) 2-methylisoborneol (b)

Figure 1.1: Structures of (a) geosmin and (b) 2-MIB

Although South Africa has no clear sensory quality standards for taste and odour in potable water, consumer complaints resulted in a survey of water bodies in South Africa in the early 1990s, which revealed that 30% of water bodies examined had odour problems and 50% of these problems were attributed to geosmin (Wnorowski, 1992).

The situation has grown worse over the years with one of the worst cases in recent years experienced by Rand Water between September and November 2005, where high

cyanobacteria concentrations in the source water resulted in high concentrations of geosmin in drinking water with a resultant consumer rejection (Swanepoel and Du Preez, 2006).

1.2.2 Impacts of Natural Occurring Organic Materials

Humic compounds, also known as natural organic materials (NOMs), occur widely in soil, water and sediments. They play a key role within several natural processes such as the global carbon geochemical cycle and the transport of organic and inorganic pollutants across the environmental compartments (Fiorentino et al*.,* 2006). Humic substances (HS) are high molecular weight materials resulting from the oxidative decomposition of plant and animal residues (Halmann, 1996). Humic substances, being the main component of NOM, are a major component of natural waters, with approximately 40-60% of dissolved organic carbon (DOC) in freshwaters occurring as HS (Smejkalova and Piccolo, 2005).

Humic acid is a major component of humic substances contributing significantly to soil chemistry and surface water chemistry; it is the fraction of humic substances that is not soluble in water under acidic conditions (pH < 2) but is soluble at higher pH values. Humic acids are sub classified into tannins, lignins and fulvic acids, and are currently believed to be supramolecules consisting of relatively small heterogeneous molecules held together mainly by weak dispersive forces (such as van der Waals, *π*-*π*, CH-*π* and hydrogen bonding), in large molecular dimensions (Smejkalova and Piccolo, 2006; 2005; Piccolo et al*.,* 2005; 2003).

Humic substances are endowed with acidic functional groups - mainly carboxylic acid - which confer on these molecules the ability to chelate multivalent cations such as Mg^{2+}, Ca^{2+}, and Fe^{2+}. These properties of humic substances have been recognised to influence the binding and transport of pesticides and other apolar organic compounds. Humic acids also have a smaller fraction of phenolic functional groups (Fiorentino et al*.,* 2006). By chelating the ions, they facilitate the uptake of these ions by several mechanisms, including preventing their precipitation, and have a direct influence on their bioavailability. From an environmental context, humic substances present in natural waters can increase the apparent solubility of non-polar compounds (Misra *et al* 1998).

The presence of humic acid in water intended for potable or industrial use can have a significant impact on the treatability of the water and the success of chemical disinfection processes, as they are known to have long residence times in the aquatic environment. These also contribute to the formation of disinfectant by-products (DBPs) as described above (US EPA 2006).

Cyanobacteria (blue-green algae) infested water presents several challenges to the water treatment process. These include a high concentration of non-floc forming solids, exopolysaccharides (EPS), taste and odour causing metabolites, and a wide array of phytotoxins. Some of these toxins are known to attack the liver (hepatotoxins) or the nervous system (neurotoxins); others attack the cells (cytotoxins) and can be limited to causing superficial symptoms such as skin irritation (endotoxins). Some treatment methods that cause cell rupture exacerbate the toxicity in the water by rupturing and releasing more cytotoxins into the water (Harding and Paxton, 2001).

An example of a phytotoxin from blue-green algae is the microcystins produced in the cyanobacteria *Microcystis aeruginosa*. Microcystins are the most common of the cyanobacterial toxins found in water, as well as being the ones most often responsible for animal and human poisoning, causing acute to sub acute liver toxicity (Harding and Praxton, 2001). Over 50 different species of microcystins have been identified with microcystin-LR (Figure 1.2), being the most commonly found and potentially toxic species in water supplies around the world (Carmichael, 2001; WHO, 1999).

1.3 Current Status of Filter Operations in Gauteng

Successful filtration at water treatment plants is dependent on the suspension load of the source water arriving at the filters and the condition of the filters. Clogged filters usually reduce the efficiency of the filtration process. Clogging of filters occurs with use and clogged filters are regenerated by flushing out particles imbedded in the filter media by the backwashing of filters.

Backwashing of clogged filters comprises of two steps. The first step involves the scouring of the dirt or thin mud layer on the filter media by a stream of air from below the filter media bed. The second step involves washing out the dislodged particles now suspended in water between the filter media with a stream of fast flowing water. In most treatment plants, especially those treating water from dams and impoundments, up to 6% of the treated water is used for backwashing the filters and is customarily wasted without reclamation. This is the situation at Roodeplaat and Rietvlei Water treatment plants, the plants under study.

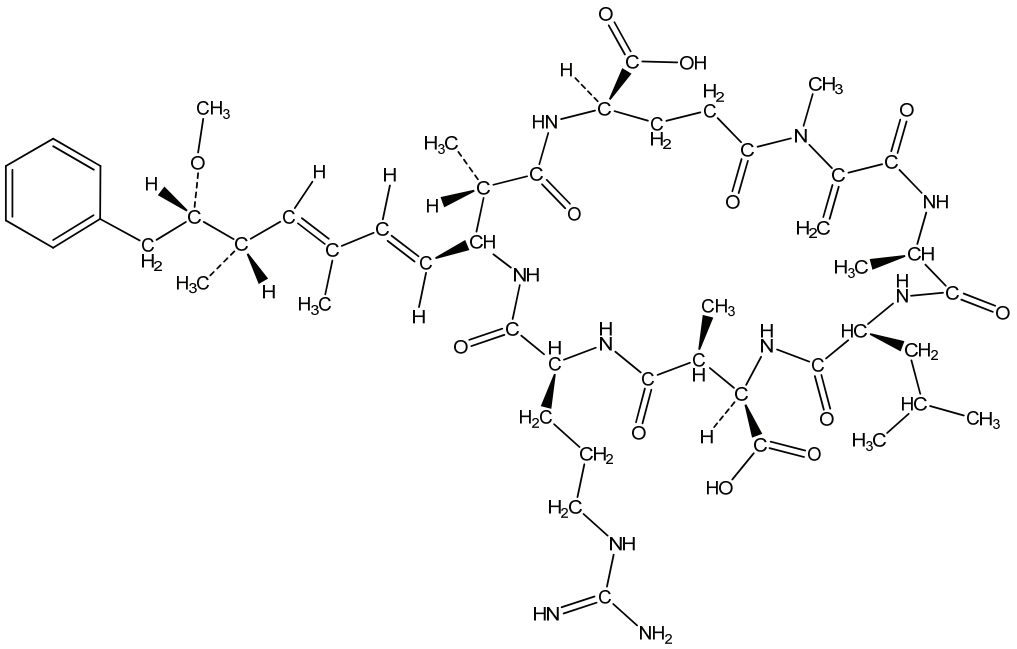

Figure 1.2: Structure of Mycrocystin-LR

1.3.1 Filter operations at the Roodeplaat Water Treatment Plant

Operated by Magalies Water, Roodeplaat Water Treatment Plant treats and supplies an average of 60 Mℓ/Day to Montana and suburbs in Pretoria North. The plant treats highly eutrophied water from the Roodeplaat Dam, which is fed by the Apies River. Less than 1 km

from the water treatment plant is the Zeekoegat Wastewater Treatment Plant, which discharges its wastewater into the Roodeplaat Dam.

Water is abstracted from the top two of five abstraction levels of the dam at a 50:50 ratio. The top level contains highly eutrophied water while the second level (10 m below top level) has an average metal content of 150 mg/ℓ. The plant operates eight rapid gravity sand filters, each with two filter bays with an area of 38 m^2 providing a combined filter area of 600 m^2. Each filter contains an average of 1150 mm filter media comprised of 150 mm of 4-8 mm pebbles, 100 mm of 2-4 mm grit and a 900 mm layer of sand with grain size of 0.6-1.35 mm. Filters are backwashed when any of the following occur:

- Filters reach the terminal headloss.
- Filtrate quality deteriorates below acceptable limits.
- The filtration period exceeds an acceptable maximum of 30 hours.

Each of the two filter bays in the filters is backwashed independently, with air at a rate of 7.5 mm/s and water at a rate of 7.5 mm/s. Filters are fitted with online headloss sensing devices, turbidity meters and time sensors that record time interval between individual filter backwashing cycles.

In practice, filters are automatically backwashed on a 30 hourly cycle (or at 45% of the filter capacity). However, during algal blooms, backwashing is carried out more frequently – on 10-hourly cycles or less during summer – to remedy clogging of the filters.

After each backwash cycle the filters are filtered to waste for one minute to ensure the complete removal of residual particles. The filter backwash water is collected in the collecting pond and allowed to settle. The supernatant is recycled to the feed water from the dam at a ratio of 1:30 (i.e. 2 Mℓ/60 Mℓ from the dam). The monthly backwash water volume for 2007 is presented in Table C-1 in Appendix C.

1.3.2 Filter Operations at Rietvlei Water Purification Works

The Rietvlei Water Purification Plant treats highly eutrophied water from the Rietvlei Dam and supplies water to some parts of Pretoria East and suburbs. The treatment plant is situated about 40 km away from the Hartbeeshoek Wastewater Treatment Plant operated by ERWAT.

The water treated in the plant is abstracted from the middle of three abstraction levels in the dam as the top level contains highly eutrophied water and the bottom level has high metal content. The plant treats an average of 40 Mℓ/Day and operates two independent filter types. The filtration system consists of 10 DAFF (dissolved air floatation filtration) filters of sand and anthracite filter media with an average filter media height of 1098 mm, and 20 GAC (granular activated carbon) filters consisting of 12 x 14 mesh carbon filter beds with an average filter media height of 1165 mm. The filters are backwashed when the turbidity of the filtered water approaches 0.3 NTU. An average of 130 (DAFF) and 44 (GAC) filter backwash operations are conducted weekly resulting in 12-hourly wash cycles for the DAFF filters and a 24-hour cycle for the GAC filters. The backwash water is sent to a sludge tank to settle; where after

the supernatant is discharged into the river. The monthly volume of water that was used in 2007 to backwash the DAFF and GAC filters is presented in Table C-1 in Appendix C.

1.4 Main Objective

The main objective of this study was to evaluate the potential of photocatalysis as a technology for treating backwash water at water treatment plants utilising highly eutrophic raw water sources. This could facilitate the reclamation and recycling of treated backwash water at a lower risk of accumulating natural and anthropogenic organic compounds, which serve as precursors for DBPs during disinfection.

1.5 Specific Tasks

The main tasks conducted to achieve the project objective included:

- Identification and quantification of natural and anthropogenic organic pollutants in raw and filter backwash water at two treatments around Pretoria.
- Evaluation of the performance of a laboratory scale treatment unit employing a chemical free photocatalytic system for the complete degradation of environmentally significant concentrations of taste and odour compounds in filter backwash water.
- Detailed kinetic analysis of the photocatalytic degradation of two taste and odour causing compounds to obtain parameters for possible use in future scale-up design.
- Cost and efficiency comparison with other known chemical oxidation technologies such as O_3 and Photo-Fenton systems.

CHAPTER TWO

2 ADVANCED OXIDATION PROCESSES

2.1 Background

An increasing number of organic molecules (natural and synthetic), often refractory to microorganisms, are detected in industrial and municipal wastewater streams. Some of these compounds inevitably find their way into surface water used as source water for potable uses. A significant component originating from anthropogenic sources such as pesticides, aromatic compounds from industrial effluent or pharmaceuticals; are often found in drinking water sources and could be potential human and animal health hazards. The effectiveness of the conventional water treatment systems in removing these compounds has become limited in light of the present challenges (Zhou and Smith, 2002). In addition to the anthropogenic aromatic compounds, vegetation and phytoplankton contribute humic acid substances that mimic these compounds (Huang et al., 2006).

The search for newer and cleaner treatment technologies to handle these challenges has led to the development of some advanced treatment methods collectively referred to as advanced oxidation processes (AOPs) (Comninellis et al., 2008; Stasinakis, 2008; Modrzejewska et al., 2007; Ljubas, 2005). Recent research has tended towards the application of advanced oxidation processes for the treatment of recalcitrant organic pollutants in water. This is reflected by the increasing number of research articles published on the application of AOPs for the degradation of a wide range of organic and inorganic pollutants in water (Li et al., 2008; Auguglisto et al., 2006; Klán and Vavrik, 2006; Bahnemann, 2004; Von Gunten, 2003; Andreozzi et al., 2000; Zhou and Smith, 2002). The immense interest in AOPs can be attributed to the diversity of technologies involved, the level of success achieved by laboratory studies and the variety of areas of potential application and commercialisation.

Advanced oxidation processes are processes that utilise the oxidative potential of reactive oxygen species such as hydroxyl radicals ($^{\bullet}OH$) or superoxide ($O_2^{-\bullet}$), generated from the reduction of water or oxygen molecules in water. The radicals are in turn used to degrade organic and inorganic pollutants or for 'contact disinfection' of water by destroying potentially harmful microorganisms. The hydroxyl radical is the most powerful oxidising agent after fluorine, with an oxidation potential of 2.80 V. This exhibits faster oxidation rates than conventional oxidants such as H_2O_2 or $KMnO_4$ (Gogate and Pandit, 2004; Mills and Lee, 2004). The oxidation potentials of commonly used oxidants are presented in Table 2.1.

Table 2.1: Oxidation potentials of some commonly used oxidants

Oxidant	Oxidation Potential (V)
Fluorine (F)	3.03
Hydroxyl Radical ($^{\bullet}OH$)	2.80
Ozone (O_3)	2.07
Hydrogen Peroxide (H_2O_2)	1.78
Potassium Permanganate ($KMnO_4$)	1.68
Chlorine	1.36

Hydroxyl radicals are reactive electrophiles that are very effective in the destruction of organic compounds because they react rapidly and non-selectively with most electron rich organic compounds. Advanced oxidation processes are characterised by their catalytic, photochemical properties and oxidative degradation reactions (Maciel et al., 2004). Due to their instability and transient nature, hydroxyl radicals are used *in situ* (Esplugas et al., 2002; Munter, 2001).

Various reactions are classified under the broad term of AOPs. The differences in the various methods lie in the mechanism of hydroxyl radical generation. These classes include the photolytic systems, chemical systems, photochemical systems and physical systems as illustrated in Figure 2.1.

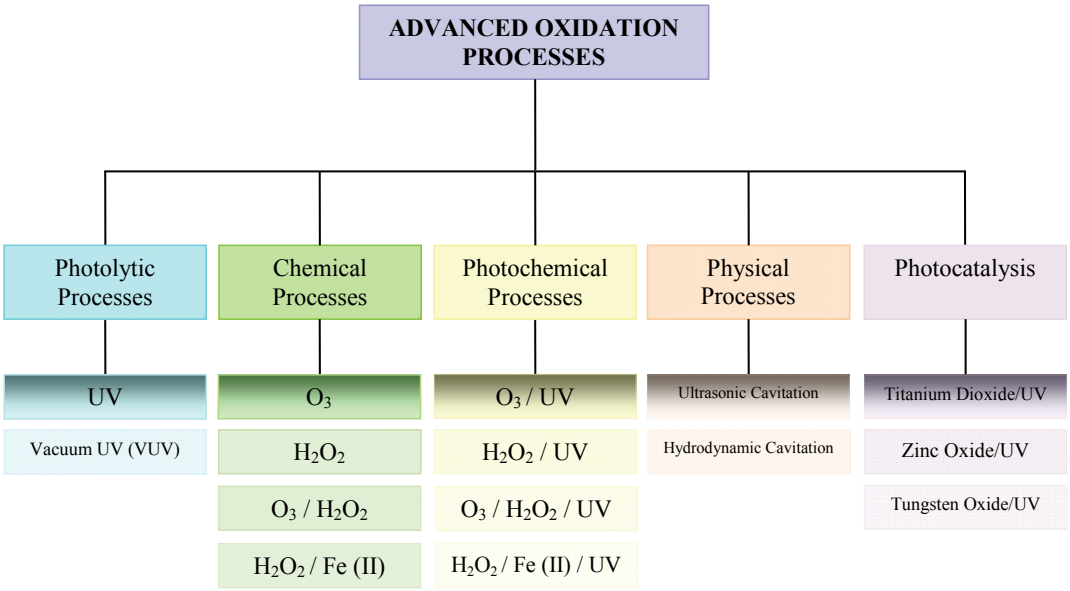

Figure 2.1: Classification of advanced oxidation processes

2.2 Photolytic Processes

Photolytic systems initiate pollutant degradation directly or indirectly by the absorption of UV radiation, either from artificial sources or from solar energy. Energy supplied by absorbed photons of light enables excitation of reactant molecules to promote degradation reactions (Parsons and Williams, 2004). In direct photolysis, the organic compounds absorb UV light, a procedure that either enables them to react with the constituents of water or induce self-decomposition. Indirect photolysis involves the photodegradation of organic compounds caused by photosensitisers like oxygen and hydroxyl or peroxy radicals produced by the photolysis of humic and inorganic substances (Giokas and Vlessidis, 2007). Sunlight induced photochemical reactions are considered as the most important abiotic processes that determine the fate of organic compounds in natural waters. Both direct and indirect photolytic processes occur in the surface layers of aquatic systems (Giokas and Vlessidis, 2007).

Application of photolysis for organic pollutant degradation has found limited application due to the lower efficiency of the photolytic systems compared to other advanced oxidation processes. Another major drawback in the use of photolysis for treating complex organic

compounds is the production of harmful intermediates, as complete mineralisation is often not achieved. Buchanan et al. (2006) in their study of UV and vacuum UV (VUV) irradiation of natural organic matter; concluded that UV or VUV photolysis cannot be used as stand alone methods. Their conclusion was based on the formation of potentially hazardous by-products due to UV radiation. Zoh et al. (2009) studied photolysis of triclosan and also concluded that UV photolysis alone was not an effective system for triclosan degradation as harmful intermediates of the dioxin type were produced. Both groups of researchers suggested that UV irradiation could be used as a pre-treatment to biological treatment. This suggestion was based on evidence of appearance of breakdown compounds of lower molecular weight compounds (Buchanan, 2004).

2.3 Chemical Processes

The oldest systems are the chemical based systems that utilise a single oxidant for the degradation of pollutants. Such systems include the ozonation systems and the hydrogen peroxide (H_2O_2) systems. A search for improvement of the degradation efficiencies of these traditional chemical processes gave rise to the hybrid chemical systems which use a combination of two or more oxidants for pollutant degradation. The hybrid chemical based systems often used for pollutant degradation in aqueous systems include the H_2O_2 and O_3 system (peroxone, or O_3/H_2O_2) and the use of Fenton's reagent. Fenton's reagent is a combination of H_2O_2 and ferrous ions (Fe II). These systems have shown higher efficiencies due to accelerated hydroxyl radical generation mechanisms. A brief description of each of the chemical systems highlighting their advantages and major drawbacks is presented below.

2.3.1 Ozonation

Ozone is a very reactive gas that is sparingly soluble in water (Zhou and Smith, 2002; Shin et al., 1999). The mechanism of pollutant decontamination by O_3 in water treatment can occur by the direct reaction between O_3 and the dissolved organic species, by reaction between generated hydroxyl radicals and the dissolved pollutants, or by a combination of both (Von Gunten, 2003, Shin et al., 1999). Direct reaction between O_3 and organic compounds is selective, occurring at sites with high electronic density. On the other hand, hydroxyl radicals are non selective oxidants. Ozonation systems would therefore be more effective for the degradation of highly unsaturated compounds such as alkenes, alkynes and amines. However, other organic compounds such as aliphatic carbon chains, amides, and nitroso compounds are not effectively oxidised by O_3. Oxidation of O_3-resistant compounds can be improved by irradiation of the system with UV or addition of H_2O_2, which enhances $^{\bullet}OH$ production by accelerating O_3 decomposition (Rosal et al., 2009; Lee et al., 2007; Beltrán et al., 2002).

In depth studies by Nadezhdin (1988), Bühler et al. (1984) and Staehelin and Hoignè (1985) gave an insight to the mechanism of O_3 decomposition in water, which they postulated occurs via a radical chain mechanism, producing intermediate species including hydroxyl radicals. Ozone decomposition is initiated by single electron transfer from hydroxide ions (Equation 2.1), which is favoured at higher pH (Bühler et al., 1984; Staehelin and Hoignè, 1985).

The process can be artificially accelerated by increasing the pH of the medium or by the addition of H_2O_2. However, high pH values and very high $^{\bullet}OH$ concentration promote decomposition of O_3 back to oxygen (Equation 2.6). The decomposition process also depletes hydroxyl radicals in solution. In light of the possible decomposition, careful balance of pH of the medium is required and optimal utilisation of molecular ozonolysis and free radical reaction with organic compounds is best achieved at a neutral pH range (Stockinger et al., 1996). The following are the key reactions for O_3 oxidation.

$$O_3 + OH^- \rightarrow HO_2 + O_2^- \quad (2.1)$$
$$HO_2 \leftrightarrow H^+ + O_2^- \quad (2.2)$$
$$O_2^- + O_3 \rightarrow O_2 + O_3^- \quad (2.3)$$
$$O_3^- + H^+ \rightarrow HO_3 \quad (2.4)$$
$$HO_3 \rightarrow O_2 + {}^{\bullet}OH \quad (2.5)$$
$$O_3 + {}^{\bullet}OH \rightarrow HO_2 + O_2 \quad (2.6)$$

The radical chain process could be inhibited or terminated by the presence of organic or inorganic species in water, acting as inhibitors or radical scavengers (Staehelin and Hoignè, 1985). Important initiators include OH^-, H_2O_2, UV radiation, photocatalyst, and some metal ions, while the main scavengers are carbonate and bicarbonate ions. As scavengers, presence of carbonate and bicarbonate ions in solution would reduce the efficacy of oxidation of pollutant molecules by ozonation.

One of the major drawbacks with ozone as an oxidant is its low solubility in water. Another is the cost of generating ozone in sufficient quantities for use as an oxidant for the complete degradation of organic compounds. Mass transfer limits the use of O3 in water treatment and engineering solutions to increasing the mass transfer rates would further enhance its effectiveness as an oxidant (Von Gunten, 2003; Shin et al., 1999).

Proposals to enhance the potential viability of the system include the integration of ozonation and a biological (post ozonation) system (Contreras et al., 2003). Ozone is considered a promising alternative to chlorine for disinfection of water. Promising as the process is, there are some potential hazards due to the conversion of bromide ions in water to bromate ions by O_3 (Michalski, 2003; Zhou and Smith, 2002).

The presence of bromate ions in water is as undesirable as the other DBPs, THMs and HAAs, especially as bromate ions are not degraded by the biological filtration process (Von Gunten, 2003). The International Agency for Research on Cancer (IARC) classified bromate in group B-2 (as a “probable human carcinogen”) and established a drinking water maximum contaminant level goal (MCLG) of zero; and maximum contaminant level of 10 µg/ℓ for bromate in drinking water (Michalski, 2003).

Despite the mass transfer limitations, research into the degradation of organic compounds by O_3 is a very active field and the ozonation of several organic compounds has been studied. Ozonation is one advanced oxidation method that has been widely applied in water treatment or pre-treatment systems, and as at 2002; over 4000 ozonation plants were already in operation globally (Zhou and Smith, 2002) with the expectation that several others would have been installed by 2010 considering the volume of research in the field.

2.3.2 Hydrogen peroxide systems

The effectiveness of the oxidation process is the ready availability of the oxidant specie in solution. Hydrogen peroxide though a moderately strong oxidant; has limited application on its own as an oxidant for the degradation of complex organic compounds. Its use alone is not effective due to kinetic limitations at reasonable peroxide concentrations. On the other hand, aqueous H_2O_2 decomposes over heterogeneous catalysts including metals (i.e. Fe, Cu, Pt, Ti, and Ni) and metal oxides immobilised on various support materials such as sand, silica, zeolites, and alumina (Kitis and Kaplan, 2007). Improvement of the oxidative capacity of H_2O_2 can be achieved by combining H_2O_2 with O_3 or with UV radiation or some transition metal salts. These hybrid chemical systems exhibit better oxidative properties due to the decomposition of H_2O_2 to release hydroxyl radicals as shown in Equation 2.7.

2.3.3 Ozone / hydrogen peroxide (peroxone) systems

The O_3/H_2O_2 system generates hydroxyl radicals by a radical chain mechanism resulting from interaction between O_3 and H_2O_2 as shown in Equation 2.7.

$$H_2O_2 + 2O_3 \rightarrow 2^{\bullet}OH + 3O_2 \qquad (2.7)$$

The O_3/H_2O_2 system is much more efficient than using O_3 alone for the removal of organic compounds from water, with better chances of complete mineralisation of both target pollutant and degradation intermediates formed in solution. Rosa et al. (2009) reported increased efficiency of the O_3 system used to degrade organic matter in effluent from secondary clarifier by the addition of H_2O_2. They observed increase in extent of mineralisation, from below 35% (O_3 alone) to 75-100% on the injection of H_2O_2 into the O_3 system. The efficiency of the O_3/H_2O_2 system can be further improved by incorporation of a UV radiation source.

2.3.4 Fenton reagent (H_2O_2/Fe(II))

The Fenton process is increasingly used in the treatment of organics in water and soil. Fenton reagent is a catalytic oxidative mixture that usually contains an oxidant (usually H_2O_2) and a catalyst (a metal salt or oxide, usually ferrous salts). Decomposition of H_2O_2 by Fe^{2+} ions in solution spontaneously produces extremely reactive and non-selective hydroxyl radicals (Raj and Quen, 2005; Wadley and Waite, 2004; Munter, 2001). The chemistry of the process is presented in Equations 2.8-2.14. The Fenton process is often modified by the use of ferric ion, which acts as a catalyst in the decomposition of H_2O_2 into H_2O and O_2 (Equations 2.9-2.14).

$$Fe^{2+} + {}^{\bullet}OH \rightarrow Fe^{3+} + OH^{-} + {}^{\bullet}OH \qquad (2.8)$$
$$Fe^{3+} + H_2O_2 \rightarrow [Fe\text{---}OOH]^{2+} + H^{+} \qquad (2.9)$$
$$[Fe\text{---}OOH]^{2+} \rightarrow Fe^{2+} + HO_2^{\bullet} \qquad (2.10)$$
$$Fe^{2+} + HO_2^{\bullet} \rightarrow Fe^{3+} + HO_2^{-} \qquad (2.11)$$
$$Fe^{3+} + HO_2^{\bullet} \rightarrow Fe^{2+} + H^{+} + O_2 \qquad (2.12)$$
$$^{\bullet}OH + H_2O_2 \rightarrow H_2O + HO_2^{\bullet} \qquad (2.13)$$
$$2HO_2^{\bullet} \rightarrow H_2O + O_2 \qquad (2.14)$$

The mechanism of the Fenton reactions is not completely understood and the reactions presented by Equations 2.8-2.14 do not take into account other species that may be present in the solution. The use of ferric ions produces Fe (II) ions *in situ*, which in turn reacts with H_2O_2 to produce more hydroxyl radicals. This could be used to avoid high concentrations of Fe (II) ions in the reaction vessel. In this reagent Fe (II) can be replaced by other metal ions and their complexes in the lower oxidation states although their application is limited due to the relative toxicity of some of these metal ions (Wadley and Waite, 2004). These metal ions have the oxidative features of the Fenton reagent and are collectively called Fenton-like reagents. They include Cu(I), Cr(II), CO(II) and Ti(III).

The main advantages of the Fenton process include: (i) the relative very low cost of the key reagents (H_2O_2 and iron salts) as iron is highly abundant and non-toxic, and dilute solution of H_2O_2 is easy to handle and environmentally friendly (Momani et al., 2004; Wadley and Waite, 2004); and (ii) the relative simplicity of the process, requiring neither special reagents nor apparatus (Andreozzi et al., 1999). The limitation in the Fenton system is the narrow pH range of efficient application (pH 2-4, but best at 2.8); hence it is not efficient in the pH range of natural waters. This is due to the tendency of ferric hydroxide precipitation at pH > 3. The precipitation can be controlled by the addition of some organic ligands, which can complex Fe(III) and enable the process to be carried out at higher pH values (Wadley and Waite, 2004 and references therein).

2.4 Photochemical Processes

The photochemical processes incorporate high powered chemical oxidant(s) and UV radiation from a light source. These usually show improved efficacy compared to the corresponding chemical systems due to accelerated production of the hydroxyl radicals in the presence of radiation. Photochemical processes include the O_3/UV system, the H_2O_2/UV system, the O_3/H_2O_2/UV system and the photo Fentons (Fe(II)/H_2O_2/UV) System.

2.4.1 Ozone/Ultraviolet system

The energy supplied by UV radiation interacts with O_3, which then readily absorbs at 254 nm to produce hydroxyl radicals. Hydrogen peroxide is believed to be produced as an intermediate species, which decomposes to produce hydroxyl radicals.

$$O_3 + H_2O + h\nu \rightarrow 2^{\bullet}OH + O_2 \qquad (2.15)$$

If water solutions contain organic compounds that strongly absorb UV light, then UV radiation usually does not give any additional effect to O_3 due to the screening of O_3 from the UV light by optically active compounds (Munter, 2001). The most common lamp used for the UV/O_3 is the low-pressure, mercury vapour lamp (LPUV) which emits radiation at 253.7 (254) nm.

2.4.2 Ultraviolet/ Hydrogen peroxide

Ultraviolet light source provides energy to photolyse H_2O_2 to hydroxyl radicals with a quantum yield of two $^{\bullet}OH$ per quantum of radiation absorbed. The photodecomposition of H_2O_2 is the most direct and efficient technique for the generation of the hydroxyl radical

(Hernandez et al., 2002). Reaction is pH and temperature dependent and it is self-limiting since H_2O_2 reacts with $^{\bullet}OH$ to produce $HO_2^{\bullet}$ and H_2O_2. This is illustrated by the following reactions.

$$H_2O_2 + hv \rightarrow 2^{\bullet}OH \quad (2.16)$$

$$H_2O_2 + {}^{\bullet}OH \rightarrow H_2O + HO_2^{\bullet} \quad (2.17)$$

$$2HO_2^{\bullet} \rightarrow H_2O_2 + O_2 \quad (2.18)$$

Where *hv* = quantum energy from UV light source with radiation 254nm (Esplugas et al., 2002; Munter, 2001).

Hydrogen peroxide in Equation 2.17 acts as a radical scavenger. Radical scavenging by H_2O_2 occurs at relatively high peroxide concentrations (Hernandez et al., 2002). Scavenging of hydroxyl radicals in solution would generally reduce the amount of oxidative species present and reduce the degradation efficiency. Therefore there is a limiting H_2O_2 concentration in this system, which should be determined experimentally.

The most common lamp used in the H_2O_2/UV AOP system is the medium pressure mercury vapour lamp (MPUV). It has significant emittance within the 200-250 nm range, which is the primary absorption range for H_2O_2. The production of hydroxyl radicals by the MPUV/H_2O_2 system is affected by several variables including temperature, pH, and concentration of the peroxide and presence of radical scavengers (Hernandez et al., 2002).

2.4.3 Ozone/Hydrogen peroxide/Ultraviolet

The irradiation of O_3/H_2O_2 by UV from solar light or artificial light accelerates the decomposition of both O_3 and H_2O_2, which results in the production of hydroxyl radicals. The synergic effects of O_3, H_2O_2 and UV irradiation make the photo O_3/H_2O_2 system, which is an improvement over the individual oxidants in the degradation of pollutants in water. It is a very powerful method that allows the fast and complete mineralisation of pollutants. It is considered to be the most effective treatment for highly polluted effluents (Esplugas et al., 2002; Munter, 2001).

2.4.4 Photo-Fenton (H2O2/Fe(II)/UV)

The efficiency of the Fenton process is improved by irradiation with UV light. Addition of UV to the Fenton system leads to the formation of additional hydroxyl radicals and recycling of the ferrous catalyst by the reduction of Fe(II). The increased efficiency of this process is mainly attributed to the photo reduction of ferric ion (Momani *et al*; 2004).

2.5 Physical Processes

Hydroxyl radicals are also generated by the physical process of cavitation. Cavitation is the formation, growth and implosion of microbubbles or gaseous cavities within a liquid. It is also called “nucleation of bubbles” (Dupree et al., 1998). Its use in water and wastewater treatment is a concept that is relatively new and still under investigation.

Cavitation is accompanied by adiabatic heating of the vapour phase inside the bubbles resulting in very high local temperatures and pressures in millions of such locations within the reactor. The effective local temperature and pressure at these transient ‘hot spots’ in

water may exceed 5000K and 50 atmospheres, respectively; (Hassoon et al., 2004). The violent collapse of cavities results in the formation of reactive hydrogen atoms and hydroxyl radicals which combine to form H_2O_2 to some extent and are responsible for promoting oxidation reactions (Findik et al., 2006; Mason and Pétrier, 2004; Gogate et al., 2003). Cavitation can also lead to cellular damage in microorganisms (Jyoti and Pandit; 2001). Cavitationally induced metal corrosion (Chen et al., 2006) may be a major factor that would limit the wide application of cavitation for water treatment, as it would be an engineering challenge during reactor design. Cavitation in a liquid can be brought about by the application of ultrasonic waves or by hydrodynamic means.

2.5.1 Ultrasonic cavitation

Ultrasonically induced cavitation, also called acoustic cavitation, is defined as the formation, growth and collapse of gaseous or vaporous bubbles under the influence of ultrasound (Liang et al., 2006). In acoustic cavitation high frequency sound waves in the range of 16 kHz-100 MHz are often required to bring about cavitational inception. Alternate compression and rarefaction cycles of the sound waves results in various phases of cavitation such as generation of the bubble cavity, growth phase and finally collapse phase releasing large amount of energy locally. The oxidation of contaminants by acoustic cavitation is thought to progress via two mechanisms – free radical attack and pyrolysis (Gogate and Pandit, 2004; and references therein).

2.5.2 Hydrodynamic cavitation

Bubble creation and collapse in hydrodynamic cavitation is brought about by hydraulic devices. In such systems cavitation is generated due to pressure variations in a flowing liquid caused by changes in the geometry of the flow system (Gogate and Pandit, 2004; Jyoti and Pandit, 2001). Pressure variations are created by the passage of the liquid through constrictions such as valves and orifice plates. Intensity of cavitation generated by hydraulic devices is lower than that of acoustic cavitation. On the other hand hydrodynamic cavitation has higher efficiency and cavitational yields compared to acoustic cavitation (Gogate and Pandit, 2001).

2.6 Semiconductor Photocatalysis

Semiconductor photocatalysis involves the photo-excitation of a solid semiconductor as a result of the absorption of electromagnetic radiation often in the near UV spectrum. The electronic structure of most semiconductor materials comprises a highest occupied band full of electrons called the valence band (VB) and a lowest unoccupied band devoid of electrons, called the conductance band (CB). The VB and the CB are separated by a region that is devoid of energy levels; the energy difference between the two bands is called the band gap energy (E_{bg}) (Bahnemann, 2004; Mills and Lee, 2004; Sumita et al., 2001).

Activation of a semiconductor photocatalyst is achieved through the absorption of a photon (*hv*) of ultra-bandgap energy, which results in the promotion of an electron, e^-, from the VB into the CB with the generation of a hole, h^+, in the VB thus forming an electron-hole pair (h^+ e^-) (Figure 2.2). Excited state CB electrons and CB holes can:

- Recombine either at the surface, or in the bulk of the semiconductor material and dissipate the input energy liberating heat (Δ);
- Get trapped in metastable surface states; or
- Make their separate ways to the surface of the semiconductor material to react directly or indirectly with electron donors and electron acceptors adsorbed on the semiconductor surface, or within the surrounding electrical double layer of the charged particles.

In the absence of suitable electron hole scavengers, the stored energy is dissipated within a few nanoseconds by recombination. If a suitable scavenger or surface defect state is available to trap the electron or hole, recombination is prevented and subsequent redox reactions may occur (Hoffmann et al., 1995).

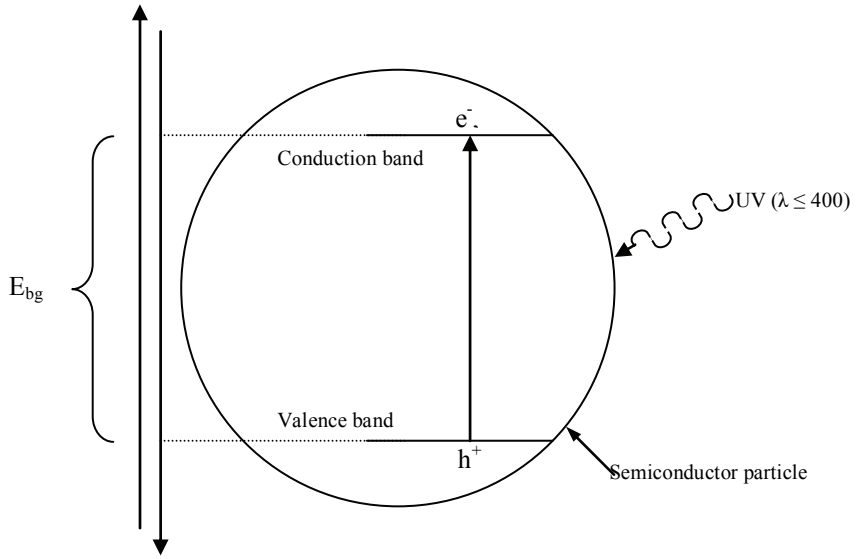

Figure 2.2: Schematic of electron-hole pair formation over a semiconductor particle

Recombination of electron hole pairs reduces the efficiency of the photocatalytic process by reducing the availability of reactive species (Mills and Lee, 2004; Bauer et al., 1999; Hermann, 1999). For a photocatalyst to be efficient, the different interfacial electron transfer processes, involving e^-, and h^+ reacting with adsorbed species must compete effectively with the major deactivation route of electron-hole recombination (Devilliers, 2006; Mills and Lee, 2004; Hoffmann et al., 1995).

Valence bond holes are powerful oxidants, with oxidation potentials of +1.0 to +3.5 V (Bahnemann, 2004; Munter, 2001; Hoffmann et al., 1995). Reactions of photogenerated electron hole pairs on the surface of the photocatalyst occur in the presence of electron donors or electron acceptors adsorbed on the photocatalyst surface. Thus, if there is an electron acceptor, A, then the photo generated electrons can react with A (directly or indirectly) generating a reduced product A^-. Similarly the photogenerated holes that migrate to the surface can react with an electron donor, D; to form an oxidised product D^+. The oxidation and reduction reactions on the surface are summarised in equation 2.19 and illustrated in Figure 2.3.

$$A + D \xrightarrow{\text{semiconducotr } (h\nu \geq E_{bg})} A^- + D^+ \quad (2.19)$$

where: A = electron acceptor, A^- = reduced product, D = electron donor
D^+ = oxidised product.

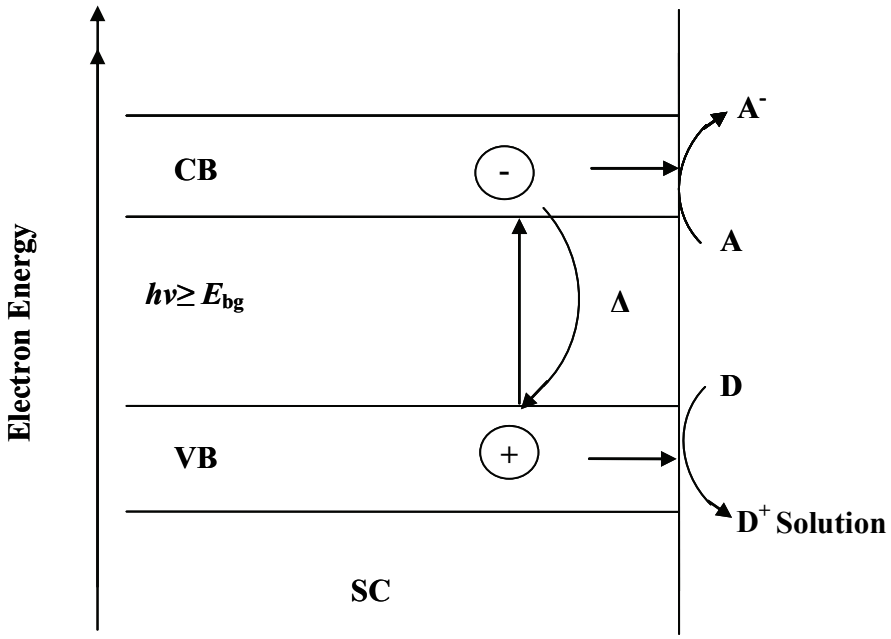

Figure 2.3: Schematic illustration of the Energetics of semiconductor photocatalysis

In water purification, the electron acceptor (A) is oxygen, and the electron donor (D) is the pollutant. The overall process is the photocatalytic oxidation of the pollutant by dissolved oxygen as represented by Equation 2.20.

$$\text{Organic pollutant} + O_2 \xrightarrow{\text{semiconductor } (h\nu \geq E_{bg})} CO_2 + H_2O + \text{Mineral acids} \quad (2.20)$$

The possible processes associated with the electron-hole pair formation and the reactions that occur on a particular photocatalyst are presented in Figure 2.4. Processes depicted by Figure 2.4 include:

(a) Formation of charged carriers (electron – hole pair) by a photon;

(b) Electron-hole recombination in the bulk;

(c) Electron – hole recombination on the surface of the particle;

(d) Direct or indirect reduction of oxygen or oxidizing intermediates by photogenerated electrons on the surface of the catalyst;

(e) Direct or indirect oxidation of pollutant, or an oxidised intermediate by photogenerated hole at the surface of the semiconductor, leading to mineralised products (usually CO_2 and H_2O).

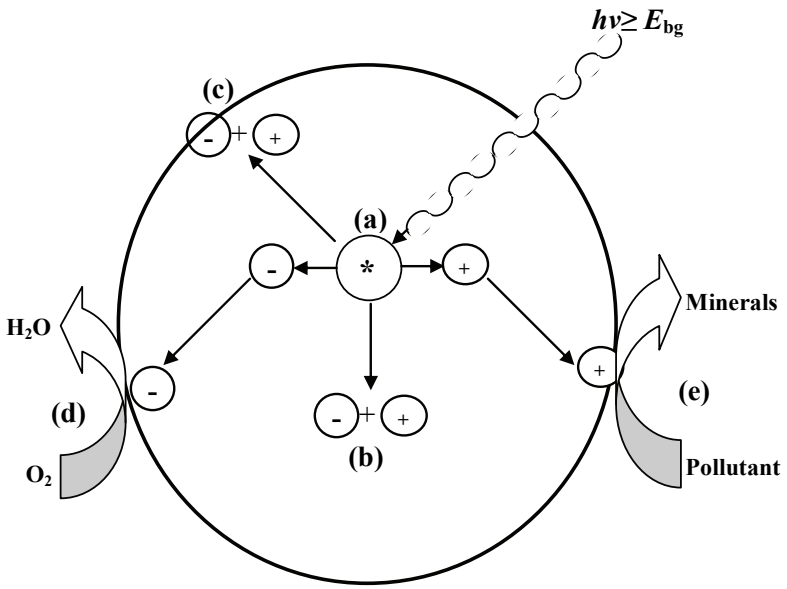

Figure 2.4: Major processes in semiconductor photocatalysis upon ultraband gap illumination

Various metal oxides act as photocatalysts. These include titanium dioxide (TiO_2), zinc oxide (ZnO), molybdenum trioxide (MoO_3), ceric dioxide (CeO_2), zirconium dioxide (ZrO_2), tungsten trioxide (WO_3), ferric oxide (Fe_2O_3), stannic dioxide (SnO_2); and metal chalcogenides including zinc sulphide (ZnS), cadmium sulphide (CdS), cadmium selenide (CdSe), tungsten disulphide (WS_2) and molybdenum disulphide (MoS_2) (Hoffmann et al., 1995; Gogate and Pandit, 2004; Devilliers, 2006). For a catalyst to act effectively as a suitable photocatalyst, it should be:

- Chemically and biologically inert;
- Easy to produce, and use; and
- Photostable

For a semiconductor to be photochemically active as a sensitiser for the reaction shown in Equation 2.20, the redox potential of the photogenerated VB hole must be sufficiently positive to generate absorbed OH radicals. The generated radicals can in turn oxidise the organic pollutants. In addition the redox potential of the photogenerated CB electron must be sufficiently negative to reduce the absorbed oxygen to superoxide (Mills et al., 1993).

No semiconductor available exhibits all of the above requirements but, of all the semiconductors tested in photocatalysis, TiO_2 has proven to be the most suitable for environmental applications.

Figure 2.5 shows some of the semiconductors that have been considered for photocatalytic reactions in water and their associated band gap energies in eV.

Titanium dioxide has a suitable bandgap energy; is biologically and chemically inert; it is stable with respect to photocorrosion and chemical corrosion; non toxic, non carcinogenic; insoluble under most conditions and it is inexpensive. Titanium dioxide does not present any

significant fire hazards or environmental risk. It has been widely reported to give the best catalytic performances and degradation efficiencies, especially in the anatase form (Malato et al., 2007; Gogate and Pandit, 2004; Mills and Lee, 2004; Andreozzi et al., 1999, Mills et al., 1993). Due to the above conditions TiO_2 has become the semiconductor material of choice for photocatalytic processes.

Metal sulphide semiconductors are unsuitable due to their instability as they undergo photoanodic corrosion. The iron oxide polymorphs are not suitable semiconductors, even though they have nominally high bandgap energies and are cheap. Iron compounds readily undergo photocathodic corrosion (Hoffmann et al., 1995).

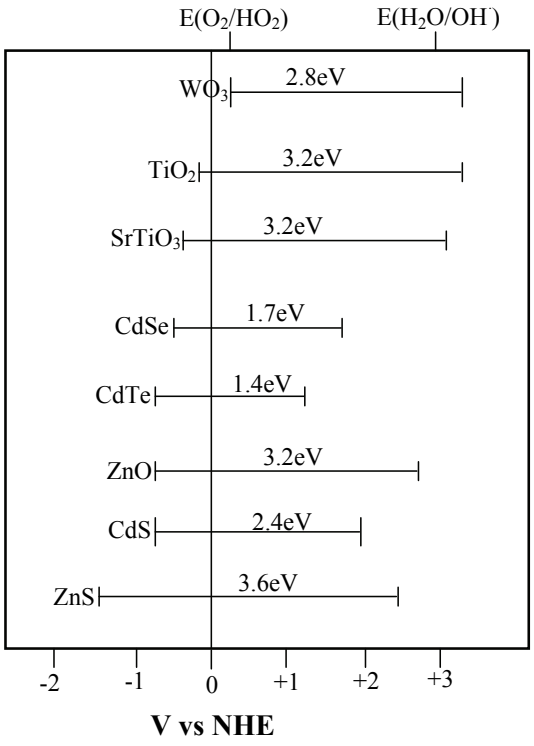

Figure 2.5: Band positions of common semiconductors used in photocatalysis and the redox potential of the $H_2O/^{\bullet}OH$ and $O_2/HO^{\bullet}_2$ redox couples at pH = 0 (Mills et al., 1993)

2.6.1 Titanium dioxide (TiO_2)

Titanium dioxide exists in three crystalline forms, namely anatase, rutile and brookite, but only the anatase forms are reported to exhibit efficient photocatalytic activities. The anatase form is also the easiest to produce. The anatase form of TiO_2 has therefore become the photocatalyst of choice for photocatalytic purification of water.

The threshold wavelength of radiation depends on the band gap energy. Titanium dioxide has large band gap energy of 3.25-3.05 eV (anatase 3.25 eV and rutile 3.05 eV). It can absorb UV light in the range of 380-405 nm, which represents a small fraction of the solar spectrum (approximately 6%). The energy input from the electromagnetic waves in this region is enough to drive the photocatalytic process (Mills and Lee, 2004). The oxidation potential of the photogenerated holes in the VB of anatase attains a value of +2.9 eV vs. Standard Hydrogen Electrode (SHE)/pH 0), which is sufficient for the complete oxidative

decomposition of most of the organic molecules to carbon dioxide and water (Kluson et al., 2005).

Some commercial forms of TiO_2 are now in use and have been reported to be efficient. The most used of these is the P25 Degussa TiO_2, a non porous 70:30% anatase to rutile mixture with a specific surface area (BET) of 55 ± 15 m^2/g and crystalline sizes of 30 nm in 0.1 μm diameter aggregates (Doll and Frimmel, 2005; Hoffmann et al., 1995). Another frequently used form of TiO_2 is the Hombikat UV100 (Doll and Frimmel, 2005).

2.7 Reactor Configurations

A wide variety of reactor configurations has been used in photocatalytic degradation of pollutants in water. Types of reactors include:

- Dispersed catalyst reactors (DCRs)
- Fixed-bed reactors

2.7.1 Dispersed catalyst reactors

In DCRs, the semiconductor catalyst is dispersed in powdered form in the reaction solution containing the pollutant. The apparatus consists of a mixing device, reactor vessel and protected UV lamp; and may be purged with air or oxygen.

The reactor can be illuminated internally (immersion of the UV lamp in the solution) – Figure 2.6(b) – or externally (irradiation of the solution from outside of the reactor, above or below the reactor) – Figures 2.6(a) and (c). Another photoreactor for semiconductor photocatalysis is the annular system, in which the reactor solution passes along the reactor length one or more times – Figure 2.6(d). This reactor configuration is very popular in the water disinfection industry. The annular system is a reverse of the externally illuminated system with multiple lamps arranged parallel to the main axis of flow.

The DCRs are easy to step up since additional photocatalyst preparation is not required. However, a major disadvantage of these slurry reactors is that the semiconductor particles must be separated from the bulk fluid phase after treatment by filtration, centrifugation and flocculation. These additional steps contribute various levels of complexity to the overall treatment process and decrease the economic viability of the slurry reactors (Mills and Lee, 2004; Hoffmann et al., 1995). Some simple commonly used slurry reactor designs are presented in Figure 2.6.

2.7.2 Fixed-bed reactors

This is an alternative configuration which comprises a solid semiconductor coated on an inert substrate. Several inert substrates have been used as a support for coating the solid semiconductor photocatalyst, including glass walls, stainless steel (Chen and Dionysiou, 2006), and glass spiral tubes (Figure 2.7 overleaf). The photocatalyst can also be coated on the outer casing of the light source.

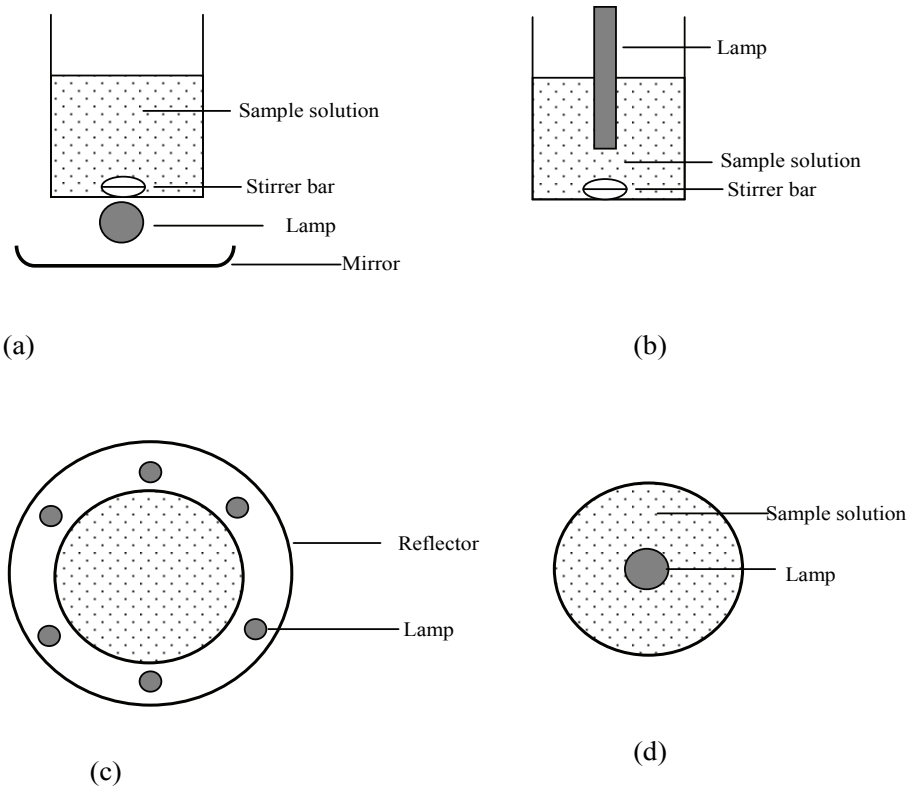

Figure 2.6: Basic photocatalytic DCR designs: (a) side of reactor with external illuminator; (b) side view of reactor with immersed lamp; (c) top view of circular reactor with several lamps; and (d) annular reactor, i.e. tubular reactor with negative illumination geometry. Adapted from Mills and Lee (2004).

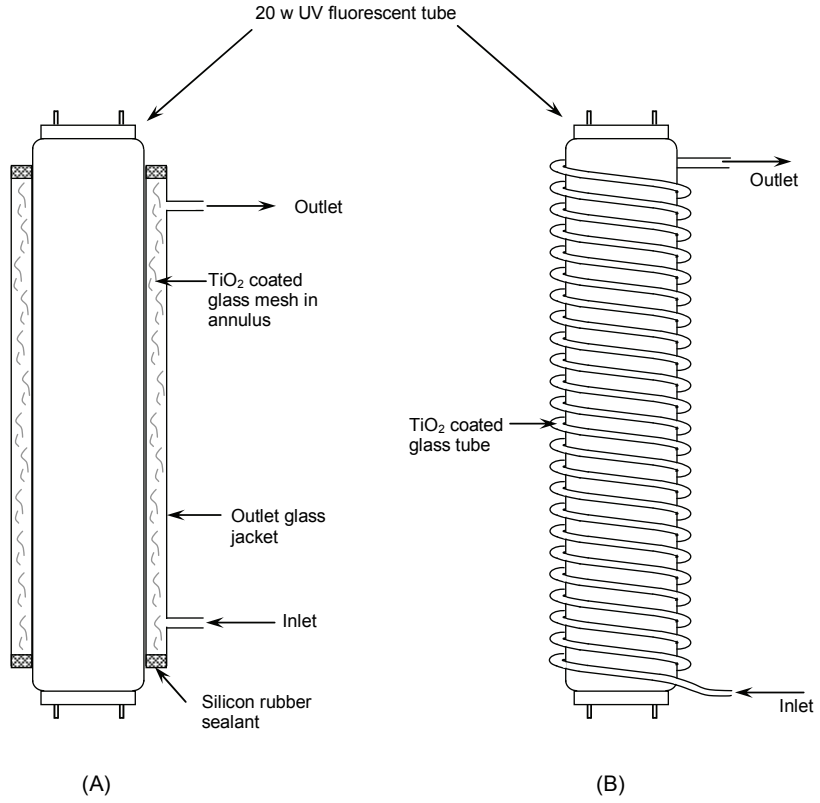

Figure 2.7: Flow reactors (a) comprising TiO_2-coated glass mesh in an annulus between UVA lamp and outer glass wall, and (b) spiral glass tube reactor coated with TiO_2

A major advantage of the fixed-bed reactors is the elimination of the catalyst recovery step. In slurry reactors, the recovery is achieved by filtration, sedimentation or other separation processes.

The limitations of the fixed bed reactors are:

- Low surface area to volume ratios, as fixed beds have limited surface area of the catalyst exposed to the irradiation source;
- Reduction of reaction efficiency due to scattering of light by the reaction medium;
- Poor mixing results in inefficient exposure of pollutant.

Due to the low surface area to volume ratio, the fixed-bed photoreactors are usually operated in a multipass (recycling mode) or series mode. Improvement of the surface area to reaction volume ratio can be achieved by suspended media systems. Suspended media in common use include alumina pellets, molecular sieves, glass beads, fibreglass, glass mesh or woven fibres.

2.8 Light Sources

The source of ultraband gap illumination in photocatalysis is one of the most important factors to consider in designing the reactor. The light source is the highest contributor of capital costs of the system. Ultraviolet light is required as a source of ultraband gap illumination and is usually obtained from arc lamps in which mercury and/or xenon vapour is activated electrically. Mercury and xenon lamps are usually inefficient in terms of UV photons produced per unit of electrical energy input as a result of conversion of a great deal of electrical energy into heat or visible light. They are also expensive with a limited lifetime of about 1000 h. Alternative light sources are the UV fluorescent lamps, which have highly efficient electrical energy to UV photon conversion.

A version of the artificial UV lamp, the black light has high UV light to electrical energy conversion efficiencies of 10-20% and long operational lifetimes of 4000-14000 hours. A major disadvantage of black light is the emission of UVC radiation (280-100 nm, far UV) which causes cancer. Unfortunately, most black light bulbs have low light intensity of ≤150 W (Mills and Lee, 2004). Such dispersed light systems show high surface area to reaction volume ratio and even distribution of the photons on catalyst particles.

2.8.1 Ultraviolet lamps

One of the major problems in semiconductor photocatalysis is the achievement of an even distribution of light in the photoreactor. Poor distribution of UV light in a semiconductor reactor will lead to a low overall efficiency of operation. Rate of reaction is reported to be directly proportional to the intensity of radiation (Equation 2.21 on page 40). At low intensities there is usually a linear relationship between reaction rate and intensity. At higher intensities rates of reaction are reported to show a square root dependence on intensity (Okimotoe et al., 1985; Ollis et al., 1991 as reported by Gogate and Pandit, 2004). A novel system for distributing the ultraband gap light more evenly and efficiently has been used by Hoffstadler and co-workers. The photocatalytic material in this system is dispersed throughout the photoreactor via a series of light conductors, such as thin glass plates, rods and fibres of hollow glass tubes (Mills and Lee, 2004).

The threshold wavelength of radiation depends on the band gap energy. Titanium dioxide has band gap energy of 3.2-3.0 eV and absorbs UV light of 380-405 nm. The rutile form has band gap energy of 3.05 eV, which would require 405 nm irradiation to generate the electron hole pair. Anatase has band gap energy of 3.20 eV corresponding to 380 nm of radiation. Use of lamps of the right wavelength is very important for an efficient system.

Table 2.2: Comparative features of dispersed and fixed-film reactors (Mills and Lee, 2004)

Feature	Dispersed semiconductor photocatalyst	Fixed film semiconductor photocatalyst
Ease of preparation of photocatalyst	Excellent. Photocatalyst easily prepared by numerous chemical routes, including hydrolysis or air oxidation of simple Ti(IV) precursors.	Can be difficult and usually involves either CVD, sol-gel, sputtering or thermal oxidation methods.
Ease of replacement of semiconductor photocatalyst	Excellent. The photocatalyst particles are simply added to the polluted water stream.	Often difficult as the usually firmly fixed film photocatalyst is often attached to the walls of the photoreactor. Photocatalyst on support materials, such as glass beads, are easier to change.
Overall ease of operation as a water purification system	Not usually very good, since a subsequent particle separation step is required, which usually brings with it the need for regular filter replacement. In addition, ideally, the filtered photocatalyst should be returned to the photoreactor, which poses another technical problem, although a recirculation system with cross-filtration appears to offer a solution. System needs constant sparging with air.	Excellent. No filtering required. In some 'close-to-ambient air' systems, oxygen sparging is really needed.
Efficiency by m^2	High due to high photocatalyst surface area to reaction solution ratio and no mass transfer effects.	Low, thus, such systems need to be cheap per m^2.
Cost	Low initial cost, but maintenance costs can be high.	High initial cost, but maintenance costs could be low, provided the water stream does not contain any deactivating contaminants.

2.8.2 Solar source

The major component of operational cost in photocatalytic systems is associated with the artificial generation of photons required for electron-hole pair formation. This cost can be significantly reduced by the use of the 'free' light source form, solar energy (Malato et al., 2007; Ljubas, 2005; Bahdalala et al., 2004; Bahnemann, 2004; Gogate and Pandit, 2004; Mills and Lee, 2004; Esplugas et al., 2002). Using a solar light source would have ecological

benefits as well as economic benefits. The sun has a typical UV-flux near the surface of the earth of 20-30 W/m^2; this translates to 0.2-0.4 mol photon/m^2 h^{-1} available in the 300-400 nm range (Bahnemann, 2004, Mills and Lee, 2004). This is estimated to be 25 times less than that from an 8 W UV fluorescent lamp (Mills and Lee, 2004). Tapping this free source would translate into significant cost savings. Solar powered applications can only be used beneficially in the parts of the world that receive enough sunlight. Fortunately, Africa is geographically located to benefit from the use of such solar powered systems.

Several solar powered photocatalytic systems are currently under test for various applications. They use only high-energy short-wavelength photons, which can be collected by conventional solar thermal collector designs, such as parabolic troughs and non-concentrating collectors (which utilise direct or diffuse sunlight). Non-concentrating collectors are, in principle, cheaper than parabolic trough concentrators (PTCs), as they have neither moving parts nor solar tracking devices (Malato et al., 2007; Rodriguez et al., 1996). The most commonly used solar reactor concepts include (Bahnemann, 2004):

- **Parabolic trough reactor (PTR)**: The PTR is a concentrating type of reactor. It concentrates the parallel (direct) rays of the photocatalytically active ultra-violet part of the solar spectrum by a factor of 30-50; it is characterised by a typical plug flow reactor. This reactor design has been installed in California (USA) and Almeria in Spain.

- **Thin film fixed bed reactor (TFFBR)**: The TFFBR does not use a concentrating system but utilises the diffuse as well as the direct portion of the sunlight. It comprises of a sloping plate coated with the semiconductor photocatalyst over which the polluted water stream flows. System performance comparison was tested between the first TFFBR test reactors installed at the Plataforma Solar de Almeria in Spain, and the PTR. In every instance TFFBR displayed superior performance than the PTR. The superior performance could be due to a greater surface area provided by the film bed compared to the plug flow system of the PTR.

- **Compound parabolic collecting reactor (CPCR)**: The CPCR is a trough reactor without light concentrating properties. The shape of its reflecting mirrors differs from those of the conventional parabolic trough reactor. The shape of a CPCR reflector usually consists of two half circular profiles side by side, and a parabolic continuation at both outer sides of the circles. The focal line is located closely above the connection of the two circles. This geometry enables light entering from almost any direction to be reflected into the focal line of the CPCR, i.e. most of the diffuse light entering the module can also be employed for the photocatalytic reaction. The reflector plates are usually made of polished aluminium, which has very good reflection properties in the UV region of the solar spectrum.

- **Double skin sheet reactor (DSSR)**: The DSSR is a new kind of non-concentrating reactor. It consists of a flat and transparent structured box made of Plexiglas in the form of several grooves. The suspension containing the model pollutant and the photocatalyst is pumped through these channels. The DSSR reactor can utilise both the direct and diffuse portions of the solar radiation. After the degradation process the photocatalyst has to be removed from the suspension either by filtering or by sedimentation from the reactor.

2.9 Reaction Mechanism

The major reactions involved in the photomineralisation of pollutants by photosensitised TiO_2 are presented in Equations 2.21 to 2.27.

$$TiO_2 + h\nu \rightarrow TiO_2\ (e^-_{CB} + h^+_{VB}) \quad (2.21)$$

$$TiO_2(h^+_{VB}) + H_2O_{ad} \rightarrow TiO_2 + {}^{\bullet}OH_{ad} + H^+ \quad (2.22)$$

$$TiO_2(h^+_{VB}) + OH^- \rightarrow TiO_2 + {}^{\bullet}OH_{ad} \quad (2.23)$$

$$TiO_2\ (e^-_{CB}) + O_2 \rightarrow TiO_2 + O_2^- \quad (2.24)$$

$$O_2^- + H^+ \rightarrow HO_2^{\bullet} \quad (2.25)$$

$$TiO_2(h^+_{VB}) + R\text{-}H \rightarrow TiO_2 + \text{oxidised products.} \quad (2.26)$$

$${}^{\bullet}OH + R\text{-}H \rightarrow \text{oxidised products.} \quad (2.27)$$

In the photomineralisation of organic pollutants sensitised by TiO_2 as represented by Equation 2.20, the photogenerated electrons reduce oxygen to water (Equation 2.24), and the photogenerated holes mineralise the pollutant (Equation 2.26). The mineralisation process is believed to involve the initial oxidation of surface hydroxyl groups ($>Ti^{IV}OH$) on the TiO_2 to hydroxyl radicals ($>Ti^{IV}\ OH^{\bullet+}$), which oxidises the pollutant and any intermediate(s). The final product is usually the mineral form of the pollutant, typically carbon dioxide and water. However, if there are heteroatoms present, then the mineral acid of the heteroatom is formed. Other intermediate species formed include Ti^{III} species ($Ti^{III}OH$) formed from the trapping of the photogenerated electrons by surface sites ($>Ti^{IV}OH$). $Ti^{III}OH$ reacts with dissolved oxygen to form superoxide, $O_2^{\bullet-}$, which can be further reduced to H_2O_2.

Hydrogen peroxide is also a possible source of hydroxyl radicals, which could be partly responsible for some degree of the mineralisation in reaction represented in Equation 2.20. Primary processes and the associated characteristic time frames for these processes are presented in Table 2.3.

The dynamic equilibrium of Equation 2.30 represents a reversible trapping of a CB electron in a shallow trap below the CB edge, thus a finite probability of e_{tr}^- transfer back into the CB at room temperature exists. From Equations 2.27-2.34, two critical processes determine the overall quantum efficiency for interfacial charge transfer. These processes are the competition between charge carrier trapping (Equations 2.28-2.30) and recombination (Equations 2.31 and 2.32) – picoseconds to nanoseconds. This is followed by the competition between trapped carrier recombination and interfacial charge transfer – microseconds to milliseconds. An increase in either the recombination lifetime of charger carriers or the interfacial electron transfer rate constant is expected to result in higher quantum efficiency of the steady state photocatalysis (Hoffmann et al., 1995).

Table 2.3: Primary processes and the associated timeframe for TiO_2 photosensitised mineralisation of organic pollutants (Hoffmann et al., 1995)

Primary process	Characteristic times	Equation
Charge carrier generation		
$TiO_2 + h\nu \rightarrow h_{vb}^+ + e_{cb}^-$	fs (very fast)	(2.28)
Charge carrier trapping		
$h_{vb}^+ + >Ti^{IV}OH \rightarrow \{Ti^{IV}OH^{\bullet+}\}$	10 ns (fast)	(2.29)
$e_{cb}^- + >Ti^{IV}OH \leftrightarrow \{Ti^{III}OH\}$	100 ps (shallow trap, dynamic equilibrium)	(2.30)
$e_{cb}^- + >Ti^{IV} \rightarrow >Ti^{III}$	10 ns (deep trap), irreversible.	(2.31)
Charge carrier recombination		
$e_{cb}^- + \{Ti^{IV}OH^{\bullet+}\} \rightarrow >Ti^{IV}OH$	100 ns (slow)	(2.31)
$h_{vb}^+ + >Ti^{III}OH \rightarrow >Ti^{IV}OH$	10 ns (fast)	(2.32)
Interfacial charge Transfer		
$\{Ti^{IV}OH^{\bullet+}\} + Red \rightarrow Ti^{IV}OH + Red^{\bullet+}$	100 ns (slow)	(2.33)
$e_{tr}^- + Ox \rightarrow Ti^{IV}OH + Ox^{\bullet-}$	ms (very slow)	(2.34)

where: >TiOH represents the primary hydrated surface functionality of TiO_2,
ecb- represents a conduction band electron,
etr- is a trapped conduction band electron,
h_{vb}^+ is a valence band hole,
Red is an electron donor (i.e. reductant),
Ox is and electron acceptor (i.e. oxidant),
>TiIIIOH is the surface trapped CB electron
fs is femtosecond (1 fs is 10-15 of a second), and
{TiIVOH•+} is the surface trapped VB holes (i.e. surface bound hydroxyl radical)

2.9.1 Application of semiconductor photocatalysis

Toxic organic compound degradation

Research into semiconductor photocatalysis has largely focused on the removal of organic pollutants from water, as it appears that a wide range of organic substrates can easily be completely mineralised in the presence of dissolved oxygen, photosensitised by TiO_2. One of the very attractive features of semiconductor photocatalysis is its effectiveness against a broad range of pollutants, including those that are recalcitrant to other water treatment processes. This makes it ideal for treating hazardous refractory organics such as herbicides and aromatic compounds (Mills and Lee, 2004). A non-exhaustive list of some classes of compounds mineralised by TiO_2 sensitised photocatalysis is presented in Table 2.4. Class of compounds of environmental interest in Table 2.4 include haloalkanes, such as chloroform and tetrachloromethane; halophenol; herbicides, especially DDT which is in the US EPA's top priority persistent organic pollutants (POP) list. The halogenated compounds are disinfection products often found in small but detectable quantities in drinking water disinfected by chlorination; and are known carcinogens.

Some examples of application of TiO_2 semiconductor photocatalysis in the destruction of organic pollutant and the key reaction conditions are presented in Table 2.5. The list is far from complete but careful choices of compounds have been made to include compounds from a variety of classes; under a variety of operational conditions.

Chen and Dionysiou (2006) concluded that photocatalytic activity depended largely on the structural properties and film thickness of the catalyst. On the other hand, findings by Doll

and Frimmel (2005) on the effectiveness of two commercial TiO_2 catalysts, indicate that the ultimate catalyst for photocatalysis could depend on the chemistry of the compound (Table 2.5). The combined contributions from diverse process parameters over a wide range of pollutants with different chemistries makes it imperative for laboratory scale kinetic studies for each pollutant type to be treated by photocatalysis.

Degradation of toxic inorganic compounds

Due to the non selective action of photocatalysis, it finds application beyond the degradation of organic species in water. Semiconductor photocatalysis has also found application in the degradation of toxic inorganic compounds to harmless or less toxic compounds; some examples are presented in Table 2.6. Thus semiconductor photocatalysis can be used to oxidise nitrite, sulphite and cyanide anions to form relatively harmless products, such as NO_3^-, SO_4^{2-} and CO_2 respectively.

Bromate formation during ozonation of compounds containing bromide ions in water is a major concern with ozonation systems. With titanium photocatalysis bromate ions in solution are decomposed to bromide and oxygen. The reactions involved are presented in Equation 2.46 (see Table 2.6). The ability to degrade bromate ions is of significant environmental advantage as there are growing concerns over its detection at environmentally significant levels in potable water that has been chlorinated (Mills and Lee, 2004).

Table 2.4: List of classes of organic compounds photomineralised by TiO_2 photocatalysis

Class of Organics	Examples
Alkanes	Isobutane, pentane, heptane, cyclohexane, paraffins
Haloalkanes	Mono-, di-, tri- and tetrachloromethane, tribromoethane, 1,1,1-trifluoro-2,2,2 trichloroethane
Aliphatic alcohols	Methanol, ethanol, propanol, glucose
Aliphatic carboxylic acids	Formic, ethanoic, propanoic, oxalic, butyric, malic acids
Alkenes	Propene, cyclohexene
Haloalkenes	1,2-dichloroethylene, 1,1,2-trichloroethylene
Aromatics	Benzene, naphthalene
Haloaromatics	Chlorobenzene, 1,2-dichlorobenzene
Nitrohaloaromatics	Dichloronitrobenzene
Phenolic compounds	Phenol, hydroquinone, catechol, methylcatechol, resorcinol, o- m-, p-cresol, nitrophenols
Halophenols	2-, 3-, 4-chlorophenol, pentachlorophenol, 4-fluorophenol
Amides	Benzamide
Aromatic carboxylic acids	Benzoic acid, 4-aminobenzoic, phthalic, salicylic, m- and p-hydroxybenzoic acids, chlorohydroxybenzoic and chlorobenzoic acids
Polymers	Polyethylene, PVC
Surfactants	Sodium dodecylsulphate, polyethylene glycol, sodium dodecyl benzene sulphonate, trimethyl phosphate, tetrabutylammmonium phosphate
Herbicides	Atrazine, prometron, propetryne, bentazon, 2-4 D, monuron
Pesticides	DDT, parathion, lindane, tetrachlorvinphos, phenitrothion.
Dyes	Methylene blue, rhodamine B, methyl orange and fluorescein.

Table 2.5: List of some TiO_2 sensitised photodegraded compounds and key reaction conditions

Pollutant	Catalyst Form	Radiation Source	Key Findings	Reference
4-chlorobenzoic acid	Transparent, dense TiO_2 film on stainless steel – prepared at different calcinations temperatures (400-600°C)	Four 15 W, integrally filtered low-pressure mercury UV tubes	Structural properties and film thickness affects photocalytic activity. Reduction of calcinations temperature improved activity significantly.	Chen and Dionysiou (2006)
Cyclopentene	Slurry (1 g/300 mℓ). Compared activity of eight (4 commercial, 4 prepared) TiO_2 catalysts.	250 W, vacuum Hg lamp	Achieved above 50% total mineralisation	Kluson et al. (2005)
Pharmaceuticals	TiO_2 suspension (Hombikat UV100 and P25 Degussa)	Solar UV simulator (1000 W, Xe short arc lamp)	P25 more effective for clofibric acid, while Hombikat 100 was more effective for iomeprol degradation	Doll and Frimmel (2005)
Formic acid	Immobilised TiO_2 (supported on glass beads) Packed bed reactor	15 W, UV lamp	Immobilisation on large beads gave better degradation. Immobilised systems gave same degradation efficiency as slurry.	Dijkstra et al. (2001)
4-Nitrophenol	Suspended TiO_2 catalyst. Optimum value of catalyst concentration of 4g/ℓ with catalyst size of <70 µm.	125 W high-pressure mercury lamp	Higher degradation at pH of 3 than at 8.5	Androzzi et al. (2000)
Dyes	Suspended TiO_2 (3 g/ℓ)	500 W super high pressure mercury lamp	Lowered pH increased degradation by about 21%. Lower concentration of acid orange dyes improved degradation rates. 75% removal achieved from about 60 min.	Tanaka et al. (2000)
Microcystin	Suspended TiO_2 slurry (1% m/v) of Degussa 25	280 W UVA spot 400 lamp (spectral output at 330-450 nm)	Noticed rapid destruction of microcystin to undetectable levels within 40-60 min	Robertson et al. (1997)

Table 2.6: Titanium dioxide sensitised photosystems for the removal of toxic inorganic compounds (Mills and Lee, 2004, Halmann 1996)

Overall Reaction Equation Number
$A + D \xrightarrow{h\nu / TiO_2} A^- + D^+$
$5O_2 + 6NH_3 \xrightarrow{h\nu / TiO_2} 2N_2 + N_2O + 9H_2O$ (2.40)
$O_2 + 2NO_2^- \xrightarrow{h\nu / TiO_2} 2NO_3^-$ (2.41)
$O_2 + 2SO_3^{2-} \xrightarrow{h\nu / TiO_2} 2SO_4^{2-}$ (2.42)
$2O_2 + H_2O + 2SO_3^{2-} \xrightarrow{h\nu / TiO_2} 2SO_4^{2-}$ (2.43)
$O_2 + 2CN^- \xrightarrow{h\nu / TiO_2} 2OCN^-$ (2.44)
$5O_2 + 4H^+ + 4CN^- \xrightarrow{h\nu / TiO_2} 2H_2O + 4CO_2 + 2N_2$ (2.45)
$2BrO_3^- \xrightarrow{h\nu / TiO_2} 2Br^- + 3O_2$ (2.46)
$HNO_3 + 6H^+ + 6e^- \xrightarrow{h\nu / TiO_2} NH_2OH + 2H_2O$ (2.47)

Degradation of organo-metallic compounds

Semiconductor photocatalysis has also found application in the degradation of some organo-metallic compounds of serious environmental concern. Serious environmental hazard of spills of mercury and other heavy metals (particularly lead and cadmium) into natural waters is due to the formation of organo-metallic derivatives of the metals. Some of these organo-metallic compounds are extremely toxic. Examples of organo-metallic compounds that have been successfully degraded by semiconductor photocatalysis include mercurochrome, some phenylmercury compounds, tributyltin chloride (TBT), and bis(tributyltin) oxide (TBTO) amongst others (Halmann, 1996).

Treatment of oil spills

Oil spills are a major source of natural water pollution in oil producing regions and during transportation in high seas. Photocatalytic oxidation of films of crude oil by sunlight or of n-octane on fresh and seawater can be achieved by spreading TiO_2 coated oleophilic glass microbubbles or beads on the polluted water surface. The possibility of a natural 'self cleaning' process has been predicted on the discovery of the photocatalytic degradation of crude oil residues in contact with beach sand on irradiation with high-pressure mercury lamp. Photocatalytic activity of the beach sand was ascribed to the catalytic properties of magnetite and ilmenite contained in the beach sand (Halmann, 1996).

Destruction of biological species (bacteria and viruses)

In addition to the photomineralisation of organic, inorganic and organo-metallic compounds, photosensitised TiO_2 has also been effectively used for the destruction of microorganisms, such as bacteria, viruses and moulds. The mode of action appears to be similar to that in the oxidative mineralisation of pollutants. The photocatalytic destruction of biological material

sensitised by semiconductor catalysts is generally referred to as photo-sterilisation or photodisinfection (Mills and Lee, 2004).

2.9.2 Case Studies

Semiconductor photocatalysis is yet to make the full transition from laboratory and pilot scale experiments to full scale application. A limited number of case studies are available in literature compared to the volume of research that is being carried out. Most attempts at pilot scale studies have been focused on the treatment of pollutants from industrial effluents. There has been very limited application of photocatalysis in the treatment of surface water contaminants and in the drinking water treatment industry.

With recorded success of photocatalysis for the degradation of a seemingly endless list of recalcitrant organic compounds coupled with the ability to destroy microorganisms, photocatalysis could emerge in the near future as a one stop alternative to disinfectant / treatment method in the potable water industry.

Despite its limited application outside laboratory studies, a few successes have been recorded in the area of surface and ground water remediation with photocatalysis. These include:

- Treatment of musty odour in Lake Biwa – Japan
- Contaminated surface water – Ontario, Canada
- Cleaning of groundwater contamination – Gainesville, Florida
- Oil Spill Clean-up in Japan
- Petrochemical waste site – Galveston, Texas

Treatment of musty odour in Lake Biwa – Japan

A flow through photoreactor packed with TiO_2 coated glass beads under illumination with black light at flow rates of 20-50 mℓ/min was developed in the laboratory to degrade 2-MIB. Concentration of 2-MIB decreased to half of its initial value of 1 000 ng/ℓ within a minute. The process was developed to degrade musty odours in Lake Biwa, Japan (Halmann, 1996).

Contaminated surface water – Ontario, Canada

The Photo-cat system was installed to treat highly contaminated surface water with high levels of oil and grease which discharges into the Thames River. The system was used to treat 136.38 kℓ from three wells continuously on a daily basis. Contaminants include trichloroethene (TCE), dichloroethane (DCA), trichloroethane (TCA), vinylchloride, oil and grease all present in the low mg/ℓ range in two wells and >1000 mg/ℓ range in the third well. A low concentration of H_2O_2 was added as an additional scavenger of photogenerated electrons to enhance overall efficiency of the system. The system is reported to have been operating since 1998 (Mills and Lee, 2004).

Cleaning of groundwater contamination – Gainesville, Florida

Clearwater Industries R2000 solar oxidation facility using a modular set of tilted flat bed solar photoreactors, with dispersed TiO_2 photocatalyst was used to treat 500 gallons of underground water aquifer contaminated with benzene, toluene, ethyl benzene and xylene (BTEX). The R2000 system reduced BTEX to below the allowed levels of 65 µg/ℓ within three hours of use on a cloudy day (UV – light intensity ≅ 31 Wm^{-2}). This was compared to

the use of activated carbon absorption and trials with both systems showed that the R2000 photocatalytic system was significantly less expensive to install and operated at a fraction of the cost of the activated carbon system (Mills and Lee, 2004).

Oil Spill Clean-up in Japan

Degradation of a thin film of crude oil spilled on seawater was achieved by photocatalytic oxidation using TiO_2 coated microbubbles of 80 µm average diameter and 0.37 cm^{-3} density. The microbubbles stayed on the air-oil interface and promoted the initial very rapid photodegradation process of the oil with air as the oxidant. The microbubbles absorbed the oil, forming oil-containing aggregates thereby leaving the water surface relatively clean. The microbubbles were reported to promote complete mineralisation with destruction of intermediates at a weekly rate of about twice their weight of oil. Photoxidation eliminated both aliphatic and aromatic compounds including polycyclic aromatics. The clean-up process was reported to be accelerated by waves thereby proceeding even in high seas where skimming of oil spills is not praticable (Halmann, 1996).

Petrochemical waste site, Galveston, Texas

A 19-Kw Photo-Cat system was used to reduce groundwater contaminants from 200 mg/ℓ to 5 µg/ℓ, in the presence of 6 000 mg/ℓ of chloride ion. The 19-Kw system was used to reduce levels of 200 mg/ℓ of bis(2-chloroethyl)ether to 20 µg/ℓ. The unit was designed to operate at 15-30 ℓ/min in fully automated mode (Mills and Lee, 2004).

With the recorded success of photocatalysis for the degradation of a seemingly endless list of recalcitrant organic compounds in the laboratory and the few reported cases for the treatment of organic compounds in surface water and groundwater, it is becoming an attractive choice for water treatment systems. The increased interest seems justified in light of enhanced awareness of the implications for use of non environmentally sensitive processes; and a subsequent global shift to ‘greener’ processes. This is in light of the fact that the photocatalytic process has the added advantage of being the only AOP system that can be classified as a completely ‘green’ process. For the potable water industry, installation of a single system that could potentially degrade recalcitrant organic compounds and act as a disinfectant for the microbial population without the production of DBPs would be an added benefit.

CHAPTER THREE

3 MATERIALS AND METHODS

3.1 Natural Water Samples

Raw and filter backwash water samples were collected from Rietvlei and Roodeplaat Water Treatment Plants and analysed to determine the chemical composition of the samples. A detailed chromatographic analysis was performed to identify the constituent organic pollutants in both the source water and the filter backwash water samples. Organic pollutants identified during chromatographic analysis were chosen as target compounds for this study. These include phenolic compounds, pesticides and the cyanobacterial metabolites geosmin and 2-MIB. Detailed quantitative analysis of the taste and odour compounds gave an indication of the extent of retention of target organic compounds by the different filter types in the treatment plants. Maximum concentrations of taste and odour compounds obtained from quantitative analyses were used as environmentally significant concentrations for subsequent laboratory photocatalytic degradation studies.

3.2 Materials and Reagents

Acetonitrile (99.9% – BDH HiperSolv), dichloromethane (99.9% – BDH HiperSolv), phenol reagent (99.5 % – Saarchem, sodium chloride (99% – Saarchem); 2-chlorophenol (98% – Merck), 4-chlorophenol (98% – Merck), 4-nitrophenol (99% – Merck); and tertiary butanol (99.5% – Merck) were supplied by Merck, South Africa. Methanol (99.9% – High performance liquid chromatography (HPLC) grade) was purchased either from Merck, South Africa or from Waters, South Africa. Hexane (99% – Fluka) and phenol analytical standard (99.7% – Fluka) were purchased from Sigma Aldrich, Germany. Acetone (99.5% – Merck) and Glacial acetic acid (100% – Merck) were purchased from Merck, Germany.

Sodium azide (99.5% - Sigma), taste and odour standards including, geosmin (99.8% – Supelco), 2-methylisoborneol (99.9% – Supelco), 2,4,6-trichloroanisole (99.1% – Supelco), 2-isopropyl-3-methoxypyrazine (99.9% – Supelco) and 2-isobutyl-3-methoxypyrazine (99.5% – Supelco) were purchased from Sigma Aldrich, Germany. The taste and odour standards were purchased as 100 mg/ℓ solutions in methanol (1 mℓ). Anatase TiO_2 powder (99.8% – Aldrich) was purchased from Sigma Aldrich. Ultra high purity helium gas (99.99%) was purchased from Afrox, South Africa.

All chemicals, with the exception of sodium chloride, were used as received without further purification. All samples were prepared using ultra pure water from a Millipore DirectQ_3 unit (0.05 µS/cm).

Long-arc 400 W, (Philips HOK 4/120 SE), medium pressure, and 9 W low pressure (Philips TUV PL-S 9W) UV lamps (Philips, Netherlands); were supplied by Technilamps, South Africa. Goldilux UV Smart Meters (Model GRP-1) equipped with UV-A, UV-B and UV-C probes (Goldilux, USA) were purchased from Measuring Instruments Technology (MIT), South Africa. The UV meter and probes were calibrated at the National Metrology Institute of South Africa (NMISA).

3.2.1 Characterisation of anatase titanium dioxide powder

Anatase titanium dioxide powder used for photocatalytic degradation studies was characterised by x-ray diffractometry (XRD) analysis and by high resolution scanning electron microscopy (SEM).

X-ray diffractometry analysis of anatase titanium dioxide powder

The crystallinity of anatase TiO_2 powder was examined by XRD with a PANalytical Xpert-Pro diffractometer system equipped with an X'celerator detector; and variable divergence and receiving slits with Fe filtered Co-Kα radiation. Anatase TiO_2 powder was prepared for XRD analysis using the back loading preparation method. X-ray diffractometry analysis was performed with the detector in continuous scan mode operating at 35 kV and 50 mA; and 2θ in the range of 5°-90°. The phases were identified using X'Pert Highscore plus software. The semi quantitative phase amounts (as percentages by weight) were estimated using the Reference Intensity Method in the X'Pert Highscore plus software. Amorphous phases, if present, were not taken into account in the quantification.

Surface morphology of anatase titanium dioxide powder

High resolution SEM images were taken of the anatase TiO_2 powder with a Zeiss Ultra Plus SECSEM electron microscope operated at 0.5 kV. Images were taken at low and high resolution of 10 000 and 30 000 magnifications respectively. The TiO_2 sample was prepared for SEM by first coating the powder on a carbon tape, drying the coated tapes in the oven at 60°C for 8 minutes and finally applying a carbon coat over the TiO_2 powder.

The catalyst used for the photocatalytic degradation studies has a mainly tetragonal crystal structure with 94% anatase and 6% rutile as shown by x-ray diffraction pattern (Figure 3.1), with non uniform particle sizes less than 0.5 μm (Figure 3.2).

3.2.2 Actinometric measurements

The amount of radiation emitted by the UV lamps (UVA, UVB and UVC) and transferred into the reactant solution was determined for the two lamps with the UV meter. Measurements were taken with the UV lamp placed in a closed box in the centre of the reactor. Ultraviolet radiation was measured with the UV probes at the outside wall of the reactor in the following configurations:

- With an empty reactor and UV sleeve (Reactor configuration A)
- Empty reactor and UV sleeve with water circulating through outer jacket of the sleeve (Reactor configuration B).

The properties of the two UV lamps used for the study are presented in Table 3.1. The lamp wattage and voltage as presented in Table 3.1(A) are values supplied by the manufactures. Ultraviolet radiation values in Table 3.1(B) are those obtained from laboratory measurements during the course of the study as described in Section 3.5.2.

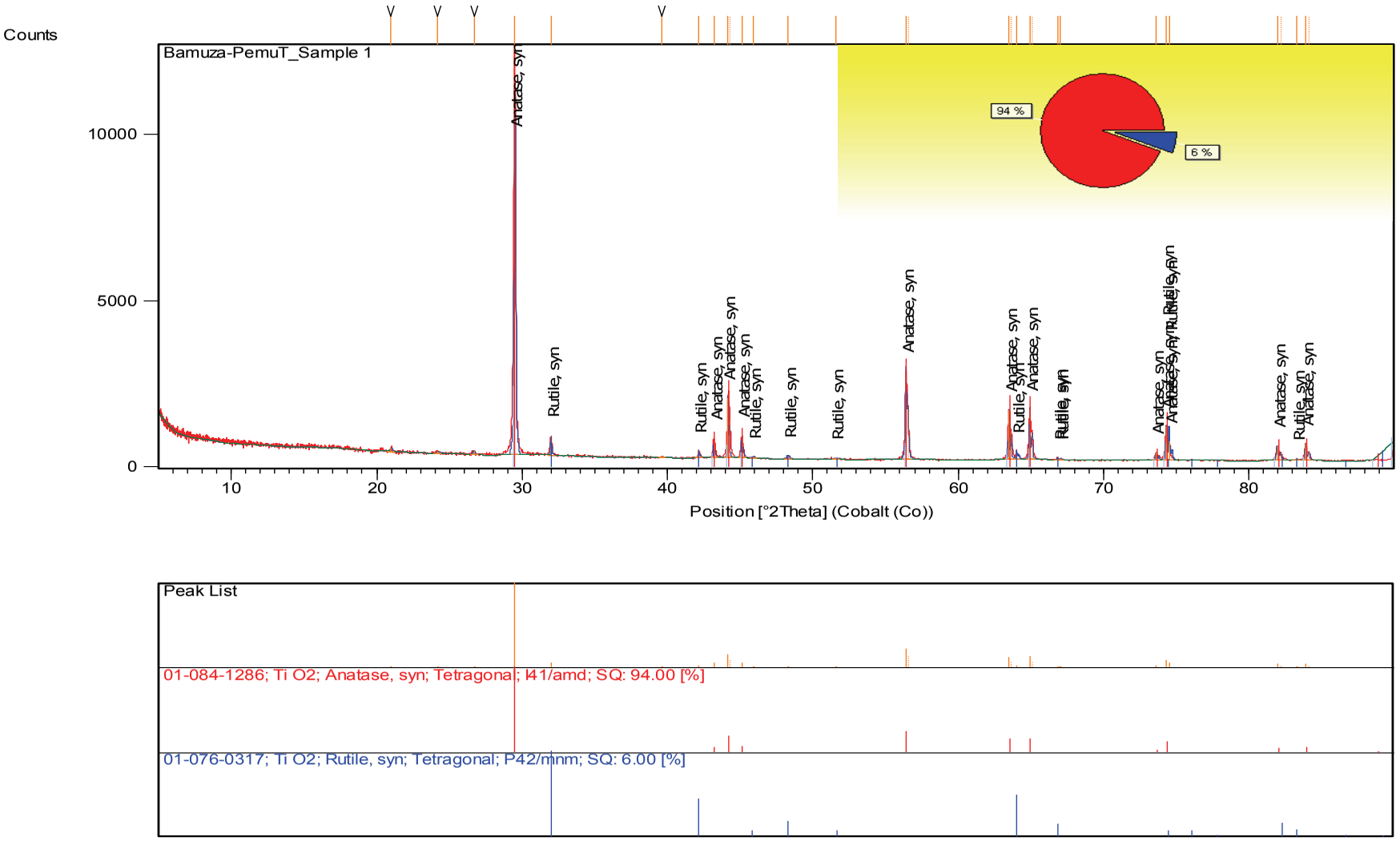

Figure 3.1: X-ray diffraction pattern of anatase titanium dioxide powder used for degradation experiments

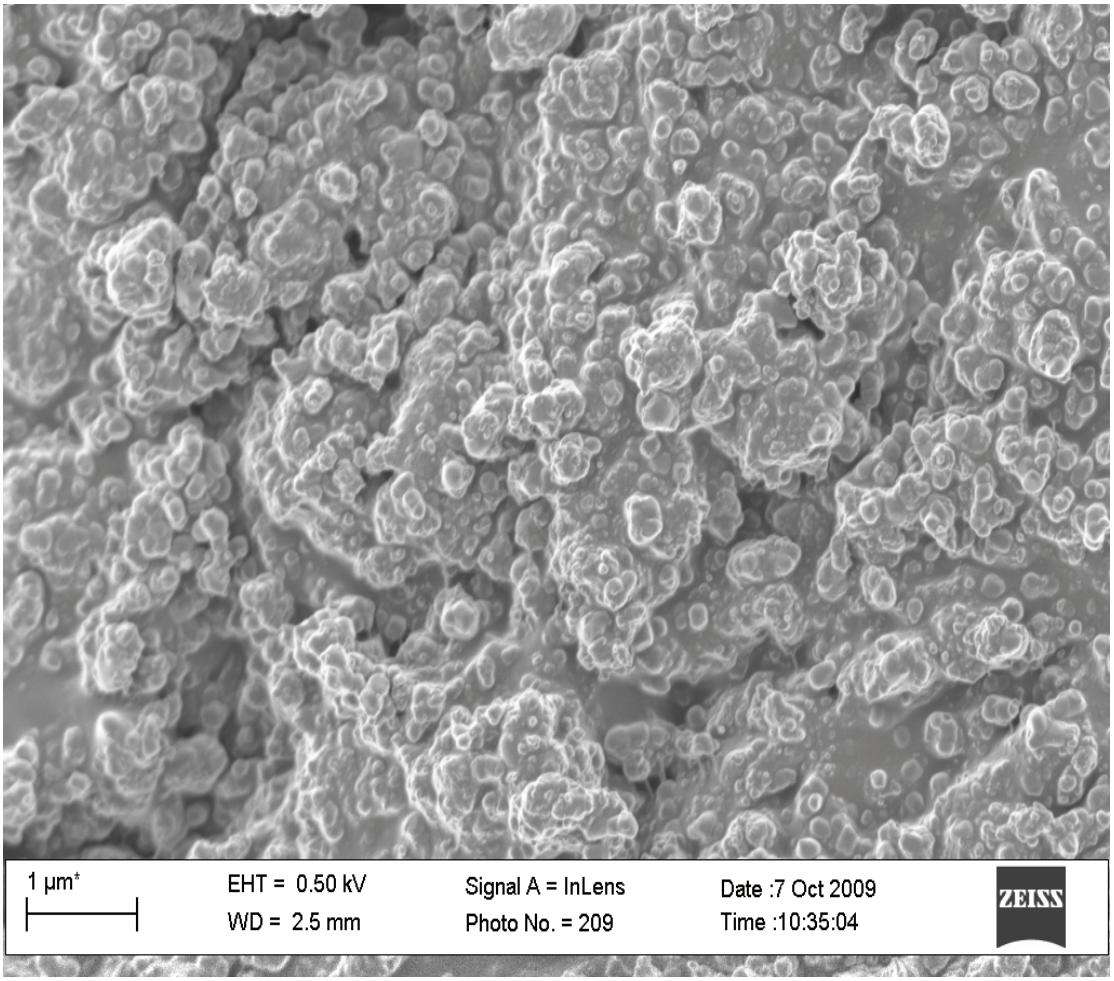

Figure 3.2: SEM image of anatase TiO_2 showing particle size distribution

Table 3.1: Properties of UV lamps

(A)

Lamp Type	Length (mm)	Width (mm)	Lamp Wattage (W)				Voltage (V)
			Elect	UVA	UVB	UVC	
400 W	110	16	400	31	32	52	125
9 W	--	28	9	--	--	2.4	60

(B)

Lamp Type	UV Radiation (n = 5)		
	UVA (mW/cm^2)	UVB(mW/cm^2)	UVC (µmW/cm^2)
	(A) With Empty Sleeve		
400 W	34.81 ± 0.50	13.98 ± 0.06	599.24 ± 0.38
9 W**	1650 ± 2.55	14.35 ± 0.03	15.20 ± 0.02
	(B) With Water Circulating Through the UV Lamp Sleeve		
400 W	33.65 ± 0.07	11.59 ± 0.01	431.28 ±0.16
9 W**	1326.14 ± 3.83	9.82 ± 0.06	9.61 ± 0.02

** Values for 9 W lamp are in µmW/cm^2

3.3 Water sources and sampling techniques

Water samples were collected from Rietvlei Water Purification Works and Roodeplaat Water Treatment Plant, both in the Tshwane Metropolis, in the Gauteng Province of South Africa.

Duplicate water samples were collected from the Water Treatment Plant at Rietvlei at three sampling points, i.e.

1. The inlet to the reservoir for raw water from the dam;
2. The collection tank for filter backwash water from the DAFF settling tanks (DAFF to river);
3. The collection tank for filter backwash water from the GAC filters (GAC to river).

Sampling was carried out between 12:30 and 13:00, immediately after the filters were backwashed and the backwash water drained into the collection tanks. Water samples were collected into 1 ℓ glass bottles (Duran Schott) filled without air space. Samples were pre-treated on site with 0.02 mg/ℓ sodium azide and 20 mℓ/ℓ of methanol. Sodium azide was added to prevent microbial degradation of water samples during transportation to the laboratory and during storage of samples prior to analysis. Temperature, pH and the turbidity of the water were measured at the sampling site immediately after sample collection. Samples were transported to the laboratory in a cooler box packed with ice.

Duplicate samples were collected at each sampling point from the Roodeplaat Treatment plant. Sampling points were:

1. The tap at the raw water inlet pipe and;
2. Point of discharge of filter backwash water out of the sand filters.

Sampling was carried out immediately after the filters were backwashed, as the backwash water was drained out of the filters. Samples were pre-treated on site with sodium azide and methanol as described earlier, and transported in ice cooled cooler boxes to the laboratory.

3.4 Sample Analysis

Initial analyses of samples from Rietvlei Water Treatment Plant in the months of June and July 2007, were conducted with a Hewlett Packard (HP) gas chromatograph/ mass spectrometer (GC/MS) at the Institute of Chromatography, in the Department of Chemistry, University of Pretoria. The GC/MS system at the Institute of Chromatography consisted of an HP GC G1530A gas chromatograph coupled to an HP 5973 quadrupole mass selective spectrometer. Subsequent analyses for samples collected during the year from January 2009 to January 2010 were performed on a Perkin Elmer GC/MS.

3.4.1 Sample pre-treatment and extraction

Pre-treatment of collected water samples involved filtration, followed by extraction and concentration of organic constituents prior to GC/MS analysis. Filtration and extraction were carried out concurrently to preserve sample integrity. The samples were filtered under vacuum and the filtrate was used for subsequent extraction.

Extraction and concentration of organic constituents in the water samples was achieved by solid phase extraction (SPE) using a method outlined by Naude (2002). The SPE setup consisted of a 12 port vacuum manifold (Waters), a vacuum pump (Edwards) and SPE cartridges (Varian – C_{18}-E, Bond Elut, 6 mℓ cartridges). The cartridges were packed with 1 g of highly cross-linked polystyrenedivinylbenzene (PSDVB) sorbent material with average particle sizes of 57 µm. Solid phase extraction of organic constituents involved three stages:

1. Conditioning of cartridges;
2. Extraction of organic compounds into SPE cartridge packing; and
3. Elution of adsorbed organic compounds from cartridge

Conditioning of cartridges

Cartridges were preconditioned by treating the cartridge packing material with three solvent systems. The solvent systems were applied in the order of increasing polarity. The conditioning solvents were allowed to flow through the SPE packing material under gravity. Solvents used include:

- 10 mℓ of 1:1 (v/v) mixture of acetonitrile: dichloromethane (DCM);
- 5 mℓ of methanol; and
- 5 mℓ of ultra pure water.

Extraction

Extraction of organic compounds from water samples into the packing of the SPE cartridges was achieved by feeding the filtered water samples through preconditioned SPE tubes under vacuum at a slow flow rate of 10 mℓ/min. The water was fed into the cartridges with slip-on filters attached to the cartridges. The cartridges containing extracted analytes were dried under vacuum before elution.

Elution

Extracted analytes in the dried cartridges were eluted drop wise into pre-washed and dried tubes with two solvent systems. Solvent systems used for elution were in the order of decreasing polarity:

- 10 mℓ of 1:1 (v/v), mixture of acetonitrile and DCM; followed by
- 5 mℓ of hexane.

Extracted organic compounds in the tubes were dried with a rotary evaporator (Bucchi) at 35°C. Dried extracts were re-dissolved in 1 mℓ of hexane. One µℓ of the hexane extract was injected directly into the GC.

A blank sample was prepared with ultrapure water containing 0.02% sodium azide and 20 mℓ/ℓ methanol. The blank sample was extracted and analysed under the same conditions as the water samples from the treatment plant. The chromatogram of the blank served as a screen for the elimination of organic contaminants from the SPE cartridges and the GC column.

Filter residues during sample filtration were extracted with 20 mℓ of methanol and dried under vacuum at 35°C with a Bucchi Evaporator. The dried extracts were re-dissolved in

1 mℓ of hexane and analysed in the GC. This was necessary to determine the possibility of the presence of undissolved organic compounds in the water adsorbed on the particulate matter in the backwash water samples.

3.4.2 Analysis of soluble semi-volatile organic compounds

Initial analyses of semi-volatile organic compounds (SVOCs) for samples from Rietvlei Water Treatment Plant in the months of June and July 2007, were conducted with a HP GC/MS at the institute of Chromatographic in the Department of Chemistry, University of Pretoria. Subsequent analyses were carried out on a Perkin Elmer GC/MS. The SPE extracts in hexane (1 µℓ) were injected directly into the GC. Organic compounds in the extracts were separated in the GC/MS using the conditions listed in Table 3.2. Total ion chromatograms (TIC) of the water samples were obtained and the compounds in chromatogram were tentatively identified by matching the electron impact spectra of the peaks with those in the Wiley chemical database.

Table 3.2: GC and MS operating conditions for analysis of semi-volatile organic compounds with HP system

GC Conditions	
Column	Restek (RTX1MS), 100% polydimethylsiloxane
Column Dimensions	30 m x 0.25 mm (0.25 µm)
Sample Introduction	
Sample Injection Mode	Direct liquid injection
Flow Mode	Splitless
Injection Volume	1 µℓ
Cooled Inlet System	Cryo trap
Cryo Cooling	Liquid nitrogen
Initial temperature	-20°C
Rate	5°C/sec
Final Temperature	250°C
Final Time	10 minutes
Oven Program	
Initial Oven temp.	30°C (5 min)
Ramp	5°C/min to 250°C (5 min)
Post Run	280°C (2 min)
Carrier Gas	Helium Afrox (UHP)
Flow Mode	Constant pressure
Column Inlet Pressure	9.43 psi
Column Carrier Gas Flow	1.3 mℓ /min
MS Conditions	
Transfer Line Temperature	250°C
Ionisation Mode	Electron impact (EI^+)
Electron Energy	70 eV
Mass Scan	45-450 amu

GC Conditions	
Mass Calibration	Perfluorotributylamine (PFTBA)
Calibration Masses	69, 219 and 502
Solvent Delay	5 minutes
Database Library	Wiley 275

3.4.3 Identification of taste and odour compounds in source water and filter backwash water

Gas chromatographic analysis for the identification of taste and odour compounds was carried out using a Clarus 600T GC/MS from Perkin Elmer coupled to a Perkin Elmer TurboMatrix 40 Trap headspace sampler. Data acquisition and interpretation were performed using TurboMass 5.0 Software. Volatile and SVOCs including taste and odour compounds were analysed following methods modified from Sung et al. (2005); and Ikai et al. (2003). The headspace, GC and MS conditions are presented in Table 3.3.

Analysis of standards

Taste and odour standard solutions were analysed as received by direct injection of 1 µℓ of each standard into the GC/MS, with the liquid injection auto sampler. The mass spectra of peaks obtained for the standard compounds were compared with the spectra of the compounds in the mass spectral database of the National Institute of Standards and Technology (NIST) library in the turbo mass software. Retention times obtained from total ion chromatograms and mass spectra of the individual compounds were used to develop single ion recording (SIR) methods used in subsequent trace analyses.

3.4.4 Trace analysis of taste and odour compounds and semi volatile organic compounds in water samples from treatment plants

Analysis of taste and odour compounds at trace levels was either by the use of solid phase micro extraction (SPME) (Sung et al., 2005; Lawton et al., 2003; Bao et al., 1997); or by SPE (Ikai et al., 2003); prior to gas chromatographic analysis. In this study, analyses of taste and odour compounds were conducted at levels between 0.5 and 1 000 ng/ℓ with the Perkin Elmer Turbo Matrix Headspace (PE TMH) without SPE or SPME. The trap in the PE TMH equipped with a purging device allows on-line extraction and concentration of organic constituents thereby eliminating the need for external SME or SPE processes. Trace analyses for geosmin and 2-MIB, were conducted with headspace at concentrations of 10-1 000 ng/ℓ in full scan mode; and 0.50-1000 ng/ℓ, in SIR mode.

Headspace extraction and sample introduction

Sodium chloride was dried in the oven at 105°C for 3 hours, then baked in the furnace at 540°C for 12 hours and cooled in a desiccator prior to use in head space vials. Sodium chloride was used to ensure complete elimination of moisture and trace organic contaminants from the sodium chloride salt. Solutions of the standards (0.5-1 000 ng/ℓ) were prepared in ultrapure water from the 100 mg/ℓ standard of the taste and odour compounds. Ten millilitres (10 mℓ) of standard solution of the required concentration was transferred into a headspace vial, 3 g of sodium chloride was dissolved in the standard solution in the headspace vial; and the vials were sealed. The organic compounds in the sealed headspace

vials were extracted from the headspace with a previously optimised method and introduced into the GC/MS for analysis through a transfer line of 0.32 µm fused silica. Detailed GC, MS and headspace conditions are presented in Table 3.3.

The MS method for trace analysis of taste and odour compounds included five functions for SIR scans for the five individual compounds. This serves to improve the sensitivity for identification of trace amounts of the compounds. The SIR scan functions and parameters are presented in Table 3.4.

Water samples from Rietvlei and Roodeplaat (inlet water and filter backwash water) were analysed using PE TMH and PE GC/MS under the same conditions as those used for the standards (Table 3.3). Quantification of the target compounds geosmin and 2-MIB were obtained from calibration curves of standard solutions in the SIR. Fresh standards were analysed with each batch of compounds on the GC/MS. Tentative peak identification for other VOCs was based on mass spectral comparison of the unknown compound with those obtained from NIST library search.

Table 3.3: Headspace, GC and MS operating conditions for analysis of semi-volatile organic compounds with the Clarus 600T GC/MS system

Head Space Conditions		
Head Space Transfer Line		0.32 mm ID fused silica tube.
Temperature Settings	Headspace oven temperature	80°C
	Trap temperature gradient	40-280°C
	Needle temperature	95°C
	Transfer line temperature	150°C
Pressure Settings	Column pressure	137.89 kPa
	Desorb pressure	103.42 kPa
	Vial pressure	206.84 kPa
Timing	Vial pressurised time	2 min
	Trap load time	1 min
	Dry purge time	5 min
	Trap hold time	6 min
	Trap repeat cycles	4 Cycles
GC Conditions	GC column	Perkin Elmer Elite – 5MS capillary column
	Column dimensions	30 m x 0.25 mm (0.5 µm)
GC Oven Conditions	Initial oven temp.	40°C (3 min)
	Ramp 1	6°C/min to 150°C
	Ramp 2	15°C/min to 250°C
Carrier Gas (helium)	Flow Rate	1 mℓ/min (Direct injection)
	Split Ratio	20:1 (Direct injection)

MS Conditions	Transfer line temperature	250°C
	Source temperature	180°C
	Ionisation mode	Electron impact (EI^+)
	Electron energy	70 eV
	Mass scan	35-350 amu
	Scan time	0.28 sec
	Inter Scan delay	0.02 sec
	Solvent delay (direct injection)	3.5 min
	Photomultiplier voltage	350 V (Direct injection – standards)
	Photomultiplier voltage	500 V (Head space – trace analysis)
Database Library		NIST

Table 3.4a: Parameters for SIR scan functions in the MS for target analytes

Compound	Function Number	Scan Time Window	Quantifier Ion	Qualifier Ions
IPMP	2	12.0-14.0	137	124,152
IBMP	3	14.0-16.0	124	94,151
2-MIB	4	15.0-18.5	95	108,110
TCA	5	18.5-20.5	195	169,210
Geosmin	6	20.5-24	112	55,125 (or 150)

Table 3.4b: Parameters for SIR scan functions in the MS for target analytes for degradation studies of field samples

Compound	Function Number	Scan Time Window	Quantifier Ion	Qualifier Ions
2-MIB	2	14.5-17.0	95	108,110
Geosmin	3	20.0-21.5	112	55,125 (or 150)
Geosmin	4	20.0-21.5	112	111,149

Detection limit for geosmin in TIC was 10 ng/ℓ and in the SIR mode was below 0.5 ng/ℓ, while detection limit for MIB in the TIC was 15 ng/ℓ; and 1 ng/ℓ in the SIR scan

3.5 Setup and Operation of Photocatalytic Reactor

Gas chromatograph/ mass spectrometer analysis of source and backwash water indicated the presence of a couple of aromatic compounds including some phenolic compounds and the herbicide, atrazine. Photocatalytic degradation of phenol and its derivatives have been studied by a number of researchers; and the degradation kinetics are known. Phenol was chosen as a model compound to represent the phenolic compounds in the water samples.

Kinetics of photocatalytic degradation of simulated polluted water containing only phenol were studied to establish the effectiveness of the photocatalytic system over a range of catalyst concentrations. Degradation experiments were also conducted on simulated polluted water containing a mixture of phenol and three substituted phenolic compounds to study the synergic effect of the presence of competing organic pollutants in solution.

The system was applied to the degradation of geosmin in water (as a model taste and odour compound). The optimum laboratory conditions obtained were used to treat filter backwash water samples, monitoring the rate of geosmin degradation. Photocatalytic degradation of

filter backwash water was conducted to test the effectiveness of the system for degradation of taste and odour compounds in the presence of other natural organic matter.

3.5.1 Laboratory photolytic and photocatalytic degradation of phenol

Experimental setup for photocatalytic degradation of phenol

Photocatalytic degradation experiments of phenol were conducted in a 1000 mℓ capacity Pyrex® glass open double jacketed reactor (Corning, NY) with inner diameter of 950 mm, outer diameter of 1300 mm and depth of 1850 mm (Figure 3.3). The schematic of the reactor setup is presented in Figure 3.3 as Configuration A. Temperature of the reactor was controlled by circulating cold water through the outer jacket of the reactor. Ultraviolet irradiation was provided by the 400 W medium pressure UV lamp encased in a quartz sleeve.

Photolytic and photocatalytic degradation procedure

Phenol solutions were prepared by spiking ultrapure water with the required amount of phenol. One litre of phenol solution was used for each batch of degradation studies with the experimental setup Configuration A. Continuous mixing of the reactor contents was achieved either by aeration or with a WiseStir MSH 30D magnetic stirrer (Wisd Laboratory Equipments, South Africa), equipped with a temperature probe for on line temperature monitoring. Variations in the pH of the reactor solutions during degradation were monitored with either an Orion3 Star portable pH Meter (Thermo Electron Corporation, USA); or an HQ11p portable pH Meter (HACH, USA, supplied by Aqualytic Environmental & Laboratory, South Africa). All experiments were conducted at natural pH.

Progress of degradation was checked by monitoring the concentration of phenol left in solution at regular intervals by HPLC analysis. In all experimental batches, 2 mℓ aliquots were withdrawn from the reactor at timed intervals, particulate matter was removed by filtration through 0.45 µm syringe filters (Millipore) prior to HPLC analysis. Total reaction time was 60 minutes for both photolytic and photocatalytic systems. The detailed HPLC method is described in Section 3.7.

Effect of oxygen on the degradation kinetics of phenol was studied by carrying out photocatalytic degradation with aeration of the reactor contents. Phenol concentration was fixed at 30 mg/ℓ and TiO_2 concentration was varied from 30 mg/ℓ to 150 mg/ℓ. Phenol and TiO_2 in the reactor in each instance were irradiated with a 400 W UV lamp under a constant flow of air. Aeration of the reactor was achieved by bubbling air through a perforated quartz disc at a flow rate of 5 mℓ/min.

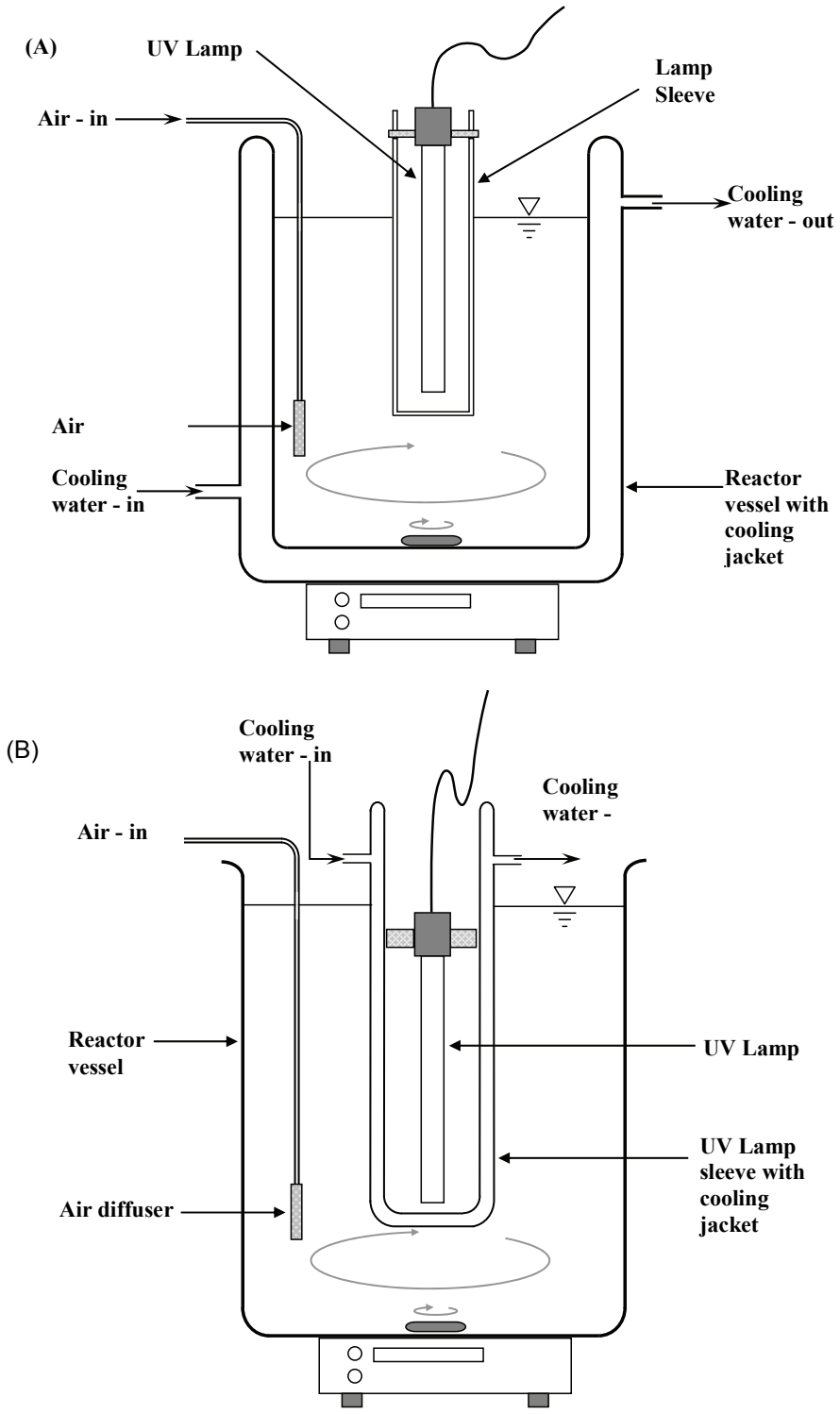

Figure 3.3: Schematics of experimental reactor setup - Configuration A and Configuration B

3.5.2 Photocatalytic degradation of mono-substituted derivatives of phenol

Results obtained during the photocatalytic degradation of phenol indicated that the optimum experimental conditions occurred when the catalyst concentration was 40-60 mg/ℓ under aeration. Photocatalytic degradation of three commonly occurring, mono-substituted phenol derivatives (2-chlorophenol, 4-chlorophenol and 4-nitrophenol) were photocatalysed under the optimum conditions obtained during phenol photocatalysis. Thirty mg/ℓ of each

compound was photocatalysed as a single pollutant in water using titanium (50 mg/ℓ) irradiated with 400 W UV lamp in reactor Configuration A. Progress of degradation was recorded for each compound by monitoring the concentration of the compound left in solution. Concentrations of phenolic compounds were measured by HPLC analysis with conditions as stated in Section 3.7. Degradation kinetics of the three phenol derivatives were compared with that of unsubstituted phenol.

3.6 Photocatalytic Degradation of Geosmin

Photocatalytic degradation of geosmin was conducted in a slightly modified reactor configuration. The setup consisted of a 2 ℓ glass reactor (Pyrex® glass (Corning, NY); with the UV lamp enclosed in a double walled quartz sleeve. Temperature in the reactor was controlled by circulating the cooling water through the outer jacket of the double walled quartz sleeve (reactor Configuration B). See Figure 3.3 for the schematics of reactor Configuration B. The reactor contents were continually aerated at a flow rate of 10 mℓ/min through an air flow meter and a perforated quartz disc or a quartz rod. Dissolved oxygen (DO) was measured with a HQ30d DO Meter (HACH, USA; supplied by Aqualytic Environmental & Laboratory, South Africa)

Photocatalytic degradation of geosmin was conducted in batch with reactor Configuration B with 1 ℓ solutions of geosmin (220 ng/ℓ). The concentration of geosmin chosen for degradation studies represents environmentally significant levels obtained from analysis of source and filter backwash water samples from Rietvlei and Roodeplaat water treatment plants conducted over a period of 11 months during the course of this study (Table 3.5). Solutions of geosmin were prepared by spiking ultrapure water with geosmin standards at the required concentrations. These were treated under three different conditions listed below:

1. With anatase TiO_2 (40 mg/ℓ); irradiated with:
   - low pressure UV lamp; and
   - medium pressure UV lamp.
2. With TiO_2 at varied concentrations (40-100 mg/ℓ), irradiated with the medium pressure UV lamp.
3. With TiO2 in the absence of UV radiation.

Table 3.5: Phenol and catalyst concentration combinations

Phenol Conc. (mg/ℓ)	**Titanium Dioxide Concentration (mg/ℓ)**									
	10	**20**	**30**	**40**	**50**	**60**	**70**	**90**	**100**	**150**
10	x	x	x	x	x	--	--	--	x	x
20	--	--	x	x	x	--	--	--	x	x
30	--	--	x	x	x	x	x	x	x	x

Aliquots (12 mℓ) were withdrawn from the reactor at predetermined intervals and filtered through 0.22 µm syringe filters (Millipore). Ten mℓ of the filtered solution was analysed in the GC/MS after the addition of 3 g of salt and 0.5 mℓ of t-butanol. Tertiary butanol was added as a radical scavenger to prevent further degradation by hydroxyl radicals in solution during analysis. Total reaction time in all instances was 60 minutes. Gas chromatograph/ mass

spectrometer conditions used to monitor the progress of degradation of geosmin are listed in Table 3.3. The SIR scan parameters used for this set of analyses are as presented in Table 3.4b.

Degradation of taste and odour compounds in water samples from treatment plants
Degradation of geosmin in the actual backwash water samples from the treatment plants was conducted under the same conditions as were used for laboratory degradation of the synthetic geosmin solutions. This set of experiments was conducted in November 2009 with the intent of using water samples with high concentrations of taste and odour compounds, but analysis of these revealed very low concentrations of geosmin and 2-MIB. Degradation experiments on field samples were therefore conducted on the filter backwash water from Rietvlei spiked with geosmin (220 ng/ℓ), representing the highest concentrations previously obtained in the analysis of the field samples.

3.7 HPLC Analysis

The HPLC system used for analysis of phenolic compounds consists of a Waters Alliance system with a Waters 2695 separation module equipped with an autosampler and a Photo Diode Array (Waters 2998 PDA) detector.

The HPLC analysis of the synthetic water containing phenolics and their degradation products was performed using the EPA Method 604 with a Symmetry C_{18}, 150 x 3.9, 5µm column. A binary gradient mobile phase consisting of 1% acetic acid in water (Solvent A) and 1% acetic acid in acetonitrile (Solvent B) was used at a flow rate of 1.2 mℓ/min.

The mobile phase gradient was from 70% of Solvent A, 30% Solvent B at Time zero to 0% of Solvent A and 100% of Solvent B at 20 minutes. Injection volume was 20 µℓ. Concentrations of phenolics were obtained at 280 nm from calibration curves of standard solutions for each of the four phenolic compounds.

CHAPTER FOUR

4 RESULTS AND DISCUSSION

4.1 Predominant Organic Compounds Identified in Water Samples

Organic compounds identified during GC/MS analysis of the water samples from Rietvlei and Roodeplaat are listed in Table 4.1. Forty-two VOCs and SVOCs belonging to ten different classes of compounds were qualitatively identified. Taste and odour compounds, geosmin and 2-MIB were positively identified and quantified with analytic standards.

Qualitative identification of organic compounds was automatically conducted by the Turbomass software using the inbuilt library of compounds. This was achieved by comparing the peak distribution in the mass spectra of the unknown compounds in the water samples with the peaks in the spectra of similar compounds in the NIST Library. The peak fitting by the software is conducted in the right to left scan (forward fit) and a left to right scan to obtain the reverse fit values (at a scale of 1 to 1 000). The most probable compound for each peak was chosen from the generated list of likely compounds using the peak fit parameter of 500 and above. The compounds, the individual retention times (t_R) in the TIC and the NIST library match parameters are presented in Table 4.1. The mass spectra of the analytes in the water samples and the spectrum of the corresponding compounds from the NIST library match of some selected compounds are presented as head to tail spectra in Appendix A. The identified compounds are discussed grouped into the different classes of compounds and by known applications.

4.1.1 Classes of compounds

Compounds listed in Table 4.1 can be classified into ten different classes, which include:

- Phenolic compounds (Phenols)
- Polycyclic aromatic hydrocarbons (PAHs)
- Quinones
- Taste and odour compounds
- s-triazine-ring herbicide
- Carbonyl compounds – ketones and aldehydes
- Acid esters
- Hydrocarbons – alkanes and alkenes
- Alcohols
- Indene

4.1.2 Phenols

Two phenol derivatives, 2-(1,1-dimethylethyl)-5-methylphenol and 2,6-bis[1,1-dimethylethyl]-4-methylphenol (butylated hydroxyltoluene) commonly used as preservatives and antioxidants (Eriksson et al., 2003) were identified in the raw inlet and filter backwash water samples from both sources**.** Phenols are classified as water pollutants and have a MCL of 0.5 µg/ℓ set by the European Community Directive (1980), and a US EPA limit of 1 mg/ℓ (US EPA, 2009; Steiner et al., 2008 (Appendix D)) in drinking water. Though specific limits are not stated in the South African drinking water quality standards (SA DWQS), the range 0-1 mg/ℓ is listed as suitable for long term intake (DWAF, 1996). The SA DWQS further states

that a toxic concentration of 3 mg/ℓ is given for phenol by the World Health Organization (WHO, 2008); and the ingestion of a concentrated solution of phenol leads to severe pain and shock leading to renal damage, circulatory collapse and eventual death. The fatal dose is of the order of 1500 mg (DWAF, 1996).

Table 4.1: List of organic compounds identified in water samples from Rietvlei and Roodeplaat

S / no.	t_R (min)	Compound	Fit	Reverse fit
1	7.645	Octane (C_8H_{18})	897	904
2	8.140	Butanoic acid, methylester ($C_5H_{10}O_2$)	844	896
3	8.290	2,5-dimethylheptane (C_9H_{20})	783	865
4	8.900	4-methyloctane (C_9H_{20})	874	893
5	9.055	3-methyloctane (C_9H_{20})	889	891
6	9.706	Nonane (C_9H_{20})	906	908
7	10.076	2,4,6-trimethylheptane ($C_{10}H_{22}$)	785	903
8	10.136	[1,3]Diazepan-2,4-dione ($C_5H_8N_2O_2$)	551	656
9	10.281	3,5-dimethyloctane ($C_{10}H_{22}$)	800	882
10	10.526	Decane ($C_{10}H_{22}$)	786	873
11	11.041	4-ethyloctane ($C_{10}H_{22}$)	712	917
12	11.206	4-methylnonane ($C_{10}H_{22}$)	867	872
13	11.291	2-methylnonane ($C_{10}H_{22}$)	887	888
14	11.461	3-methylnonane ($C_{10}H_{22}$)	879	889
15	12.057	2-octanone ($C_8H_{16}O$)	883	889
16	12.222	Decane ($C_{10}H_{22}$)	928	934
17	12.622	2,4,6-trimethylheptane ($C_{10}H_{22}$)	732	863
18	12.697	4-ethylheptane (C_9H_{20})	515	746
19	12.697	2,6,7-trimethyldecane ($C_{13}H_{28}$)	781	874
20	13.692	5-methyldecane ($C_{11}H_{24}$)	844	844
21	13.787	4-methyldecane ($C_{11}H_{24}$)	835	845
22	13.902	2-methyldecane ($C_{11}H_{24}$)	904	908
23	14.066	3-methyldecane ($C_{11}H_{24}$)	923	932
24[1]	14.309	Acetophenone	718	891
25	14.828	Octadecanoic acid, ethenylester ($C_{20}H_{38}O_2$)	617	654
26	15.072	Nonanal ($C_9H_{18}O$)	693	829
27[2]	16.93	2-Methylisoborneol (2-MIB) ($C_{11}H_{20}O$)	636	654
28	16.935	3,4,5,6,7,8-hexahydro-4a,8a-dimethyl-1 H-Naphthalen-2-one ($C_{12}H_{20}O$)	700	725
29	16.935	2-Propylcyclohexanol ($C_9H_{18}O$)	556	602
30	17.422	Naphthalene ($C_{10}H_8$)	675	810
31	17.496	1-methylene -1H –indene	663	828
32	18.202	2,2,3,3-tetramethylcyclopropanemethanol ($C_8H_{16}O$)	688	736
33	20.087	Propanoic acid, 2-methyl-2,2-dimethyl-1-[2-hydroxylmethyl]propylester($C_{12}H_{24}O_3$)	562	679
34[3]	21.293	2-(1,1-dimethylethyl)-5-methylphenol ($C_{11}H_{16}O$)	481	607
35	21.778	2-methyl-3-hydroxy-2,4,4-trimethylpentylester, propanioc acid	788	820
36	2.053	2-ethenylnaphthalene	794	838
37[2]	22.694	Geosmin ($C_{12}H_{20}O$)	662	778

[1] Detected in DAFF and GAC backwash water only
[2] Identified with standards (Fit parameters from TIC of standards)
[3] Detected in both SPE Extracts and Headspace Analysis

S / no.	t_R (min)	Compound	Fit	Reverse fit
38	23.195	2,5-di-tert-butyl-1,4-benzoquinone ($C_{14}H_{20}O_2$)	695	722
39	23.195	2-(1,-methylethyl)naphthalene ($C_{13}H_{14}$)	441	681
40[3]	23.653	2,6-bis[1,1-dimethylethyl]-4-methylphenol also known as Butylated hydroxytoluene ($C_{15}H_{24}O$)	879	886
41	24.834	Propanoic acid, 2-methyl-1-[1,1-dimethyl]-2-methyl-3-propanediylester ($C_{16}H_{30}O_4$)	866	885
42[4]	32.36	Atrazine		

The SA DWQS suggest oxidation for the treatment of phenols as they are not effectively removed from water using conventional water treatment techniques, and discourages the use of chlorine due to the strong tendency of formation of chlorophenols on chlorination (DWAF, 1996). In addition to the formation of chlorophenols, phenols are a major source of DBP precursors during chlorination. They are prone to partial degradation forming acetates and other short-chain fatty acids that readily combine with chlorine to form HAAs in water.

Butylated hydroxyltoluene can be classified as a phenol and a toluene. Potential health effects from toluene ingestion include nervous system, kidney or liver problems and the US EPA has set the MCL and MCLG for toluene at 1 mg/ℓ (US EPA, 2009).

4.1.3 Polycyclic aromatic hydrocarbons

Analysis of the water samples from both treatment plants revealed the presence of three polycyclic aromatic hydrocarbons (PAHs). These include naphthalene, 2-ethenylnaphthalene and 2-(1-methylethyl)naphthalene. Polycyclic aromatic hydrocarbons are compounds of environmental concern arising from incomplete combustion of organic material. They are common constituents of petroleum, coal tar and shale oil, but are most frequently formed by incomplete combustion of fossil fuels or formed in industrial activities, in vehicle exhaust fumes; and from domestic heating (Bacaloni et al., 2004; Maila and Cloete, 2002). Another potential source of PAH contamination is leaching from linings of storage tanks. Potential health risks include reproductive difficulties and carcinogenity (US EPA, 2009). Polycyclic aromatic hydrocarbons are resistant to conventional oxidation and biodegrade slowly; requiring 60 days for complete degradation of naphthalene and 120 days to achieve 5-87% degradation for higher members (Ashok et al., 1995). Possibility of faster degradation of these classes of compounds would enhance their removal from filter backwash water and reduce the chances of their build up back in the treatment train.

4.1.4 Quinones

Other compounds present include 2,5-di-tert-butyl-1,4-benzoquinone (DBBQ), which has been identified as the major auto-oxidation product of the antioxidant 2,5-di-tert-butyl-4-hydroxyanisole (Daniel et al., 1973).

4.1.5 Carbonyl compounds

Four of the forty-two compounds identified were carbonyl compounds, including one aldehyde (nonanal) and three ketones. The ketones were acetophenone, 2-octanone and 3,4,5,6,7,8-hexahydro-4a,8a-dimethyl-1-H-Naphthalen-2-one. Nonanal is used in flavours

[4] GC/MS analysis of SPE Extracts with HP GC/MS

and perfumery; and has a strong fruity smell. It is also produced by the human body and is believed to attract some species of mosquitoes. 2-octanone is used as a flavouring agent and as a solvent. Acetophenone finds use as a flavouring agent in foods, non alcoholic beverages; and in perfumery as a fragrance ingredient in soaps, detergent, creams, lotions and perfumes. In addition, it is used as a speciality solvent for plastics. The South African DWAF has a threshold concentration of 0.5 mg/ℓ for acetophenone for tainting of organism flesh in water (DWAF, 1995), while it is classified as a group D compound by the US Environmental Protection Agency (US EPA, 2000). In this study Acetophenone was detected only in the backwash water from the DAFF and GAC filters. This could be due to the retention and concentration of the compound in the filters during the process of filtration.
3,4,5,6,7,8-hexahydro-4a,8a-dimethyl-1-H-Naphthalen-2-one is often used as a precursor or an intermediate in the preparation of geosmin (Saito et al., 1996, Hansson et al., 1990) and might be a degradation product (intermediate) in the process of natural degradation of geosmin in surface water samples.

4.1.6 Acid esters

Four acid esters were identified in the water samples. These include three short chain acid esters (C_3-C_4) and one long chain fatty acid (C_{18}). The short chain acid esters include Propanoic acid; 2-methyl-2,2-dimethyl-1-[2-hydroxylmethyl]propylester (MDHP), Propanoic acid, 2-methyl-1-[1,1-dimethyl]-2-methyl-3-propanediylester (MDMP) and butanoic acid, methyl ester. The only long chain fatty acid identified in all the water samples is octadecanoic acid, ethenylester.

Esters have distinctive fruit-like odours, and are commonly used in artificial flavourings and fragrances; and widely used as chemical additives in plasticisers. Due to their various applications they have been identified in diverse environmental samples including groundwater, river water, drinking water, open ocean water, soil, lake and marine sediments (Jianlong et al., 2004).

Although methyl esters in the range of C_8-C_{18} are believed to be non toxic, some research suggests that women have a unique exposure profile to phthalates, which raises concern about the potential health hazards posed by such exposures (Lovekamp-Swan and Davis, 2003).

4.1.7 s-Triazine-ring herbicide (Atrazine)

Gas chromatograph/ mass spectrometer analysis of SPE extracts of water samples from the Rietvlei Treatment Plant revealed the presence of a very weak atrazine peak only in the raw water and the DAFF backwash water samples. Atrazine was not detected in the GC spectrum of filter backwash water from the GAC filters. This could be due the adsorption of organic compounds on the surface of activated carbon. Atrazine was not detected in samples analysed on the headspace GC/MS system. This could be due either to its extremely low concentrations in the water samples, or to the limitation of the use of headspace for the extraction of sufficiently volatilisable compounds with boiling points above 280°C.

Atrazine is commonly discharged in industrial effluents and as runoff from agriculture land. It is an s-triazine-ring herbicide that is used globally to stop pre- and post-emergence

broadleaf and grassy weeds in major crops, and the US EPA (2000) has set a 3 µg/ℓ limit for atrazine.

Though the use of atrazine on heavy clay soils was withdrawn in 1977 in South Africa and the industrial use of atrazine was withdrawn on 31 March 1995, no strong measures have been put in place to enforce the ban. In a study of residual amounts of atrazine, Tshipala (2000) reported levels of 3-20 µg/ℓ in South African surface waters and 0.29-4.36 µg/ℓ in ground waters indicating its continued use.

4.1.8 Alcohols and hydrocarbons

Alcohols identified in the samples include 2-Propylcyclohexanol and 2,2,3,3-tetramethylcyclopropanemethanol. A majority (19) of the compounds identified are straight and branched chains hydrocarbons (paraffins) ranging from C_6-C_{10}. These are major components of fractionation products of petrol and are often found in surface waters especially in environments with high boating activities. There are no reported health or environmental hazards associated with alcohols and lower molecular weight hydrocarbons.

4.2 Taste and Odour Compounds in Water Samples

Taste and odour compounds occur in very low concentrations and their presence or absence in the water samples collected from the raw inlet and the filter backwash water from both Rietvlei and the Roodeplaat water treatment facilities was confirmed with environmental standards. Only two (geosmin and 2-MIB) out of the five taste and odour compounds were detected in the water samples from Rietvlei and Roodeplaat treatment plants. 2-Isopropyl-3-methoxypyrazine (IPMP), 2-methoxy-3-isobutylpyrazine (IBMP) and TCA were not detected in any of the water samples tested.

4.2.1 Quantification of geosmin and 2-MIB

Geosmin and 2-MIB were quantified by SIR scans from linear calibration curves of the individual environmental standards. The values obtained for the geosmin and 2-MIB in the water samples from Rietvlei and Roodeplaat treatment plants are presented in Tables 4.2 and 4.3 respectively.

Table 4.2: Geosmin concentration in water samples from Rietvlei and Roodeplaat Water Treatment Plants

Sample	Geosmin Concentration (ng/ℓ)			
	Jan 2009	May 2009	Aug 2009	Nov 2009
Rietvlei raw	71	74 ± 3	NA	3 ± 0
Rietvlei DAFF	89	221 ± 2	30 ± 1	10 ± 3
Rietvlei GAC	81	88 ± 36	29 ± 1	8 ± 1
Roodeplaat raw	NA	125	28 ± 1	NA
Roodeplaat backwash	NA	111	28 ± 0	NA

Table 4.3: 2-MIB concentration in water samples from Rietvlei and Roodeplaat Water Treatment Plants

Sample	2-MIB Concentration (ng/ℓ)			
	Jan 2009	**May 2009**	**Aug 2009**	**Nov 2009**
Rietvlei raw	NA	91 ± 6	NA	5 ± 0
Rietvlei DAFF	NA	182 ± 59	NA	26 ± 2
Rietvlei GAC	NA	91 ± 1	NA	0.50 ± 0
Roodeplaat raw	NA	151	NA	NA
Roodeplaat backwash	NA	194	NA	NA

NA – Not available

Occurrence of geosmin and 2-MIB in the water samples from Rietvlei and Roodeplaat were at concentrations above the human threshold for all samples, with the exception of the Rietvlei raw inlet water sample of November 2009. Very low concentrations of geosmin (3 ng/ℓ) and 2-MIB (5 ng/ℓ) were observed in the month of November 2009, respectively.

The low values obtained in the summer month of November are contrary to the expected trend of occurrence of taste and odour compounds in South African surface waters as reported by Swanepoel and Du Preez (2006). The reversal in trend could be attributed to climatic changes and heavy rainfalls experienced in and around Pretoria in the summer of 2009. Sampling in November 2009 was conducted after two days of heavy rainfall, and samples were stored under refrigeration for one week prior to analysis. Some degree of auto degradation during storage may have occurred.

The highest concentrations of both geosmin and 2-MIB in the samples analysed were obtained in the autumn month of May 2009. Concentrations of geosmin in May 2009 ranged from 74 ng/ℓ in the Rietvlei Raw inlet water to 221 ng/ℓ in the DAFF filter backwash water. Concentrations of 2-MIB ranged from 91 ng/ℓ in the Rietvlei Raw inlet and GAC water samples to 194 ng/ℓ in the Roodeplaat backwash water samples. In the month of August 2009, relatively low values of geosmin (28-31 ng/ℓ) were obtained for all water samples analysed. However, results from one year of analysis are not enough to draw conclusions on the seasonal occurrence of the compounds.

4.2.2 Retention of organic compounds on filters

Higher values of geosmin and 2-MIB in the filter backwash water samples indicate that organic compounds are filtered out of the water and retained on the filters during the filtration process. Retention was calculated using Equation 4.1:

$$\text{Retention (\%)} = \left(\frac{[C_b] - [Ci]}{[C_i]} \right) \times 100 \qquad (4.1)$$

Where:
$[C_i]$ is the concentration organic compound in raw inlet water
$[C_b]$ is the concentration organic compound in filter backwash water.

Retention was most prominent in the DAFF filters both for geosmin, recording 276%, and to a lesser extent for 2-MIB, showing retention of 44% in the November, 2009 samples.

Backwash water from GAC filters showed lower retention for both geosmin (14-167%) and no retention for 2-MIB as shown in Table 4.3.

Retention of geosmin in the sand filters of the Roodeplaat treatment plant was not observed in the samples analysed during this study, as the geosmin concentrations were either the same in both inlet and backwash water (November 2009), or lower in the backwash water (August 2009). However, retention of 2-MIB (28.49%) was observed in the water from the sand filters of the Roodeplaat treatment plant (Table 4.3).

Geosmin was chosen as a representative test compound for taste and odour compounds for degradation studies. Concentrations obtained were used in setting up the laboratory photocatalytic degradation experiments for the geosmin degradation.

4.3 Turbidity

Filter backwash water is highly turbid, with turbidity values obtained from the GAC and DAFF filters ranging from 37-135 mg/ℓ to 63-161 mg/ℓ respectively (Table C-2 in Appendix C). No serious health impacts are associated with highly turbid waters, but SA DWQS states that a "slight chance of adverse aesthetic effects and infectious disease transmission exists" (DWAF, 1996). Concerns regarding highly turbid water are due to the possible screening of UV photons by particles in solution during water treatment with processes involving UV radiation. The high turbidity of filter backwash water might be a major setback in reclamation systems, especially if treatment involves the use of UV radiation as used in photocatalytic systems.

4.4 Photocatalytic Degradation of Test Compounds

4.4.1 Degradation of geosmin

Effect of light intensity on degradation efficiency of geosmin

Environmentally significant concentrations of geosmin were rapidly degraded by photocatalysis with the medium pressure lamp achieving 95.8% removal in 60 minutes. The low pressure lamp under the same reaction conditions achieved only 49.6% removal after 60 minutes of treatment. Results showing the progress of degradation (as percentages removed) for both lamps are presented in Table B-1 (Appendix B). Under these conditions geosmin levels below human detection threshold were obtained with the medium pressure lamp. Based on its superior performance, further experiments to optimise the catalyst concentration were performed with the medium pressure lamp.

Effect of catalyst loading

The effect of catalyst loading on the degradation efficiency of geosmin at 220 ng/ℓ was evaluated over a catalyst concentration range of 40-100 mg/ℓ, irradiated with the medium pressure lamp. These effects are presented graphically in Figure 4.1. A system containing only TiO_2 (100 mg/ℓ) without UV irradiation was used as a control.

Rapid degradation was obtained for all TiO_2 concentrations under photocatalysis. Observed degradation rates increased with increasing TiO_2 concentration to an optimum of 60 mg/ℓ. This is expected for photocatalytic systems, as stated by Herrmann (1999) and Lawton et al. (2003). Complete degradation was achieved at catalyst concentrations of 60 mg/ℓ after

40 min of treatment. This is in line with findings from other studies on photocatalytic degradation of phenolics (Barakat et al., 2005; Hong et al., 2001; Serpone, 1997). Although literature reports showing effect of catalyst loading for geosmin degradation are lacking, the general observed trend reflects an increase in organic degradation rate with increasing catalyst concentration to a maximum beyond which a negative effect is observed (Herrmann, 1999; Serpone, 1997). Negative effects at higher catalyst concentration are attributed to screening of photons of light by excess catalyst particles dispersed in water.

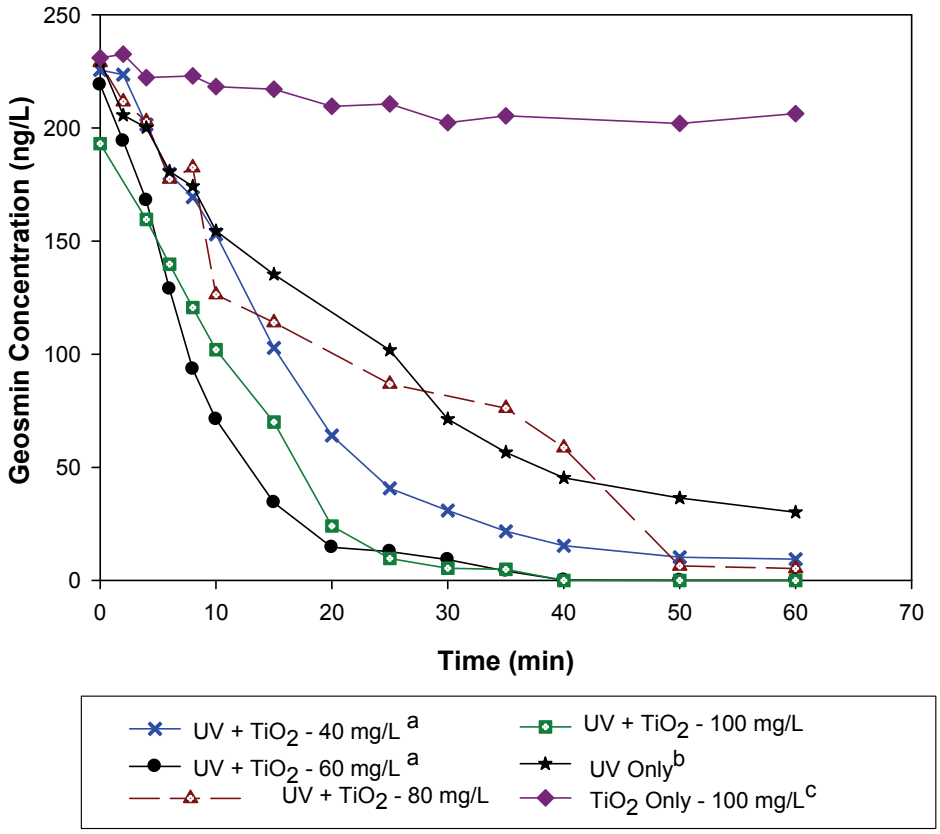

Figure 4.1: Degradation profile of geosmin (220 ng/ℓ) under various experimental conditions: (a) photocatalysis - UV 400 W and TiO_2 (40-100 ng/ℓ); (b) photolysis - UV (400 W) only; and (c) TiO_2 only (100 ng/ℓ). All systems were aerated.

The control (TiO_2 and aeration only) achieved only about 10% degradation, which is an indication that the catalyst and/or aeration are ineffective for geosmin removal. Activation of reactive sites on the catalyst by UV irradiation process is thus a key factor to an efficient photocatalytic system.

Ultraviolet irradiation alone in the absence of the catalyst (photolytic system) achieved about 86% degradation after 60 minutes. Residual concentration obtained of 30 ng/ℓ, after 60 minutes of treatment was above the human threshold.

4.5 Kinetic Considerations

4.5.1 Kinetics of semiconductor photocatalytic reactions

Kinetics for the destruction of single organic pollutant systems by semiconductor photocatalysis exhibit similar features. The initial kinetics of photomineralisation of a single

general pollutant, *P*, by oxygen sensitised by TiO_2, upon steady state illumination, generally fit a Langmuir-Hinshelwood kinetic scheme (Mills and Lee, 2004; Hong et al., 2001; Herrmann 1999; Hoffmann et al., 1995; Mills et al., 1993), represented by equation 4.2:

$$R_i = \frac{-\mathrm{d}[C]o}{\mathrm{d}t} = \frac{k\mathrm{K}[C]o}{1+\mathrm{K}[\mathrm{C}]o} \tag{4.2}$$

Where: R_i = initial rate of pollutant degradation (ng/ℓ. min^{-1}),
$[C]_o$ = initial concentration of pollutant (ng/ℓ),
K is equilibrium adsorption constant (mg/$ℓ^{-1}$), and
k =pseudo first order reaction rate constant (min^{-1}).

$$\ln\left(\frac{C_o}{C}\right) = k \times t \tag{4.3}$$

Where: C_o is the initial concentration of geosmin at time *t*=0, and
C is the residual concentration of geosmin left in solution at time *t*.

Plots of $\ln C_o/C$ as a function of time for the various test solutions gave linear curves, typical of pseudo first order kinetics of photocatalytic systems. Pseudo first order rate constants were obtained from linear transforms of the plot of $\ln C_o/C$ as a function of time from apparent first order kinetic equation. The linear transform for geosmin degradation for the degradation profile in Figure 4.2. These are presented in Table 4.4 for geosmin.

4.5.2 Photonic efficiency

Photocatalytic degradation occurs due to the oxidation of organic compounds by hydroxyl radicals generated from reduction of oxygen on the surface of the catalyst and by the photogenerated holes. Both processes depend on the effective utilisation of UV radiation on the catalyst surface. The efficiency of the photocatalytic process can be measured indirectly by the photonic efficiency (δ) of the UV radiation on the surface of the catalyst, or by the quantum yield (Φ) (Ao et al., 2008; Mills and Lee, 2004; Serpone, 1997). Values for photonic efficiency for the system were obtained from Equation 4.4.

The photonic efficiency δ is used as a rough guide to the efficiency of semiconductor photocatalytic systems and δ is defined as:

$$\delta = \frac{\text{Overall rate of photocatalytic reaction}}{\text{Intensity of incident light}} \tag{4.4}$$

The values for the rate constants *k*, initial reaction rates R_i, photonic efficiency δ, and quantum yield Φ of the various systems studied are given in Table 4.4.

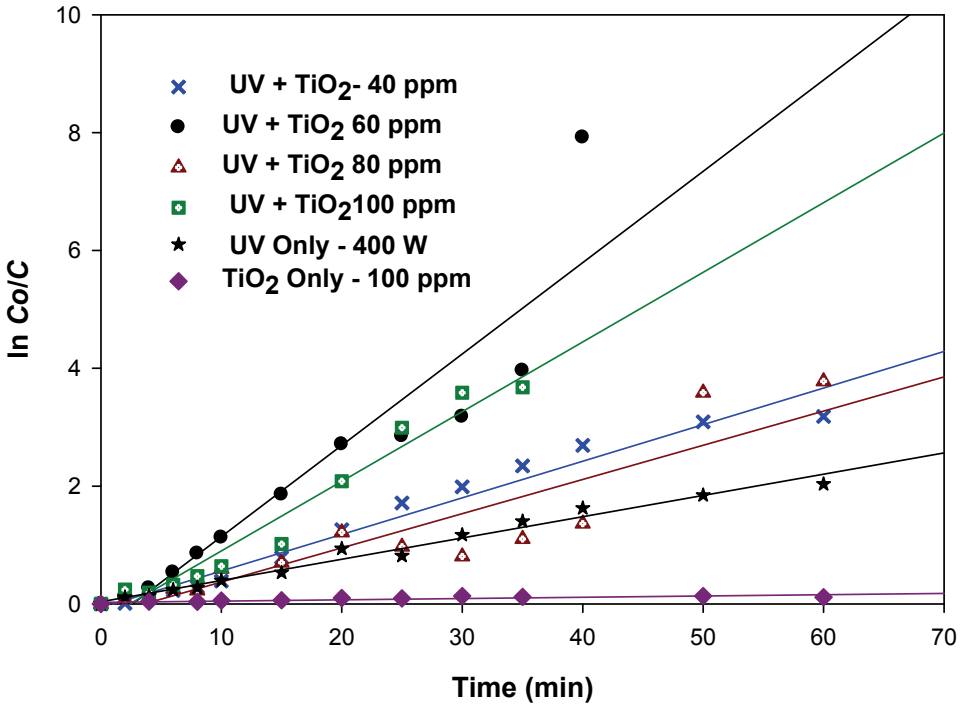

Figure 4.2: First order linear transform $\ln(C_o/C) = f(t)$ of the kinetics of geosmin degradation for degradation profile in Figure 4.1

Table 4.4: Kinetic parameters and photonic efficiencies: geosmin degradation

Reaction Conditions	R_i (ng/ℓ min^{-1})	$k \times 10^{-2}$ (ng/ℓ min^{-1})	R^2	$K \times 10^{-3}$ (ng/ℓ $^{-1}$)	$\delta \times 10^{-2}$	$\Phi \times 10^{-2}$
TiO_2 40 mg/ℓ /UV – 9W	3.312	1.03	0.98	4.582	5.282	5.44
TiO_2 40 mg/ℓ /UV - 400W	7.262	6.21	0.97	4.471	2.929	0.96
TiO_2 60 mg/ℓ /UV - 400W	14.784	15.50	0.87	4.614	7.311	1.96
TiO_2 80 mg/ℓ /UV - 400W	10.269	5.80	0.84	4.392	2.360	1.36
TiO_2 100 mg/ℓ /UV - 400W	9.110	11.82	0.96	5.248	5.575	1.21
**Geosmin	--	4.8×10^{-3} µM Min^{-1}		24.55 µM^{-1}	2.24	--

** Lawton et al. (2003)

4.6 Degradation of Phenol

4.6.1 Effect of titanium dioxide loading on degradation efficiency

The effect of catalyst loading on photocatalytic degradation performances for 10 mg/ℓ and 30 mg/ℓ solutions of phenol are presented in Figures 4.3 and 4.4 respectively. The degradation progress calculated as percentages removed from solution with time is presented in Appendix B (Tables B1 and B2 respectively). The comparative performance of photolysis alone with photocatalysis at the various catalyst concentrations is also presented in Figure 4.5; and in Tables B1 and B2.

Degradation efficiency increased with increasing catalyst concentration to a maximum at the catalyst concentration of 50 mg/ℓ for phenol solution of 10 mg/ℓ. Further catalyst loading beyond 50 mg/ℓ was detrimental to the system, as shown by the longer reaction times for complete degradation at catalyst concentrations of 100 mg/ℓ (20 minutes) and 150 (30 minutes) (Figure 4.3).

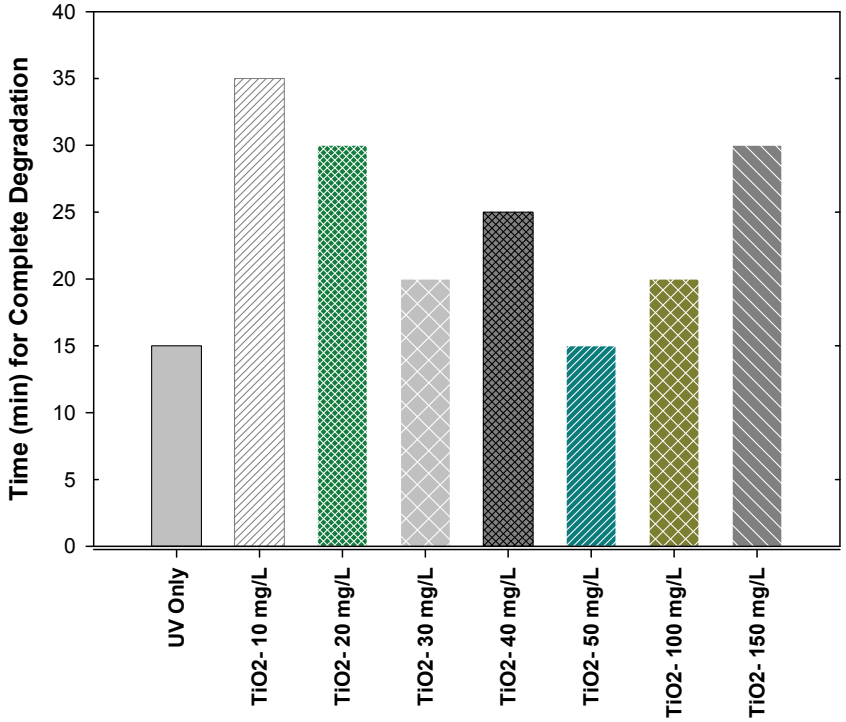

Figure 4.3: Comparative photolysis and photocatalytic degradation performance for phenol at an initial concentration of 10 mg/ℓ using 400 W UV lamp and TiO_2 (10-150 mg/ℓ)

Comparative performance efficiencies were observed for the photolytic system and the best performing photocatalytic system at 50 mg/ℓ catalyst concentration. This suggests that at catalyst concentrations higher than 50 mg/ℓ, there are reduced active sites due to reduced UV light transmittance in solution as a result of screening effect of the UV radiance by excess catalyst. This trend is in line with findings other researchers (Hong et al., 2001; Hermann, 1999).

Although longer reaction times were required for complete degradation of phenol at 20 mg/ℓ phenol concentration, the best performing system was that of the photocatalytic system at 50 mg/ℓ catalyst. At higher phenol concentration, the contribution from the catalyst becomes apparent. Relatively comparable performance of the photolytic and the photocatalytic system was observed at catalyst concentrations between 30-40 mg/ℓ.

4.6.2 The role of oxygen on degradation efficiency

The initial assumption was that oxygen supply into the magnetically stirred open vessel reactor was adequate for the oxygen requirements given in Equation 4.2 for mineralisation of phenol. Degradation rates and the first order kinetic constants obtained were low and too close in magnitude to those obtained for the photolytic system. This led to the introduction of the aeration component into the reactor system. Aeration led to improved degradation of

both the photolytic the photocatalytic systems at all catalyst concentrations studied; improvement in rates was observed when the systems were aerated, as shown in Figure 4.4.

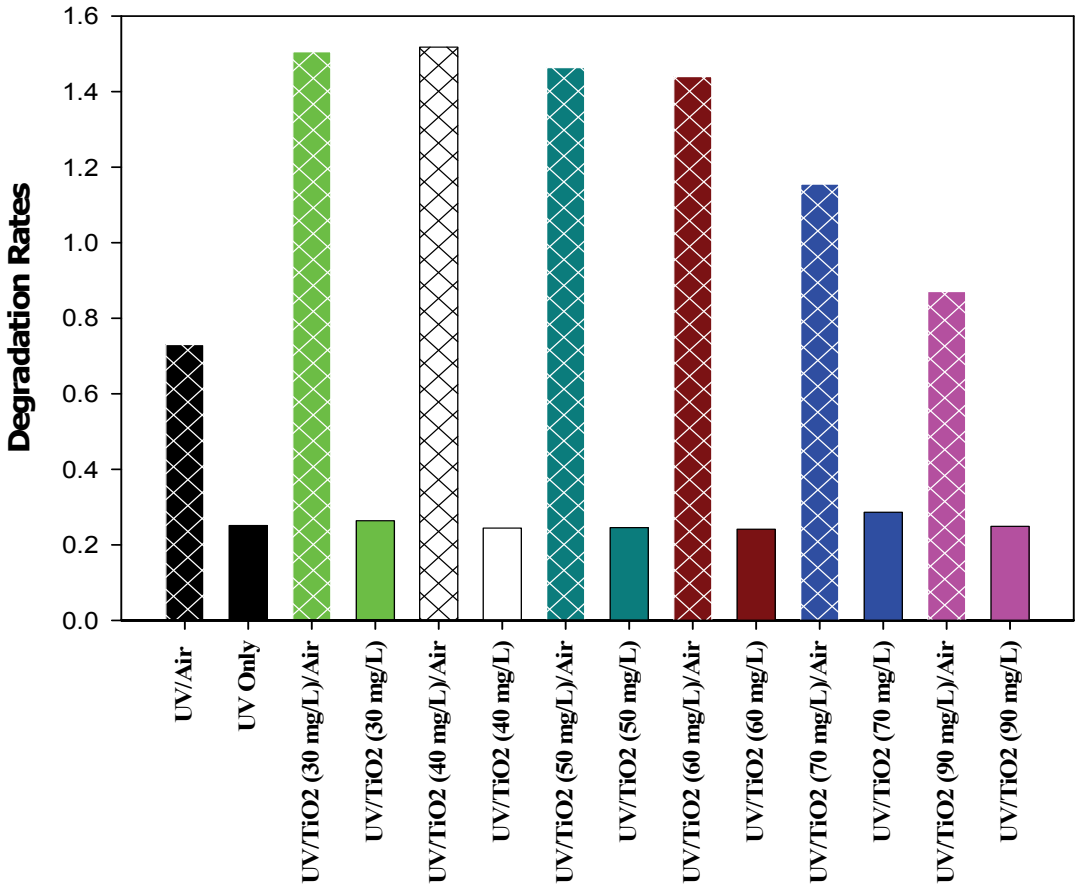

Figure 4.4: Effect of aeration on phenol degradation rates at an initial phenol concentration of 30 mg/ℓ

This is an indication that with a limited supply of oxygen, degradation might be due primarily to oxidation by reactive holes formed on the catalyst surface and photolysis. Higher rates of aeration could be due to the synergic effect of oxidation due to photolysis, oxidation from the holes on the surface of the catalyst and from hydroxyl radicals formed from the reduction of oxygen by photogenerated electrons on the catalyst surface. This is supported by the very close rates obtained for the photolytic and photocatalytic systems in the unaerated systems (Figure 4.4).

Aeration resulted in complete mineralisation within 30-50 minutes of treatment while the unaerated samples required 120 minutes. Mineralisation was not achieved after 120 minutes at catalyst concentration of 90 mg/ℓ.

The first order linear transforms for phenol at different catalyst concentration are presented in Figure 4.5. At lower phenol concentration (10 and 20 mg/ℓ) degradation rates as obtained increased with increase in catalyst concentration. The most remarkable increase was recorded at a low phenol concentration of 10 mg/ℓ with a 132% increase in rates recorded for an increase in catalyst concentration from 10 to 50 mg/ℓ. The highest rates were obtained at

a catalyst concentration of 50 mg/ℓ. Further increase in catalyst concentration to 100 and 150 mg/ℓ resulted in a decrease in rates to 0.49 and 0.32 mg/ℓ/min respectively, corresponding to a 24.6 and 50.8% drop in efficiency from the maximum rate of 0.65 mg/ℓ/min at 50 mg/ℓ catalyst concentration. This suggests that at catalyst concentrations higher than 50 mg/ℓ, there are reduced active sites due to reduced UV light transmittance in solution as a result of a screening effect on the UV radiance by excess catalyst. This trend is in line with findings of other researchers (Rao et al. 2009; Hong et al., 2001; Hermann, 1999).

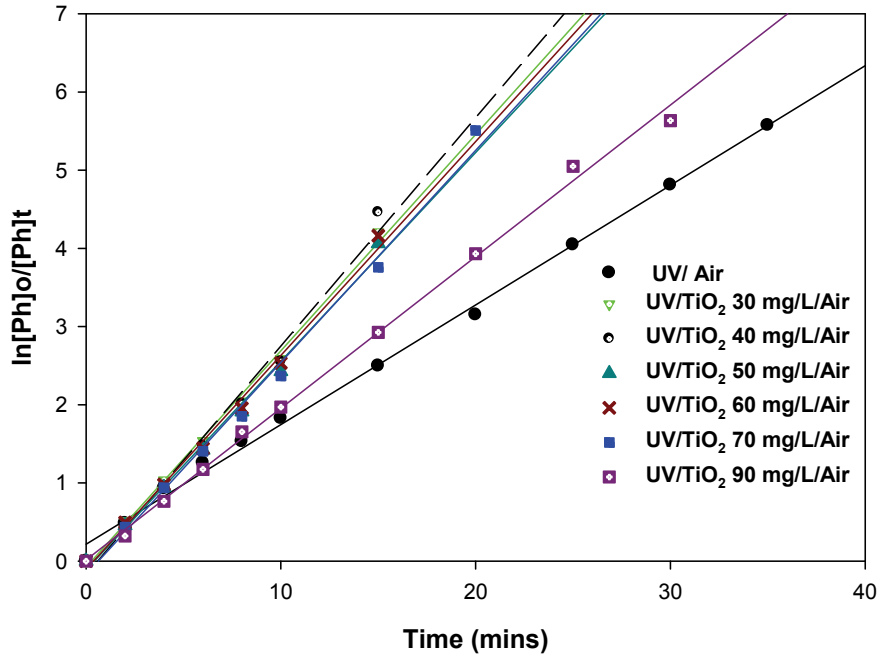

Figure 4.5: First order rate plot for photolytic and photocatalytic degradation of phenol at various catalyst concentrations

Photocatalytic degradation of phenol has been reported with TiO_2 at much higher catalyst concentrations; between 1-4 g/ℓ (Hong et al., 2001) and 0.2 g/ℓ (Li et al., 2008). The current study achieved faster degradation rates at much lower catalyst concentrations of 50 mg/ℓ (0.05 g/ℓ) than have been previously reported in literature.

4.6.3 Effect of initial pollutant concentration

For both the photolytic and the photocatalytic system at all catalyst concentrations studied, a similar trend with the effect of increasing phenol concentration on the degradation rates was observed. The effects of catalyst concentration and aeration on the degradation rates are presented in Table 4.5.

Table 4.5: First order kinetic parameters for phenol (30 mg/ℓ) for photolytic and photocatalytic systems ([TiO_2] = 30-90 mg/ℓ)

[TiO_2] mg/ℓ	Non Aerated System			Aerated System		
	k (min^{-1}) x 10^{-2}	$t_{1/2}$ (min)	R^2	k (min^{-1}) x 10^{-1}	$t_{1/2}$ (min)	R^2
UV	4.01	17.30	0.963	1.53	4.53	0.99
30	3.35	20.70	0.954	2.77	2.51	0.99
40	3.10	22.38	0.939	2.92	2.37	0.99
50	4.32	16.03	0.951	2.67	2.59	0.99
60	4.27	16.22	0.952	2.74	2.53	0.99
70	4.59	15.10	0.955	2.77	2.56	0.99
90	4.25	16.31	0.958	1.94	3.57	1.0

The optimum catalyst concentration for phenol degradation in the system studied is 50-60 mg/ℓ, above which catalyst screening of the light occurs, resulting in lowered degradation rates.

4.7 Degradation of Mono-Substituted Derivatives of Phenol

Degradation efficiencies of individual phenolic compounds photocatalysed in a noncompeting environment are shown in Figure 4.6, and the degradation rates are presented in Table 4.6.

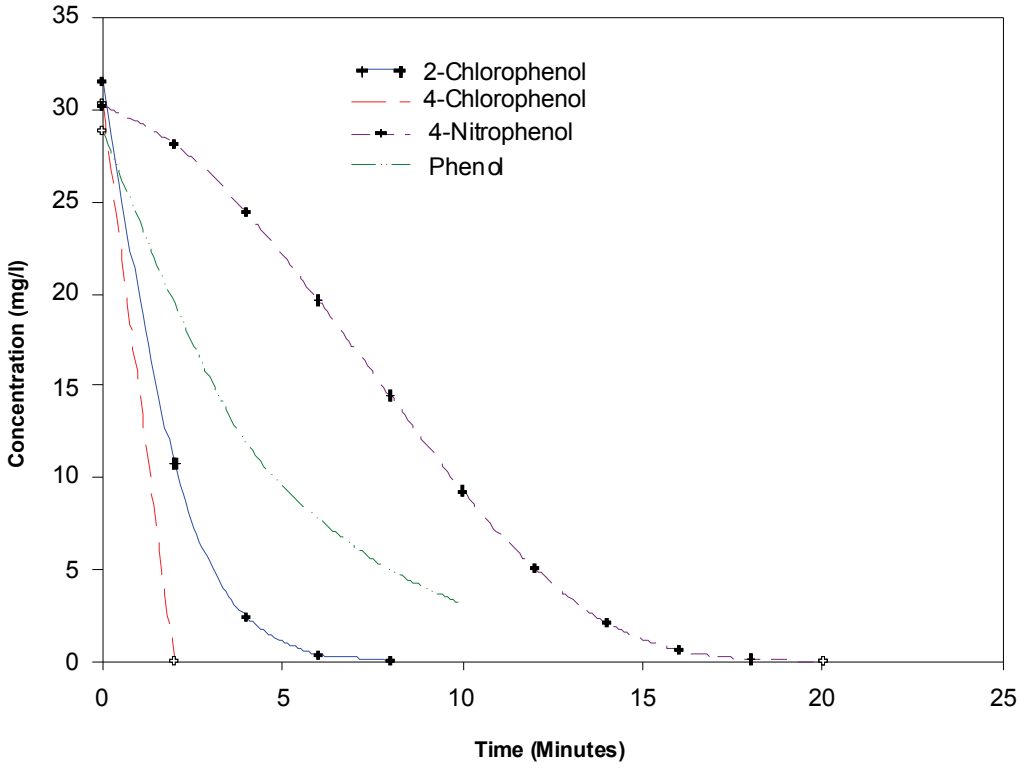

Figure 4.6: Degradation efficiency of individual phenolic compounds (30 mg/ℓ) photocatalysed with 50 mg/ℓ TiO_2

Table 4.6: Degradation rates of phenolic compounds

Compound	Degradation Rates (ng/ℓ min^{-1})
2-Chlorophenol	3.94
4-Chlorophenol	15.20
4-Nitrophenol	1.51
Phenol	2.06

The compounds 2-CP and 4-CP exhibited superior photocatalytic degradation rates to the parent phenol and 4-nitrophenol when tested as individual pollutants in solution. Complete degradation of 4-CP was achieved after 2 minutes of treatment while 2-CP degradation required 8 minutes - four times longer than the time requirement for 4-CP degradation (Figure 4.6). Phenol was completely degraded in 14 minutes and 4-nitrophenol in 20 minutes.

Photocatalysis with anatase TiO_2 appeared to be a promising method for degradation of aromatic chlorinated phenolic compounds.

CHAPTER 5

5 CONCLUSIONS AND RECOMMENDATIONS

Organic pollutants of concern were detected in the raw water and backwash water of the local water treatment plants (Rietvlei and Roodeplaat Water Treatment Works). The organics of concern detected in the water were the taste and odour causing compounds *trans*-1,10-dimethy-*trans*-9-decalol (geosmin) and 2-methyl-isoborneol (2-MIB), the phenolics – naphthalene, 2-ethenylnaphthalene, 2-(1-methylethyl)naphthalene, 2-(1,1-dimethylethyl)-5-methylphenol and 2,6-bis[1,1-dimethylethyl]-4-methylphenol (butylated hydroxyltoluene), and trace amounts of the herbicide atrazine. The investigation into the biodegradability of these families of compounds was conducted using geosmin to represent the semivolatile groups and phenol to represent the aromatic compounds. The taste and odour compound, geosmin completely degraded in the solution after exposure for 40 minutes under an optimum TiO_2 concentration of 50-60 mg/ℓ.

The degradation of the taste and odour compound geosmin at a concentration as high as 220 ng/ℓ is of practical importance since the tested value was an order of magnitude higher than the levels that result in complaints from consumers (1.3 to 6.3 ng/ℓ). The tested range of concentration of phenolics was too high for the purpose of measuring impacts on the drinking water treatment train.

One of the challenges of the current system is the high temperature generated due to the high wattage of the UV lamps used in the study. To circumvent this problem, the lamp sleeve was surrounded by the cooling water jacket. However, this increased the effective circumference of the photoreactor thereby decreasing light intensity. This could drastically increase the power input to the system to achieve the same efficiency.

In future, the cost related to power input using electricity could be lowered by using UV radiation from the sun. Several configurations that could be adopted for use in photocatalysis have been suggested in the report.

REFERENCES

ANDREOZZI R, CAPRIO V and INSOLA A (2000) Kinetics and mechanisms of polyethyleneglycol fragmentation by ozone in aqueous solution. Water Research **30** 2955-2960.

ANDREOZZI R, CAPRIO V, INSOLA A and MAROTTA R (1999) Advanced oxidation processes (AOP) for water purification and recovery. Catalysis Today **53** 51-59.

ANDREOZZI R, CAPRIO V, INSOLA A, MAROTTA R and SANCHIRICO R (2000) Advanced oxidation Processes for the treatment of mineral oil-contaminated wastewaters. Water Research **34 (2)** 620-628.

APHA, AWWA and WEF (1995) *Standard methods for the examination of water and wastewater.* 18th ed., American Public Health Association, Washington D.C., USA

ASHOK BT, SAXENA S, SINGH KP and MUSARRAT J (1995) Biodegradation of polycyclic aromatic hydrocarbons in soil around Mathura oil refinery, India. World Journal of Microbiology and Biotechnology. **11 (6)** 691-692.

AUGUGLISTO V, LITTER M, PALMISANO L and SORIA J (2006) The combination of heterogenous photocatalysis with chemical and physical operations: A tool for improving the photoprocess performance. Journal of Photochemistry and Photobiology Part C: **7** 127-144.

BACALONI A, CAFARO C, DE GIORGI L, RUOCCO R and ZOCCOLILLO L (2004) Improved analysis of polycylic aromatic hydrocarbons in atmospheric particulate matter by HPLC-Fluorescence. Annali di Chimica **94 (9-10)** 751-759

BAHNEMANN D (2004) Photocatalytic water treatment: solar energy applications. Solar Energy **77** 445-459.

BAO M-L, BARBIERI K, BURRINI D, GRIFFINI O and PANTANI F (1997) Determination of trace levels of taste and odor compounds in water by microextraction and gas chromatography-ion-trap detection-mass spectrometry. Water Research **31 (7)** 1719-1727.

BARAKAT MA, TSENG JM and HUANG CP (2005) Hydrogen peroxide-assisted photocatalytic oxidation of phenolic compounds. Applied Catalysis Part B: Environmental **59,** 99-104.

BASSON MS, VAN NIEKERK PH and VAN ROOYEN JA (1997) *Overview of Water Resources Availability and Utilisation in South Africa.* Department of Water Affairs and Forestry, Pretoria, South Africa.

BAUER R, WALDNER G, FALLMANN H, HAGER S, KLARE M, KRUTZLER T, MALATO S and MALETZKY P (1999) The photo-Fenton reaction and the TiO_2/UV process for wastewater treatment-novel developments. Catalysis Today **53** 131-144.

BELTRÁN FJ, RIVAS FJ and MONTERO-DE-ESPINOSA R (2002) Catalytic ozonation of oxalic acid in an aqueous TiO_2 slurry reactor. Applied Catalysis Part B: Environmental **39** 221-231.

BOURGEOIS JC, WALSH ME and GAGNON GA (2004) Treatment of drinking water residuals: comparing sedimentation and dissolved air flotation performance with optimal cation ratios. Water Research **38 (5)** 1173-1182.

BUCHANAN W, RODDICK F and PORTER N (2004) Enhanced biodegradability of UV and VUV pre-treated natural organic matter. Water Science and Technology **4 (4)** 103-111.

BUCHANAN W, RODDICK F and PORTER N (2006) Formation of hazardous by-products resulting from the irradiation of natural organic matter: Comparison between UV and VUV irradiation. Chemosphere **63** 1130-1141.

CARMICHAEL WW (2001) Human fatalities from cyanobacteria: Chemical and Biological cyanotoxins. Environmental Health Perspectives **109** 663-668.

CHEN D, WEAVERS LK and WALKER HW (2006) Ultrasonic control of ceramic membrane fouling by particles: Effect of ultrasonic factors. Ultrasonics Sonochemistry **13** 379-387.

CHEN Y and DIONYSIOU DD (2006) Correlation of structural properties and film thickness to photocatalytic activity of thick TiO_2 films coated on stainless steel. Applied Catalysis Part B: Environmental **69** 25-34.

COMNINELLIS C, KAPALKA A, MALATO S, PARSONS SA, POULIOS I and MANTZAVINOS D (2008) Perspective – Advanced oxidation processes for water treatment: advances and trends for R&D. Journal of Chemical Technology and Biotechnology **83** 769-776.

CONTRERAS S, RODRIGUEZ M, AL MOMANI F, SANS C and ESPLUGAS S (2003) Contribution of the ozonation pre-treatment to the biodegradation of aqueous solutions of 2,4-dichlorophenol. Water Research **37** 3164-3171.

DANIEL JW, GREEN T and PHILLIPS PJ (1973) Metabolism of the phenolic antioxidant 3,5-di-tert-butyl-4-hydroxanisole (Topanol 354). III. The metabolism in rats of the major autooxidation product, 2,5-di-tert-butyl-1,4-benzoquinone . Food and Cosmetics Toxicology. **11**(5) 793-796.

DEVILLIERS D (2006) Semiconductor Photocatalysis: Still an Active Research Area Despite Barriers to Commercialization. Energeia **17 (3)** 1-6.

DIJKSTRA MFJ, BUWALDA H, DE JONG AWF, MICHORIUS A, WINKELMAN JGM and BEENACKERS AACM (2001) Experimental comparison of three reactor designs for photocatalytic water purification. Chemical Engineering Science **56** 547-562.

DOLL TE and FRIMMEL FH (2005) Removal of selected persistent organic pollutants by heterogeneous photocatalysis in water. Catalysis Today **101** 195-202.

DWAF (1996) *South African water quality guidelines. Volume 1: Domestic water use.* Department of Water and Forestry, Pretoria, South Africa

EEC (1980) *Drinking Water Directive 80/778/EEC*. Commission of the European Economic Community, Brussels, Belgium.

ERIKSSON E, AUFFARTH K, EILERSEN A-M, HENZE M and LEDIN A (2003) Household Chemicals and Personal Care Products as Sources for Xenobiotic Organic Compounds in Grey Water. Water SA **29 (2)** 135-146.

ESPLUGAS S, GIMENNEZ J, CONTRETRAS S, PASCUAL E and RODRIGUEZ M (2002) Comparison of different advanced oxidation processes for phenol degradation. Water Research **36** 1034-1042.

FIORENTINO G, SPACCINI R and PICCOLO A (2006) Separation of molecular constituents from a humic acid by solid-phase extraction following a transesterification reaction. Talanta **68** 1135–1142.

GIOKAS DL and VLESSIDIS AG (2007) Application of a novel chemometric approach to the determination of aqueous photolysis rates of organic compounds in natural waters. Talanta **71** 288-295.

GOGATE PR and PANDIT AB (2004) A review of imperative technologies for wastewater treatment I: oxidation technologies at ambient conditions. Advances in Environmental Research **8** 501-551.

GOGATE PR, MUJUMDAR S, PANDIT AB (2003) Sonochemical reactors for waste water treatment: comparison using formic acid degradation as a model reaction. Advances in Environmental Research **7** 283-299.

HALMANN MM (1996) *Photodegradation of Water Pollutants.* CRC Press Inc, New York, 254-255.

HANSSON L, CARLSON R, and SJÖBERG A-L (1990) Synthesis of (±)-Geosmin. Part 1. On the Synthesis and Epoxidation of 1,4a-Dimethyl-4,4a,5,6,7,8-hexahydronaphthalen-2(3H)-one. Acta Chemica Scandinavica **44** 1036-1041.

HARDING WR and PRAXTON BR (2001) Cyanobacteria in South Africa. Research report no. TT 153/01, Water Research Commission, Pretoria, South Africa.

HASSOON S, BULATOV V, YASMAN Y and SCHECHTER I (2004) Fluorescence monitoring pf ultrasound degradation processes. Analytica Chimica Acta **512** 125-132.

HERNANDEZ R, ZAPPI M, COLUCCI J and JONES R (2002) Comparing the performance of various advanced oxidation processes for treatment of acetone contaminated water. Journal of Hazardous Materials **92** 33-50.

HERRMANN J (1999) Heterogenous photocatalysis: fundamentals and applications to the removal of various types of aqueous pollutants. Catalysis Today **53** 115-129.

HO L, HOEFEL D, BOCK F, SAINT CP and NEWCOMBE G (2007) Biodegradation rates of 2-methylisoborneol (MIB) and geosmin through sand filters and in bioreactors. Chemosphere **66 (11)** ***2210-2218.***

HO L, NEWCOMBE G, CROUE´ J-P, (2002) Influence of the character of NOM on the ozonation of MIB and geosmin. Water Research **36** 511-518.

HOFFMANN MR, MARTIN ST, CHOI W, and BAHNEMANN DW (1995) Environmental applications of semiconductor photocatalysis. Chemical Reviews. **95** 69-96.

HONG SS, JU CS, LIM CG, AHN BH, LIM KT and LEE GD (2001) Photocatalytic Degradation of Phenol over TiO_2 Prepared by Sol-Gel Method. Journal of Industrial and Engineering Chemistry. **7 (2)** 99-104.

HUANG W-J, CHENG B-L, HU S-K and CHU C (2006) Ozonation of algae and odour causing substances in eutrophic waters. Journal of Environmental Science and Health Part A **41**1587-1605.

JIANLONG W, XUAN Z and WEIZHONG W (2004) Biodegradation of phthalic acid esters (PAEs) in soil bioaugmented with acclimated activated sludge. Process Biochemistry **39** 1837-1841.

JYOTI KK and PANDIT AB (2001) Water disinfection by acoustic and hydrodynamic cavitation. Biochemical Engineering Journal **7** 201-212.

KITIS M and KAPLAN SS (2007) Advanced oxidation of natural organic matter using hydrogen peroxide and iron-coated pumice particles. Chemosphere **68** 1846-1853.

KLÁN P and VAVRIK M (2006) Non-catalytic remediation of aqueous solutions by microwave-assisted photolysis in the presence of H_2O_2. Journal of Photochemistry and Photobiology A: Chemistry **177** 24-33.

KLUSON P, LUSKOVA H, CERVENY L, KLISAKOVA J and CATJTHAML T (2005) Partial photocatalytic oxidation of cyclopentene over titanium (IV) oxide. Journal of Molecular Catalysis A: Chemical **242** 62-67.

LAWTON LA, ROBERTSON PKJ, ROBERTSON RF and BRUCE FG (2003) The destruction of 2-methylisoborneol and geosmin using titanium dioxide photocatalysis. Applied Catalysis B: Environmental **44** 9-13.

LEE C, YOON J and VON GUNTEN U (2007) Oxidative degradation of N-nitrosodimethylamine by conventional ozonation and the advanced oxidation process ozone/hydrogen peroxide. Water Research **41** 581-590.

LI S, MA Z, ZHANG J, Wu Y and GONG Y (2008) A comparative study of photocatalytic degradation of phenol of TiO2 and ZnO in the presence of manganese dioxides. Catalysis Today **139** 109-112.

LIANG Z, ZHOU G, LIN S, ZHANG Y and YANG H (2006) Study of low-frequency ultrasonic cavitation fields based on spectral analysis technique. Ultrasonics **44** 115-120.

LJUBAS D (2005) Solar photocatalysis – a possible step in drinking water treatment. Energy **30** 1699-1710.

LOVEKAMP-SWAN T and DAVIS BJ (2003) Mechanisms of phthalate ester toxicity in the female reproductive system. Environmental Health Perspectives **111 (2)** 139-145.

MACIEL R, SANT'ANNA GL (Jnr) and DEZOTTI M (2004) Phenol removal from high salinity effluents using Fenton's reagent and photo-Fenton reactions. Chemosphere **54** 711-719.

MAILA MP and CLOETE TE (2002) Germination of *Lepidium sativum* as a method to evaluate polycyclic aromatic hydrocarbons (PAHs) removal from contaminated soil. International Biodeterioration and Biodegradation **50** 107-113.

MALATO S, BLANCO J, ALARCÓN DC, MALDONADO MI, FERNÁNDEZ-IBÁÑEZ P and GERNJAK W (2007) Photocatalytic decontamination and disinfection of water with solar collectors. Catalysis Today **22 (1-2)** 137-149.

MICHALSKI R (2003) Toxicity of Bromate Ions in Drinking Water and its Determination Using Ion Chromatography with Post Column Derivatisation. Polish Journal of Environmental Studies **12 (6)** 727-734.

MILLS A and LEE S (2004) Semiconductor photocatalysis. In: *Advanced Oxidation Processes for Water and Wastewater Treatment*, PARSONS S. IWA Publishing, London, UK, 137-180.

MILLS A, MORRIS S and DAVIES R (1993) Photomineralisation of 4-chlorophenol sensitised by titanium dioxide: a study of intermediates. Journal of Photochemistry and Photobiology A: Chemistry **70** 183-191.

MISRA V, PANDEY SD and VISWANATHAN PN (1998) Chemical approach to study the environmental implications interaction of humic acid and gamma-HCH. Chemistry and Ecology **14** 97-106.

MODRZEJEWSKA B, GUWY AJ, DINSDALE R and HAWKES DL (2007) Measurement of hydrogen peroxide in an advanced oxidation process using an automated biosensor. Water Research 41 260-268.

MOMANI F, SANS C and ESPLUGAS S (2004) A comparative study of the advanced oxidation of 2,4-dichlorophenol. Journal of Hazardous Materials B **107** 123-129.

MUNTER R (2001) Advanced oxidation processes – current status and prospects. Proceedings of the Estonian Academy of Sciences **50** 59-80.

NADEZHDIN AD (1988) Mechanism of ozone decomposition in water. The role of termination. Industrial and Engineering Chemistry Research **27** 548-550.

NAUDE Y (2002) The extraction of persistent organic pollutants from samples from selected sites in South Africa. *Analitika 2002*, Stellenbosch, South Africa, December 2002.

PARSONS SA and WILLIAMS M (2004) *Advanced Oxidation Processes for Water and Wastewater Treatment*. IWA Publishing, London, UK.

PICCOLO A, CONTE P and TAGLIATESTA P (2005) Increased conformational rigidity of humic substances by oxidative biomimetic catalysis. Biomacromolecules **6** 351-358.

PICCOLO A, CONTE P, SPACCINI R and CHIARELLA M (2003) Effects of some dicarboxylic acids on the association of dissolved humic substances. Biology and Fertility of Soils **37** 255-259.

PLUMMER JD and EDZWALD JK (1998) Effect of ozone on disinfection by-product formation of algae. Water Science and Technology **37 (2)** 49-55.

RAJ CBC and QUEN HL (2005) Advanced oxidation processes for wastewater treatment: Optimization of UV/H_2O_2 process through a statistical technique. Chemical Engineering Science **60** 5305-5311.

ROBERTSON PKJ, LAWTON LA, MÜNCH and ROUZADE J (1997) Destruction of cyanobacterial toxins by semiconductor photocatalysis. Chemical Communications 393-394.

ROSAL R, RODRÍGUEZ A, JA PERDIGÓN-MELÓN, PETRE A and GARCÍA-CALVO E (2009) Oxidation of dissolved organic matter in the effluent of a sewage treatment plant using ozone combined with hydrogen peroxide (O_3/H_2O_2). Chemical Engineering Journal **149** 311-318.

SAITO A, TANAKA A and ORITANI T (1996) A Practical Synthesis of Enantiomerically Pure (-)-Geosmin via Highly Diastereoselective Reduction of (4aS, 8S)-4,4a,5,6,7,8-Hexahydro-4a,8-dimethyl-2(3H)-naphthalenone. Tetrahedron: Assymmetry **7 (10)** 2923-2928.

SERPONE N (1997) Relative photonic efficiencies and quantum yield in heterogenous photocatalysis. Journal of Photochemistry and Photobiology A: Chemistry **104** 1-12.

SHIN W-T, MIRMIRAN A, TIACOUMI S and TSOURIS C (1999) Ozonation using microbubbles formed by electric fields. Separation and Purification Technology **15** 217-282.

SMEJKALOVA D and PICCOLO A (2005) Enhanced molecular dimension of a humic acid induced by photooxidation catalyzed by biomimetic metalporphyrins. Biomacromolecules **6** 2120-2125.

SMEJKALOVA D, and PICCOLO A, (2006) Rates of Oxidative Coupling of humic phenolic conomers catalyzed by a ciomimetic iron-porphyrin. Environmental Science and Technology **40** 1644-1649.

STAEHELIN J and HOIGNÉ J (1985) Decomposition of ozone in water in presence of organic solutes acting as promotors and inhibitors of radical chain reactions. Environmental Science and Technology **19** 120-126.

STEINER F, MCLEOD F, ROHRER J, FABEL S, LANG L, QUN X and JING C (2008) Determination of phenols in drinking and bottled mineral waters using online solid-phase extraction followed by HPLC with UV detection. Dionex Product Notes (see Appendix D).

STOCKINGER H, KUT OM and HEIZLE E (1996) Ozonation of wastewater containing N-methylmorpholine-N-Oxide. Water Research **30** 1745-1748.

SUMITA T, YAMAKI T, YAMAMOTO S. and MIYASHITA A (2001) A new characterization method for photocatalytic activity in semiconductor photocatalysis. Japanese Journal of Applied Physics **40** 4007-4008.

SUNG YU-H, LI TY and HUANG SD (2005) Analysis of earthy and musty odors in water samples by solid-phase microextraction coupled with gas chromatography/ion trap mass spectrometry. Talanta **65** 518-524.

SWANEPOEL A and DU PREEZ H (2006). An Incident of High Cyanobacteria Concentrations, Causing Large-Scale Problems in Water Purification. In: *Proceedings of 2nd Water Research Showcase,* University of Pretoria, Pretoria, Oct. 2006.

TSHIPALA KE (2000) Implications of residual atrazine for wheat. M. Inst. Thesis, Department of Microbiology and Plant Pathology, University of Pretoria, Pretoria, South Africa. Available on request from http://upetd.up.ac.za/thesis/available/etd-12112006-170846/.

US EPA (2000) *Hazard Summary*. http://www.epa.gov/ttn/atw/hlthef/acetophe.html. (Accessed 9th December 2009).

US EPA (2009) *National Primary Drinking Water Regulations*. EPA 816-F-09-004 http://www.epa.gov/safewater/consumer/pdf/mcl.pdf. (Accessed 21 June 2010).

Wadley S and Waite TD (2004) Fenton Processes: In: *Advanced Oxidation Processes for Water and Wastewater Treatment*, PARSONS S. IWA Publishing, London, UK. 111-132.

WHO (1999) *Toxic Cyanobacteria in Water: A guide to their public health consequences, monitoring and management.* World Health Organization, Geneva, Switzerland.

WHO (2008) *International Standards for Drinking Water*, 3rd Ed. World Health Organization, Geneva, Switzerland.

WNOROWSKI AU (1992) Taste and odour forming micro-organisms in South African Surface waters. Research report no. 320/1/93, Water Research Commission, Pretoria, South Africa.

YOUNG WF, HORTH H, CRANE R, OGDEN T and ARNOTT M (1996) Water Research **30** 331.

ZAITLIN B and WATSON SB (2006) Actinomycetes in relation to taste and odour in drinking water: Myths, tenets and truths. Water Research **40** 1741-1753.

ZHOU H and SMITH DW (2002) Advanced technologies in water and wastewater treatment. Journal of Environmental Engineering and Science **1** 247-264.

APPENDIX A

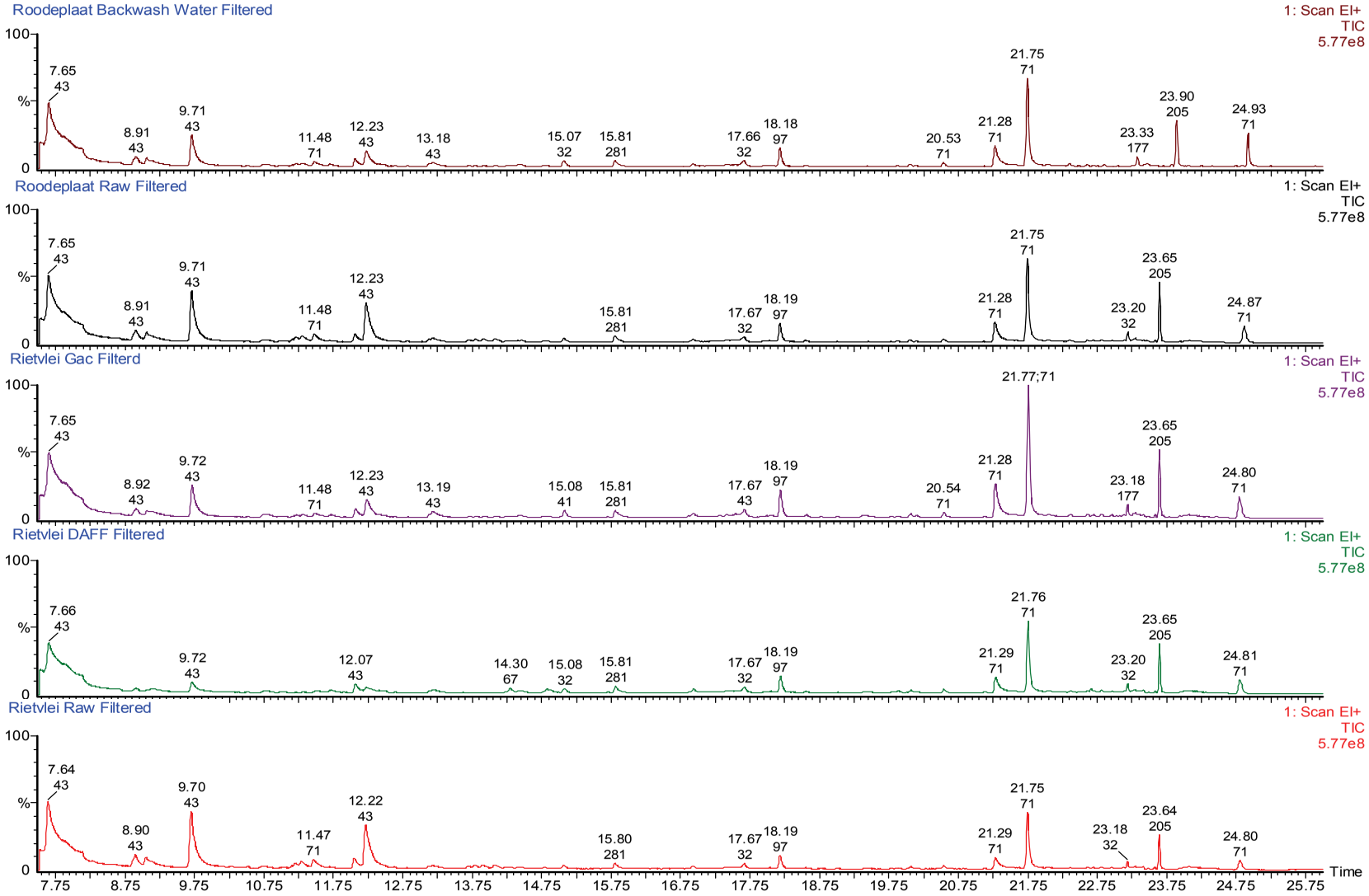

Figure A-1: Chromatogram of water samples from Rietvlei and Roodeplaat

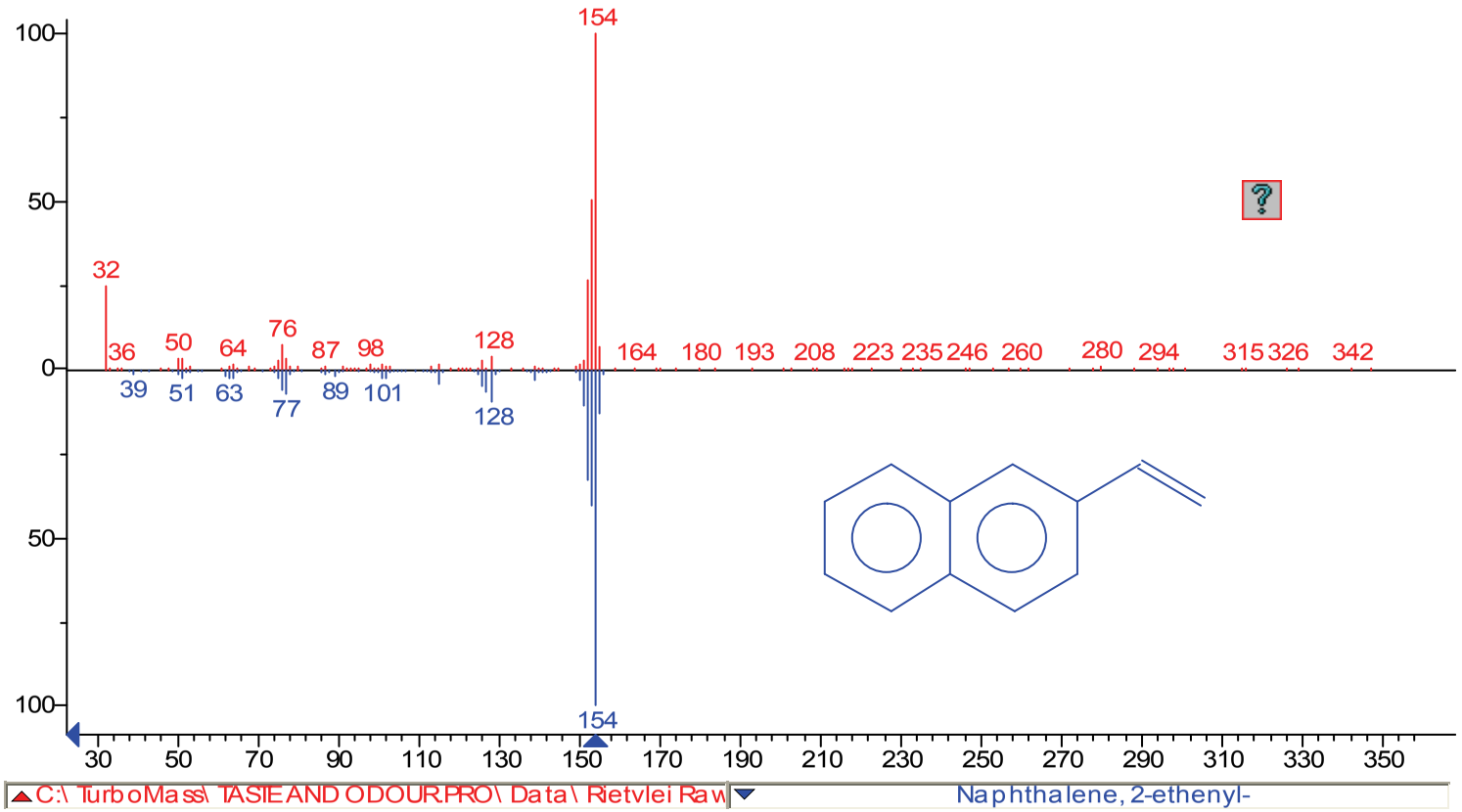

Figure A-2: Spectrum of 2-ethhenylnaphthalene from water samples and the corresponding library match

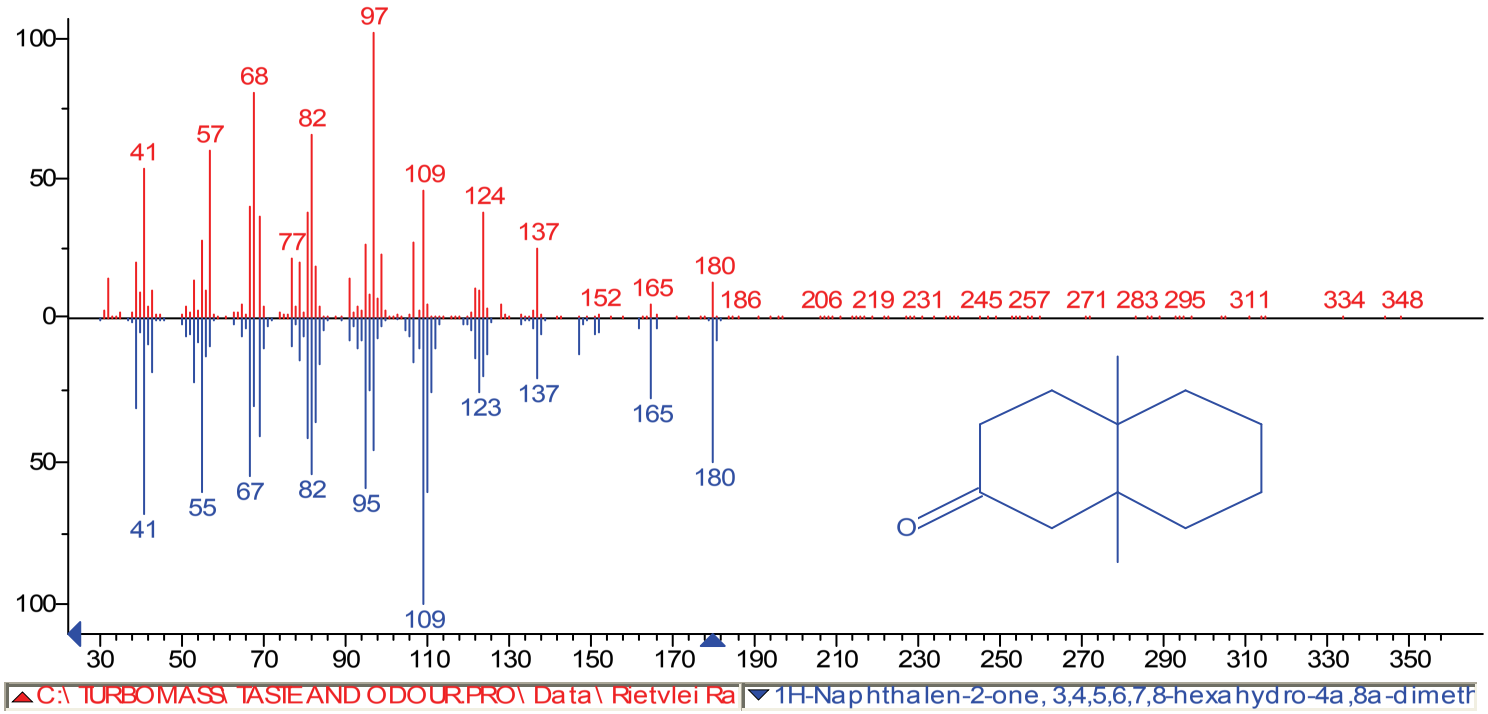

Figure A-3: Spectrum of 3,4,5,6,7,8-hexahydro-4a,8a-dimethyl-1 H-naphthalen-2-one from water samples and the corresponding library match

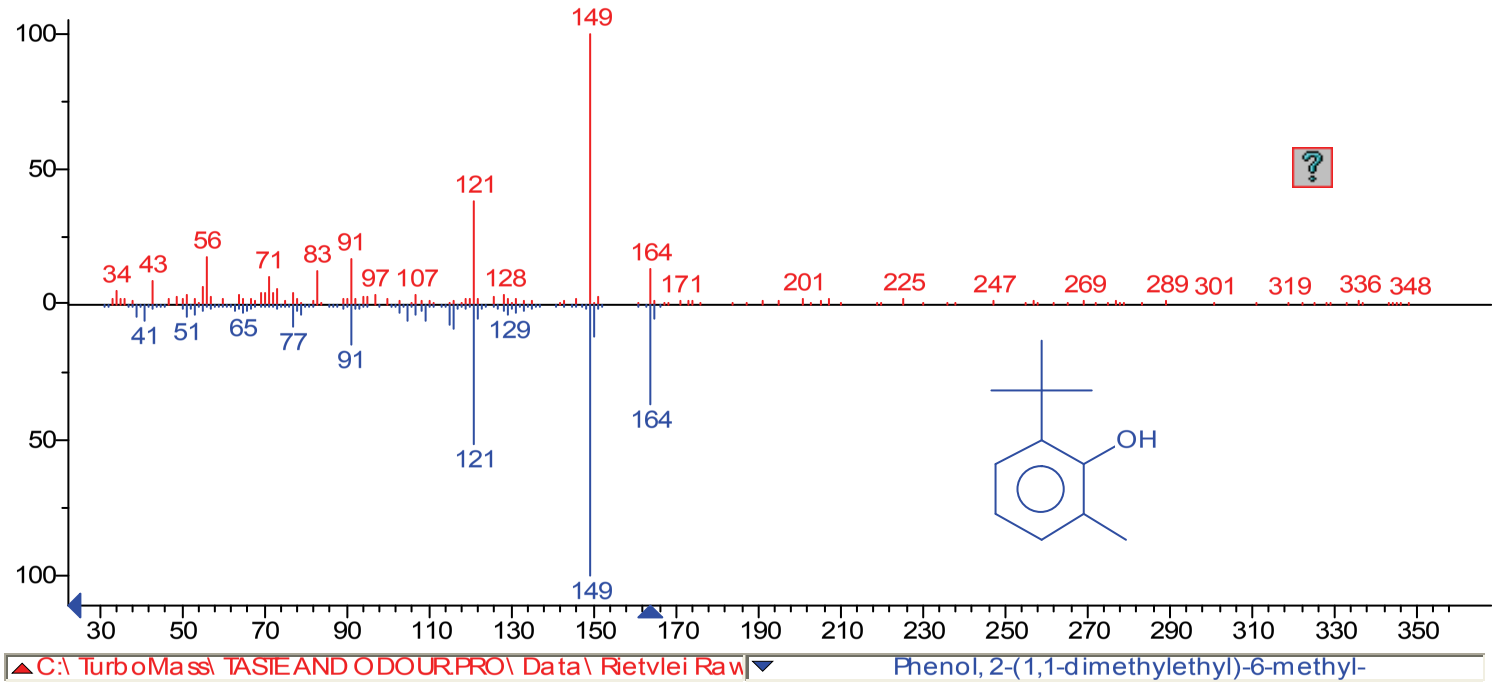

Figure A-4: Spectrum of 2,6-bis[1,1-dimethylethyl]-4-methylphenol (butylated hydroxytoluene) from water samples and the corresponding library match

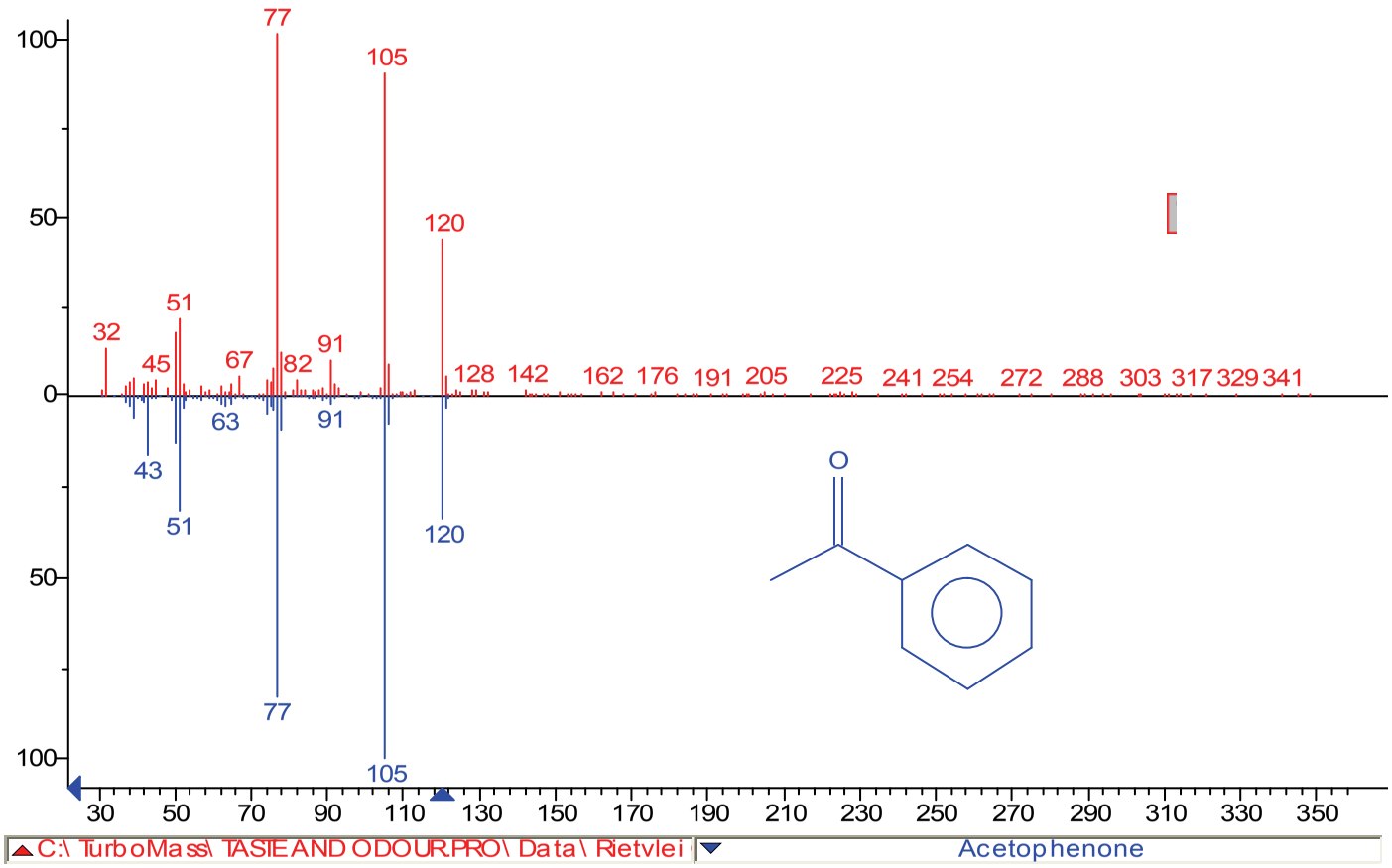

Figure A-5: Spectrum of acetophenone from water samples and the corresponding library match

APPENDIX B

Table B-1: Removal efficiencies for photolytic and photocatalytic degradation of 10 mg/ℓ phenol with 400 W UV lamp and catalyst concentrations of 10-150 mg/ℓ

	Photolysis		Photocatalysis degradation of 10 mg/ℓ phenol with TiO_2 concentrations of 10-150 mg/ℓ catalyst concentrations and percentage removal												
Time (mins)	**UV Only**	**% Removal**	**10 mg/ℓ**	**% Removal**	**20 mg/ℓ**	**% Removal**	**30 mg/ℓ**	**% Removal**	**40 mg/ℓ**	**% Removal**	**50 mg/ℓ**	**% Removal**	**100 mg/ℓ**	**150 mg/ℓ**	**% Removal**
0.00	10.00	0.00	9.90	0.00	9.80	0.00	9.80	0.00	9.25	0.00	9.75	0.00	9.86	9.65	0.00
2.00	5.20	48.00	5.10	48.48	4.50	54.08	5.10	47.96	5.19	43.87			6.14	6.47	32.97
4.00	2.30	77.00	2.40	75.76	2.40	75.51	1.90	80.61	2.36	74.51	2.13	78.11	3.11	4.04	58.20
6.00	1.10	89.00	1.40	85.86	1.20	87.76	1.00	89.80	1.36	85.27	0.95	90.24	1.69	2.32	75.99
8.00	0.60	94.00	0.80	91.92	0.60	93.88	0.53	94.64	0.70	92.41	0.51	94.72	0.85	1.24	87.15
10.00	0.30	97.00	0.50	94.95	0.40	95.92	0.37	96.27	0.51	94.53	0.31	96.85	0.39	0.93	90.33
15.00	**ND	100.00	0.30	96.97	0.30	96.94	0.17	98.26	0.23	97.51	ND	100.00	0.18	0.33	96.60
20.00			0.20	97.98	0.20	97.96	ND	100.00	0.13	98.58			ND	0.35	96.34
25.00			0.30	96.97	0.20	97.96			ND	100.00				0.14	98.55
30.00			0.10	98.99	ND	100.00								ND	100.00
35.00			ND	100.00											

**ND – Not Detected

Table B-2: Removal efficiencies (%) for photolytic; and photocatalytic degradation of 20 mg/ℓ phenol with 400 W UV lamp and catalyst concentrations of 30-150 mg/ℓ

	Photolysis		Photocatalysis degradation of 20 mg/ℓ phenol with TiO_2 concentrations of 30-150 mg/ℓ catalyst concentrations and removal efficiency									
Time (mins)	UV Only	% Removal	30 mg/ℓ	% Removal	40 mg/ℓ	% Removal	50 mg/ℓ	% Removal	100 mg/ℓ	% Removal	150 mg/ℓ	% Removal
0.00	20.68	0.00	19.88	0.00	20.79	0.00	20.82	0.00	19.38	0.00	19.16	0.00
2.00	12.43	39.89	11.27	43.34	13.56	34.79	12.21	41.36	12.58	35.10	13.77	28.13
4.00	8.37	59.54	6.63	66.64	8.55	58.90	10.02	51.90	7.95	59.00	9.04	52.81
6.00	5.95	71.22	4.77	75.99	5.80	72.09			5.31	72.59	6.22	67.54
8.00	4.74	77.06	4.01	79.85	4.21	79.77	6.92	66.78	4.06	79.04	4.72	75.35
10.00	4.03	80.53	3.76	81.10	3.47	83.32	4.36	79.04	3.61	81.36	4.16	78.29
15.00	2.98	85.60	2.75	86.19	2.50	87.99	2.32	88.85	2.62	86.47	3.27	82.93
20.00	2.34	88.68	2.17	89.07	2.00	90.38	1.64	92.13	2.00	89.68	2.78	85.50
25.00	1.83	91.15	1.68	91.55	1.56	92.48	1.21	94.17	1.46	92.49	2.22	88.43
30.00	1.47	92.90	1.20	93.96	1.32	93.64	0.73	96.51	1.26	93.49	1.79	90.66
35.00	1.29	93.77	0.89	95.50	1.03	95.04	0.58	97.20	1.00	94.86	1.44	92.48
40.00	0.90	95.64	0.68	96.56	1.04	95.01	0.45	97.84	0.72	96.26	1.16	93.93
50.00	0.54	97.38	0.37	98.12	0.79	96.20	0.20	99.04	0.42	97.82	0.73	96.21
60.00	0.30	98.56	0.18	99.07	0.30	98.56	ND	100.00	0.24	98.78	0.51	97.33
80.00	ND	100.00	ND	100.00	ND	100.00			ND	100.00	0.16	99.16
100.00											0.00	100.00

APPENDIX C

Backwash Water Volumes Generated in treatment Plants

Filter backwash water volumes collated for a period of twelve months (January to December 2007) from Rietvlei and Roodeplaat treatment plants are presented in Table C-1.

Table C-1: Summary of monthly backwash water volumes

MONTH (2007)	GAC FILTERS BACKWASH WATER VOL./Mℓ	DAFF FILTERS BACKWASH WATER VOL./ Mℓ	RIETVLEI TOTAL BACKWASH VOL./ Mℓ	RAPID SAND FILTERS BACKWASH VOL./ Mℓ
January	15.00	37.13	52.13	63.09
February	12.48	48.38	60.86	117.18
March	10.24	62.00	72.24	32.63
April	9.28	62.63	71.91	48.32
May	16.56	80.00	96.56	39.84
June	16.72	82.75	99.47	39.03
July	14.88	103.38	118.26	47.81
August	11.04	67.88	78.92	44.13
September	13.92	55.75	69.67	39.58
October	10.40	69.00	79.40	45.73
*November	10.24	34.13	44.37	40.35
December	12.56	44.50	57.06	24 .45
TOTAL	**153.32**	**747. 53**	**900.85**	**433.63**

* Volumes for November are for the 2nd to the 22nd of November

A total of 747.53 Mℓ/year of treated water was used to backwash ten DAFF filters at Rietvlei (2.08 Mℓ/day) in 2007. A total of 153.32 Mℓ of treated water was used to backwash GAC filters at Rietvlei (0.43 Mℓ/day). The average daily backwash water volume for Rietvlei in 2007 was 2.50 Mℓ. For a plant with a daily capacity of 40 Mℓ/day, an average of 6.26% of the daily production was spent in backwashing the 30 filters in the plant.

A total volume of 433.63 Mℓ in the twelve month period of 2007 was used to backwash the sand filters in the Roodeplaat treatment plant (1.20 Mℓ/day).

Table C-2: General water quality of raw inlet water, DAFF and GAC filter backwash water

Determinants	Units	Raw Inlet Water	DAFF Effluent	GAC Effluent
pH @ 25ºC		8.68-9.17	7.71-8.07	7.68-8.11
Conductivity	mS/m	49.50-51.40	49.30-59.10	49.30-51.50
Total Dissolved Solids	mg/ℓ	332-344	330-396	330-345
Chloride as Cl	mg/ℓ	47.25 -54.90	48.43-53.26	49.46- 55.72
Ammonia as N	mg/ℓ	0.06-0.82	0.05-0.53	0.01-0.16
Nitrite as N	mg/ℓ	0.14-0.28	0.01-0.20	0.01-0.10
Nitrate as N	mg/ℓ	0.03-0.88	1.30-2.40	1.45-2.15
Orthophosphate as PO_4	mg/ℓ	0.65-0.71	0.54-0.59	0.56-0.67
Sulphate as SO_4	mg/ℓ	46.91-51.43	46.81-47.83	46.81-50.57
Tot. Oxid. Nitrogen as N	mg/ℓ	0.17-1.06	1.35-2.44	1.46-2.25
Suspended Solids	mg/ℓ	2.00-6.00	74.00-131.00	50.00-169.00
Turbidity	Ntu	2.70-6.36	62.80-160.60	36.79-134.64
Chem. Oxygen Demand	mg/ℓ	24-124	144-165	32-165

APPENDIX D

Determination of phenols in drinking and bottled mineral waters using online solid-phase extraction followed by HPLC with UV detection